DISSERTATION

Disentangling neuronal pre- and post-response activation in the acquisition of goal-directed behavior through the means of co-registered EEG-fMRI

For the degree of Doctor rerum naturalium (Dr. rer. nat.)

Presented to the Faculty of Mathematics and Natural Sciences, Technische Universität Dresden by

Dipl.-Psych. Fabian Baum

Born on the 14th of January, 1984, in Hoyerswerda

Submitted on July 31th, 2020

This dissertation was written between 01/2013 and 07/2020 at the Institute of General Psychology, Biopsychology and Methods of Psychology, Chair of General Psychology.

Contact: Fabian.Baum@mailbox.tu-dresden.de

Statement

The following experimental studies included in this dissertation are already published:

Study 1 (Chapter 4):

Baum F., Wolfensteller, U. and Ruge, H., (2017). *Learning-Related Brain-Electrical Activity Dynamics Associated with the Subsequent Impact of Learnt Action-Outcome Associations.* Front. Hum. Neurosci. 11:252. https://doi.org/10.3389/fnhum.2017.00252

Please note that the analysis method presented in chapter 4 differs from the approach that finally made it to the publication. In both cases different measures were implemented to account for the highly explorative nature of the research question. In the analysis that is part of this work I performed a k = 2 cross validation procedure of the EEG data while in the published version this was achieved via Monte Carlo-based cluster-extent thresholding. These diverging approaches led to a slightly different outcome with regard to temporal and spatial maxima of the presented effects. However, in both cases there is no difference regarding the nature and the interpretation of the main results.

This publication is currently not part of any other dissertation than this one. Further, it is not planned to be used in any other dissertation than this one.

Table of contents

List of Figures

List of Tables

List of Abbreviations

AAL	Automatic anatomic labeling atlas
AAS	Average artifact subtraction
ANOVA	Analysis of variance
AS	Anticipative stimulus
BCG	Cardioballistic artifact
BOLD	Blood oxygenation level dependent
CR	Conditioned response
CS	Conditioned stimulus
ECG	Electrocardiographic channel
EEG	Electroencephalography
EPI	Echo planar imaging sequence
ERP	Event related potential
fMRI	Functional magnetic resonance imaging
FWE	Family-wise error
GA	Gradient artifact
GLM	General linear model
gPPI	Generalized psychophysiological interaction
HRF	Hemodynamic response function
Hz	Hertz
IC	Independent component
ICA	Independent component analysis
IS	Imperative stimulus
ITI	Inter trial interval
LPFC	Lateral prefrontal cortex
mm	Millimeter
ms	Milliseconds
n.s.	Not significant

O	Outcome
OBS	Optimal basis set
OFC	Orbitofrontal cortex
OIFG	Orbital inferior frontal gyrus
O-R	Outcome-response
PCA	Principal Component analysis
PCG	Precentral gyrus
PSG	Parietal superior gyrus
PPI	Psychophysiological interaction
R	Response
RF	Radio frequency
R-O	Response-outcome
ROI	Region of interest
RT	Reaction time
SMA	Supplementary motor area
SNR	Signal-to-noise ratio
S	Stimulus
S-O	Stimulus-outcome
SOA	Stimulus onset asynchrony
S-R	Stimulus-response
S-R-O	Stimulus-response-outcome
SRO-rep	Stimulus-response-outcome repetition
TE	Echo time
TR	Repetition time
TTL	Transistor-transistor logic
UR	Unconditioned response
US	Unconditioned stimulus

1 Summary

1.1 Introduction

Intentional behavior in higher animals differs from mere habitual behavior in terms of goal-directedness (Goschke, 2004). Behavior is considered goal-directed when the actor integrates information about the subsequent outcome of an action (Balleine & O'Doherty, 2010; Dickinson & Balleine, 1994; Kiesel & Koch, 2012), potentially enabling the anticipation of consequences of an action. Thus, goal-directed behavior requires knowledge about which behavior shown in the past led to the expected goal state. Technically speaking, it requires prior acquisition of knowledge about the current contingencies between behavioral responses and their outcomes under certain stimulus conditions (J. Hoffmann & Engelkamp, 2013). This association chain enables events lying in the future to be mentally represented and assessed in terms of value and achievability. Furthermore, goal-directed behavior is independent from stimulus conditions. Preceding stimuli and consecutive actions are not linked to each other like automatized behavior or reflexes but instead are mentally represented in an arbitrary manner. This way the anticipative stimulus and its consecutive reaction can be decoupled leading to an enormous increase in the degrees of freedom of an individual. Thus, higher animals are capable of reacting differently to the same stimulus, depending on its predominant present goal. This allows agents to react differently to varying environmental conditions or changed goal states, while habits are continuously performed in the same manner without regard to stimulus conditions or value of different outcomes. In all higher animals, knowledge about contingencies between a stimulus, a response and a specific effect of an action can be acquired via trial and error where learning relies on evaluating retrospectively whether a behavioral response yielded a desirable outcome. Additionally, only humans are capable of accelerating the learning process using explicit instructions, which specify prospectively how to yield intended outcomes under the appropriate stimulus conditions (Doll, Jacobs, Sanfey, & Frank, 2009a; Ruge & Wolfensteller, 2016; Wolfensteller & Ruge, 2012). This short route has an important evolutional advantage by cutting down time demanding trial-and-error sequences and thus avoiding potentially harmful behavior. Exploring and trying to understand this learning process has a long research tradition.

Historically, the acquisition of goal-directed behavior was researched in two separate schools of thought. The instrumental learning approach follows the paradigm of Behaviorism first developed by John B. Watson (Watson, 1913). Based on the principles of instrumental conditioning proposed by Thorndike, learning from a behavioristic view is defined as an association between a certain stimulus (S) and a behavior (R) that leads to a certain (rewarding) outcome (O). According to the so called “law of effect” (E. L. Thorndike, 1905)

responses that produce a rewarding effect in a particular situation become more likely to occur again under the same stimulus conditions (while likewise responses with a discomforting effect will become less likely). The importance of the rewarding effect lies only in its function to provide reinforcement to the S-R association without becoming part of the associational chain itself. According to the behaviorist dogma, the O is the mere glue that tights S and R together.

The second research line is deeply bedded into particularly the German research tradition of cognitive psychology (Stock & Stock, 2004) in which the acquisition of goal-directed behavior is explored mainly based on the so called ideomotor principle (Elsner & Hommel, 2004; J. Hoffmann, Butz, Herbort, Kiesel, & Lenhard, 2007; B. Hommel, Musseler, Aschersleben, & Prinz, 2001; Kunde, 2001a). The foundation of the ideomotor theory has been defined already in the late 19th century by William James (1890). The ideomotor hypothesis postulates bidirectional associations between an action (R) and its outcome (O) and assumes a two-step learning process of goal-directed actions (Elsner & Hommel, 2001, 2004; Kunde, 2001a). In a first step contingencies between an action and its effect are formed based on trial-and-error principle (i.e. random actions lead to a desired outcome). In a second step these contingencies can then be used in a goal-directed manner (anticipation of the desired outcome activates the necessary motor program).

However, while neural correlates of instructed goal-directed action integration processes have already been examined in a functional magnetic resonance imaging (fMRI) study using this paradigm (Ruge & Wolfensteller, 2015), there has been no information if those processes are also reflected in Electroencephalography (EEG) and if so which specific EEG parameters are modulated by them. Gaining insight into EEG related correlates of outcome response learning could also help to address a shortcoming of fMRI studies lying in its poor temporal resolution. A fMRI map with regional activations alone does not necessarily permit inferences about the exact time and order in which these activations have occurred. This phenomenon is known as the temporal inverse problem (Logothetis, 2008). The core aim of this work was to make use of the temporal highly resolved EEG signal to dissect the sluggish fMRI Blood-Oxygen-Level-Dependent (BOLD) signal within a trial in order to extract distinct activation connected to different cognitive sub-processes of outcome response learning.

1.2 Study Objectives

This dissertation set out to investigate neurocognitive mechanisms of instructed outcome response learning utilizing two different imaging methods, namely EEG and fMRI. Study 1 was an exploratory study to answer the question what kinds of learning-related EEG correlates were to expect. The O-R outcome integration specific EEG correlates identified in

Study 1 served as regressors in a unified general linear model (EEG-informed fMRI analysis) in the co-registered EEG-fMRI study (Study 2). One of the key questions in this study was if the EEG signal could help to differentiate between BOLD activation associated with processes related to response preparation or initiation and activation associated with post-response outcome integration processes.

1.3 Methods

The foundation to both studies of this work was an experimental paradigm of instructed S-R-O learning, which included a learning and a test phase. The experimental design was based on a modified version of the differential outcome paradigm (Colwill & Rescorla, 1985; Noonan, Mars, & Rushworth, 2011; Shin, Proctor, & Capaldi, 2010; Trapold, 1970; Urcuioli, 2005) where differential auditory response outcomes were presented during instruction-based visuo-motor learning (Ruge & Wolfensteller, 2015; Wolfensteller & Ruge, 2014). Stimuli were four abstract visual patterns that differed in each block. Each visual stimulus required a distinct manual response and was predictably followed by a distinct auditory outcome. Instructions were delivered via a 'guided implementation' procedure in which the instruction was embedded within the first three successful behavioral implementation trials. In these first three trials the visual stimulus was followed by an imperative stimulus highlighting the correct response. The guided implementation phase was followed by an unguided implementation phase where the correct response now had to be retrieved from memory. Behaviorally, the strength of acquired O-R associations can be analyzed via O-R compatibility effects measured in a subsequent outcome-priming test phase (Greenwald, 1970). In this test phase a previously learned outcome becomes an imperative stimulus that requires either the response, which produced that outcome in the preceding learning phase (O-R compatible), or a response, which produced a different outcome (O-R incompatible).

The experimental design was embedded into an EEG recording setup in study 1 while study 2 comprised a simultaneous EEG-fMRI recording setup in which EEG scalp potentials were continuously recorded during the experimental session inside the MR scanner bore. Study 1 comprised an exploratory approach to identify event-related potetials (ERP) engaged in S-R-O learning. Study 2 followed up on these results and utilized the spatiotemporal EEG parameters in an EEG-informed fMRI analysis approach.

1.4 Results

Study 1 revealed various ERP markers correlated with outcome response learning. An ERP post-response anterior negativity following auditory outcomes was increasingly attenuated as a function of the acquired association strength. This suggests that previously reported action-induced sensory attenuation effects under extensively trained free choice conditions can be established within few repetitions of specific R-O pairings under forced choice conditions. Furthermore, an even more rapid development of a post-response but pre-outcome fronto-central positivity, which was reduced for high R-O learners, might indicate the rapid deployment of preparatory attention towards predictable outcomes. Finally, the study identified a learning-related stimulus-locked activity modulation within the visual P1-N1 latency range, which was thought to reflect the multi-sensory integration of the perceived antecedent visual stimulus with the anticipated auditory outcome.

In general, study 2 was only partially able to replicate the EEG activity dynamics related to the formation of bidirectional R-O associations that were observed in study 1. Primarily, it was able to confirm the modulation in EEG negativity in the visual P1-N1 latency range over the learning course. The EEG-informed analysis revealed that learning-related modulations of the P1-N1 complex are functionally coupled to activation in the orbitofrontal cortex (OFC). More specifically, growing attenuation of the EEG negativity increase from early to late SRO repetition levels in high R-O learners was associated with an increase in activation in the OFC. An additional exploratory EEG analysis identified a recurring post outcome effect at central electrode sites expressed in a stronger negativity in late compared to early learning stages. This effect was present in both studies and showed no correlation with any of the behavioral markers of learning. The EEG-informed fMRI analysis resulted in a pattern of distinct functional couplings of this parameter with different brain regions, each correlated with different behavioral markers of S-R-O learning. First of all, increased coupling between the late EEG negativity and activation in the supplementary motor area (SMA) was positively correlated with the O-R compatibility effect. Thus, high R-O learners exhibited a stronger coupling than low R-O learners. Secondly, increased couplings between the late EEG negativity and activation in the somatosensory cortex as well as the dorsal caudate, on the other hand, were positively correlated with individual reaction time differences between early and late stages of learning.

1.5 Discussion

The EEG-informed analysis succeeded in dissecting the fMRI BOLD signal within a trial by correlating specific parameters in the EEG signal with it. This resulted in activation patterns linked to ERP parameters prior to the response that are more likely to reflect action selection

or response initiation processes. On the other hand, activation patterns functionally coupled to EEG activity subsequent to the response and even subsequent to outcome presentation are most likely engaged in outcome integration processes.

Prior to the behavioral response the results indicate that the OFC could serve as a (multimodal) hub for integrating stimulus information and information about its associated outcome in an early pre-stage of action selection and initiation. Learnt S-O contingencies would facilitate initiating the motor program of the action of choice. Hence, the earlier an outcome is anticipated (based on stimulus outcome associations), the better it will be associated with its response, eventually leading to stronger O-R compatibility effects later on. This account is consistent with the general notion that more salient events (here outcomes that are pre-activated sooner) will be associated with other events (here the action) more easily and more rapidly (Le Pelley & McLaren, 2003; Mackintosh, 1975). Thus, one could speculate that increased activation in response to S-R-O mappings possibly embodies a marker for the ongoing transition from mere stimulus-based behavior to a goal-directed behavior troughout the course of learning.

Post-response activations coupled with a late centro-parietal EEG negativity increase revealed a seemingly two-fold feedback integration stream of O-R contingencies, each mediated by different behavioral performance markers. On one hand the SMA seems to be engaged in bidirectional encoding processes of O-R associations. The results promote the general idea that the SMA is involved in the acquisition of goal-directed behavior (Elsner et al., 2002; Melcher, Weidema, Eenshuistra, Hommel, & Gruber, 2008; Melcher et al., 2013). Together with prior research (Frimmel, Wolfensteller, Mohr, & Ruge, 2016) this notion can be generalized not only to extensive learning phases but also to learning tasks in which goal-directed behavior is acquired in only few practice trials. However, there is an ongoing debate on whether SMA activation can be clearly linked to sub-processes prior or subsequent to an agent's action (Nachev, Kennard, & Husain, 2008). With the means of co-registered EEG-fMRI acquisition it is possible to gain a deeper insight in answering this question since it is possible to attain distinct BOLD activation information within a trial with the help of additional EEG information. All in all, the results provide additional evidence favoring an involvement of the SMA only following a performed action in response to an imperative stimulus and even more, subsequent to the perception of its ensuing effect. This may give rise to the interpretation that the SMA is associated with linking the motor program of the performed action to the sensory program of the perceived effect, hence establishing and strengthening O-R contingencies. This link is basically the core of what defines outcome response learning, i.e. acquiring goal-directed behavior according to both instrumental learning as well as ideomotor approaches.

Furthermore, the analysis identified an increased coupling of a late negativity in the EEG signal and activation in the dorsal parts of the caudate as well as the somatosensory cortex. The dorsal caudate has not particularly been brought into connection with O-R learning so far. I speculate that the coupling effect in this part of the caudate reflects an ongoing process of an early automatization of the acquired behavior. It has already be shown in a similar paradigm that behavior can be automatized within only few repetitions of novel instructed S-R mappings (Mohr et al., 2016). Automatization of behavior in this sense, however, has to be distinguished from habitualization of behavior requiring far longer learning periods. Still, the dorsal caudate could function as a region in which the acquired behavior might already be prepared to work in a more automatized manner relying less and less on the online evaluation of the ensuing effect as training continues.

Overall, co-registered EEG-fMRI recording has been proven beneficial in the context of researching underlying mechanisms of goal-directed behavior. The results can provide an additional piece in grasping the complex mechanisms involved into outcome response learning. However, due to the highly explorative approach of the studies and the nature of the EEG-informed analysis method more confirmatory research is strongly recommended to eventually attain a comprehensive understanding on the neurocognitive mechanisms of outcome response learning.

2 Theoretical Background

2.1 Introduction

When I was still being a student of psychology I fulfilled one of my dreams of staying in Japan for one year attending a Japanese university. While I was in Japan I enjoyed going to restaurants for several reasons. First of all, the food offered there is extraordinary. On the other hand, due to high prices for groceries, home cooked food isn´t that much cheaper than prepared food in a restaurant or at a food stall. I remember one special kind of restaurant, which was quite famous because it offered delicious food prepared in a very short amount of time, perfectly complementing the short breaks during university lectures. This restaurant basically only consisted out of a computer terminal in which one was supposed to place the order and an outlay where you could pick up the prepared meal. However, this computer terminal had no English translation of the menu, containing meal names and explanations only in Kanji (Japanese characters). So for the first few times whenever I went there I was stuck picking something completely random from the menu since I could not read nor translate the Japanese characters. Doing so a few times, I slowly started to memorize which sequence of Japanese characters would result in which meal. After some time, I could start actually picking meals on purpose. For example if I wanted to eat some certain type of Ramen I now knew which button I had to press. By learning the association between the Kanji sequence and the affiliated meal I was able to start ordering the food based on my intentions rather than by surprise. Back then, little did I know that my daily struggle with Japanese written language would basically define the topic of my dissertation more than a decade later.

No species other than *Homo sapiens* shows this immense amount of adaptation with regards to constantly changing and even extreme living conditions on this planet. The evolutionary basis of this enormous adaptation process can be described by four basic neural circuits of action control, which differ in complexity (Goschke, 2002). The oldest circuit with respect to phylogenesis includes innate reaction programs known as instincts. These programs are triggered by certain stimuli and are performed always in the same manner making them predestined to operate in a fix non-changing environment. Throughout the process of evolution higher animals learned to adapt their behavior based on experience in an associative learning process, giving them an advantage in ever evolving eco systems.

Additional to this long term adaptation processes the development of internal motivational states gave rise to even more degrees of freedom. Action selection now could also be altered on a shorter time scale based on acute needs or goals. This intentional behavior differs from the one described above specifically in terms of goal-directedness (Goschke,

2004). Behavior is considered goal-directed when the actor integrates information about the consecutive outcome of an action (Balleine & O'Doherty, 2010; Dickinson & Balleine, 1994; Kiesel & Koch, 2012). It can be separated from mere habitual or automatized behavior by anticipation of consequences of the action in question. Thus, goal-directedness requires knowledge about which behavior shown in the past led to the expected goal state. Technically speaking, it requires prior acquisition of knowledge about the current contingencies between behavioral responses and their outcomes under certain stimulus conditions (J. Hoffmann & Engelkamp, 2013). This association chain enables events lying in the future to be mentally represented and assessed in terms of value and achievability in the present. Furthermore, goal-directed behavior is characterized by independence from stimulus conditions. Preceding stimuli and consecutive actions are not linked to each other like automatized behavior or reflexes but instead are mentally represented in an arbitrary manner. This way the anticipative stimulus and its consecutive reaction can be disentangled leading to an enormous increase in the degrees of freedom of an individual. Thus, higher animals are capable of reacting differently to the same stimulus depending on its predominant present goals which expresses a huge evolutionary step over mere habitual behavior. It allows agents to flexibly react to different environmental conditions or changed goal states while habits are continuously performed in the same manner without regard to stimulus conditions or value of different outcomes. In all higher animals, knowledge about contingencies between a stimulus, a response and a specific outcome can be acquired via trial and error where learning relies on evaluating retrospectively whether a behavioral response yielded a desirable outcome. Additionally, only humans are capable of accelerating the learning process using explicit instructions, which specify prospectively how to yield intended outcomes under the appropriate stimulus conditions (Doll et al., 2009a; Ruge & Wolfensteller, 2016; Wolfensteller & Ruge, 2012). This short route has an important evolutional advantage by cutting down time demanding trial-and-error sequences and thus avoiding potentially harmful behavior. Exploring and trying to understand this learning process has a long research tradition.

Historically, the acquisition of goal-directed behavior was researched in two separate schools of thought. The instrumental learning approach follows the paradigm of Behaviorism first developed by John B. Watson (Watson, 1913). Based on the principles of instrumental conditioning proposed by Thorndike, learning from a behavioristic view is defined as an association between a certain stimulus (S) and a behavior (R) that leads to a certain (rewarding) outcome (O). According to the so called *law of effect* (E. L. Thorndike, 1905) responses that produce a rewarding effect in a particular situation become more likely to occur again under the same stimulus conditions (while likewise responses with a discomforting effect will become less likely). According to the instrumental learning approach importance of the

rewarding effect lies only in its function to provide reinforcement to the S-R association without becoming part of the associational chain itself. The O acts as a mere glue that tights S and R together.

The second research line is deeply bedded into particularly the German research tradition of cognitive psychology (Stock & Stock, 2004) in which the acquisition of goal-directed behavior is explored mainly based on the so called *ideomotor principle* (i.e. Elsner und Hommel, 2004; Hoffmann, 2003; Hommel et al., 2001; Kunde, 2001). The foundation of the ideomotor theory has been defined already in the late 19th century by William James (1890). The ideomotor hypothesis postulates bidirectional associations between an action (R) and its outcome (O) and assumes a two-step learning process of goal-directed actions (Elsner & Hommel, 2001, 2004; Kunde, 2001a). In a first step contingencies between an action and its effect are formed based on trial-and-error principle (i.e. random actions lead to a desired outcome). In a second step these contingencies can then be used in a goal-directed manner (anticipation of the desired outcome activates the necessary motor program).

On the following pages I will describe both research lines in detail, displaying key findings with regards to behavioral and neurophysiological correlates. I will conclude the chapter with a section giving an introduction into the methods used in the individual studies comprising this dissertation. It will feature a description of the method of Electroencephalography (EEG) and functional magnetic resonance imaging (fMRI), each separately. Additionally, it will focus on implications on combining both methods in a co-registered study and give an overview over several conjoint analysis methods of the two data modalities.

2.2 Theories of acquiring goal-directed behavior

2.2.1 Instrumental learning

2.2.1.1 Behavioral aspects

The principle of instrumental learning or instrumental conditioning was established based on the school of behaviorism developed by John B. Watson (1913) and further elaborated by Edward Lee Thorndike (E. L. Thorndike, 1927, 1933). The behaviorists wanted to understand human behavior only by observing its measurable overt aspects without having to rely on introspection. This consideration had a deep implication on learning as how they defined it. From the behaviorists point of view there is no S-R-O association chain per definition. Especially the incentive value of an anticipated outcome (as anticipation is to be

considered an introspective aspect of behavior) was denied to be a relevant part of response selection. Instead, a (rewarding) outcome following a certain response merely was thought to serve as reinforcement of the S-R association (Edward L. Thorndike, 1911). This led Thorndike to formulate what he called the *law of effect* stating that "responses that produce a satisfying effect in a particular situation become more likely to occur again in that situation, and responses that produce a discomforting effect become less likely to occur again in that situation" (Gray, 2011). The incentive value of the outcome influences the learning process merely in a sense that greater reward fosters greater learning success. According to his reasoning, the outcome is not part of the newly formed S-R association per se.

There has been a great debate over this critical claim with accumulating evidence against it. Hull (1930) and Spence (1950) first combined Thorndike's paradigm with the *stimulus substitution theory* (Pavlov, 1927). In this account an action can be initiated either by a stimulus (S) or through a substitute, i.e. the anticipation of a reward. This anticipation is based on an association between the stimulus S and the outcome O following the correct response (S-O). This account was later elaborated in the *Two-Process-Theory* (Rescorla & Solomon, 1967). According to this theory principles of classical conditioning come into effect during the process of instrumental learning. There are various studies providing evidence that the conditioned stimulus (CS) activates an anticipative state (i.e. expectation of a reward), which then itself motivates the instrumental behavior (Corbit & Balleine, 2005; Ostlund & Balleine, 2007).

Another important impulse on the question on whether the outcome is or is not part of the learned association came from Burrhus F. Skinner (1938) who elaborated on Thorndike's studies, specifically on the "law of effect". He took a different approach from mere classical conditioning in which the response is perfectly determined by the stimulus condition (Pavlov, 1927). Skinners experimental setup, known as *operant conditioning*, involved specially designed animal cages ("Skinner boxes") in which small rodents, such as rats, learned to push a lever in order to receive a reward (food). He showed that rats increasingly performed the behavior that led to a reward. The rats seemed to have made a connection between the performed action (R) and its specific outcome (O). In other words, they seemed to have acquired a response-outcome association (R-O).

It was not until forty years later that this key question would finally be solved by Colwill and Rescorla (1985) who came up with a paradigm designed to prove the existence of R-O associations. The experiment was divided into three separate phases. In the first phase rats were trained to push a lever either to the left or to the right. The two behavioral options led to differential outcomes. Pushing the lever to the left was rewarded with food pellets, while

pushing it to the right resulted in a different reward (sucrose). In the second phase one of the rewards was devaluated by administering a substance causing nausea to the rats, right after they received the reward. According to the principles of classic conditioning this nausea would now be associated with the food leading to a devaluation of the reward. In the third phase of the experiment the rats had free choice of pushing the lever either to the left or to the right. The rats now avoided the direction of the devalued reward and preferred the opposite, non-devalued, direction. This important observation could however not be explained with S-R or S-O learning alone. If the rats had formed an S-R association in which the outcome is not part of the learned behavior the devaluation wouldn´t have had any effect on the behavior of the rats in the third phase, leading to an approximately equal amount of lever pushes to the left or to the right. If the rats had formed only an S-O association on the other hand, the devaluation should have restrained both behavioral options (pushing to the left or to the right) in the third phase since both responses were associated with the same stimulus condition (the lever). These important results, which could be replicated a number of times (Adams & Dickinson, 1981; Balleine & Dickinson, 1998), strongly suggest that the rats indeed displayed goal-directed behavior in the sense that they formed specific R-O contingencies based on prior S-O associations containing knowledge about the causal relationship between their actions and its consequences. They were able to anticipate the outcome of the two action modes and according to that knowledge they chose the action which led to the non-devaluated outcome more often.

Another important study utilized the so called *degraded contingency effect* originally reported by Rescorla (1966, 1968). This effect is observed when unconditioned rewards (food) are administered during training with a conditioned reward following a conditioned response. The additional unconditioned reward leads to a diminished response to the conditioned reward independent of baseline responding in the context. The critical finding of these experiments was that the conditioned response was reduced if the chances of occurrence of unconditioned and conditioned reward were exactly the same. The association between response and outcome (R-O) degraded due to the additional reward. Dickinson et al. (1998) showed that over-trained rats were insensitive to contingence degradation when compared to undertrained rats. In contrary to undertrained rats the overtrained group was not able to actually hold back an action when it was necessary in order to gain the reward. Reversing the contingency from *R → O* to *not R → O* affected untrained, non-automatized actions in rats. Although it still lacks human studies up to this point there is strong evidence suggesting that the effect of sensitivity to R-O contingency degradation found in rats is also present in humans (Balleine & O'Doherty, 2010)

Response-outcome learning of differential outcomes

Trapold (1970) also utilized distinct outcomes as a consequence of performed actions in experiments of response-outcome learning. He showed that learning to react upon two different stimulus conditions was faster if the response led to two different rewarding outcomes (as opposed to the same reward). Trapold called this the *differential outcome effect.* In his experiment rats learned to discriminate two separate S-R associations. Two different tones required two distinct responses (pushing two buttons). In one group the two different responses led to two distinct incentive outcomes (sucrose and food pellets). In the control group both responses were rewarded with sucrose. The differential outcome group performed better and showed less errors compared to the control group. Going even further, it has also been shown that differential outcomes also led to a reduction in error rates when compared to randomly assigned rewards (Urcuioli, 2005). Those studies finally provided strong evidence that the incentive effect of the outcome not only reinforces the S-R connection but instead becomes part of a triple S-R-O association itself (Silvetti & Verguts, 2012).

With regard to differential response-outcome effects it has been shown in an abundance of studies that R-O associations can be contextualized on the basis of the incoming stimulus information (Colwill & Rescorla, 1985, 1990; Kunde, 2001b; Ruge, Krebs, & Wolfensteller, 2012; Wolfensteller & Ruge, 2011; Ziessler, Nattkemper, & Frensch, 2004b). In an exemplary study by Colwill and Rescorla (1990) rats were first trained to associate two differential outcomes of different responses with a certain stimulus. If a light flash was presented, pulling a string led to food pellets while pushing a button resulted in sucrose. On the other side if a tone was presented instead, the two response alternatives led to exactly the opposite reward. Now, one of the two rewards was devaluated. In the final test phase the rats were presented again either the light flash or the tone. Depending on the stimulus, the rats chose the non-devaluated response option. Thus, the experiment demonstrated that choosing a response alternative in anticipation of a certain goal can change from situation to situation, depending on the stimulus condition.

In human studies, it has been shown that such S-R-O associations can be established very rapidly. Ruge and Wolfensteller (Ruge et al., 2012; Wolfensteller & Ruge, 2011, 2014) have had subjects establish stimulus based R-O (S-R-O) associations using differential outcomes in a first learning phase. Specifically, each distinct link between a visual stimulus and a manual response was predictably followed by a distinct auditory outcome. In a second short test phase the strength of the established R-O association was probed by demanding the subjects to respond correctly to the differential outcomes presented in the learning phase (O-R) making use of the so called compatibility effect (Greenwald, 1970). Now the previously

learned outcome became an imperative stimulus that required either the response, which produced that outcome in the preceding learning phase (O-R compatible), or a response, which produced a different outcome (O-R incompatible). Ruge and Wolfensteller observed faster response times and higher accuracy if the demanded response in the test phase was compatible to the response, which invoked the outcome in the learning phase. The result provided strong evidence supporting the hypothesis that R-O associations can be established within few repetitions (from eight to twelve, depending on the experimental design) of specific S-R-O mappings.

Recent accounts in investigating goal-directed behavior

Recent developments in cognitive learning theories now additionally take internal motivational states into account. In classic conditioning, it is assumed that the presentation of a conditioned stimulus (CS) leads to the anticipation of an unconditioned stimulus (US). In instrumental learning, based on a previously established R-O association, an action leads to anticipation of the corresponding outcome (J. Hoffmann & Engelkamp, 2013). The fact that both, outcome as well as the conditioned stimuli predicting an outcome have a motivational influence on the performance of an agent suggests that these processes have a complementary influence on action selection (Balleine & O'Doherty, 2010).

This consideration ultimately led to the use of incentive outcomes as both discriminant stimuli (O^s) as well as discriminant goals (O^G) in a number of studies (de Wit, Kosaki, Balleine, & Dickinson, 2006; Dickinson & de Wit, 2003). In these studies, the outcome always preceded the response and in doing so, it acted as a discriminant stimulus, thus influencing action selection. On the other hand, the outcome always followed a certain response serving as a discriminant goal state. It has been shown that devaluation of the outcome influenced the response with which it was associated as a discriminant goal but did not influence responses if those were associated with the outcome as a discriminant stimulus. Those results strongly suggest that both stimuli as well as goals influence action selection and action initiation in a complementary manner.

According to Balleine and O'Doherty (2010) an action is influenced by an outcome on two different levels. On one hand, it is influenced through means of an O^S-R association in which the outcome functions as a stimulus with which the appropriate action can become associated. On the other hand, the action is influenced by an R-O^G association, basically representing a pure R-O association, in which an action produces its outcome in the sense of a goal. O^S-R associations enable activation of an outcome representation mediated by a trigger-stimulus associated with that outcome (S-O). This representation then itself serves as a discriminant stimulus, which primes the required action. Action selection and initiation again

result in the activation of the outcome representation except this time labeled as a goal (O^G). Hence, O^S and O^G together enable goal-directed behavior. It has been shown that outcome devaluation only has impact on actions if they are associated with the value of the outcome while discriminant cues to the outcome are not affected (Colwill & Rescorla, 1990; Holland, 2004; Rescorla, 1994). On the other hand, action selection after re-establishment of the action by outcome delivery subsequent to an experimental extinction phase, is not impacted from outcome devaluation, although the response rate is reduced. This suggests that in initial learning only O^S related action selection processes are involved while in later learning stages evaluation-based O^G processes primary control behavior (Balleine & Ostlund, 2007). Moreover, this motivational account provides an explanation of acquiring habitual behavior and specifically long training phases as a prerequisite of habits. Training trials strengthen O^S-based action selection in order to initiate actions without a need of online outcome evaluation. Even more likely, habitual actions tend to be initiated impulsively before the relatively slow outcome evaluation is finished. However, how those hypothesized integrative processes are implemented on a neural level has yet to be fully researched (Balleine und O'Doherty, 2010).

2.2.1.2 Neurophysiological correlates

Neurophysiological correlates have been investigated in a number of lesion studies with animals. In those studies, various cortical structures could be identified with goal-directed behavior. There is some evidence that regions corresponding to medial and orbitofrontal cortex as well as the basal ganglia in humans seem to be involved in the formation of R-O or S-R-O associations. Activation in these areas were able to be experimentally isolated from activation in other areas more related to stimulus driven S-R as well as S-O associations (Ashby, Turner, & Horvitz, 2010; Balleine & O'Doherty, 2010; M. Van Der Meer & Redish, 2010; Yin & Knowlton, 2006).

In human studies, the research focus depends on the imaging method used. EEG studies were mainly centered on the processing of response and outcome especially in error trials (Holroyd & Coles, 2002). In a recent study Luque et al. (2015) investigated the temporal dynamics of instrumental conditioning systematically manipulating the predictive value of the discriminant stimulus as well as the incentive value of the outcome. The main event related potential (ERP) analysis, however, only included the very late training phase in which R-O associations were already overlearned. The subjects were consecutively presented with two visual stimuli with one stimulus being predictive and the other one non-predictive. The sequence in which the two stimuli followed each other was balanced. A predictive stimulus enabled a reliable prediction of the correct response as well as the value of the outcome

whereas a non-predictive stimulus contained no information about the above. A predictive stimulus forecasting a small outcome value had a high predictive and a low incentive property while a stimulus that forecasted a high value outcome had both a high predictive and incentive property. Subjects were now required to choose one of two possible response alternatives with one of them being associated with loss or gain in reward depending on the predicted incentive value of the outcome. In case of a high predictive value a correct response led to a win of 100 points and an incorrect response to a loss of 1 point. In trials with low predictive value correct responses led to a win of 1 point and incorrect responses to loss of 100 points. The sequence of EEG correlates, which were identified in the study, could be matched to specific sub-processes prominent in outcome response learning, which proclaims that instrumental conditioning enables both S-O as well as O-R learning (Balleine & O'Doherty, 2010; de Wit & Dickinson, 2009). The authors reported several important findings. First, they found that the P2 component in response to a predictive stimulus, regardless of its incentive value, was significantly increased compared to a non-predictive stimulus. Subsequent to this effect, an increase in the P3b correlated only with the incentive value of a stimulus. Finally, a late negative increase over a time range of 350 ms prior to components supposedly integrated predictive and incentive dimensions of a stimulus as it was most expressed for predictive stimuli with high incentive value. The results gave rise to the interpretation that discriminant stimuli activate the representation of an outcome (S-O) which itself then activated the response with which it has been associated with (O-R).

In human fMRI research there are two predominant research paradigms (Wolfensteller & Ruge, 2012) utilizing either outcome devaluation to investigate neural correlates of differential outcomes (de Wit, Corlett, Aitken, Dickinson, & Fletcher, 2009; Valentin, Dickinson, & O'Doherty, 2007) or either investigate how manipulation of R-O contingency modulates neural activation (Tanaka, Balleine, & O'Doherty, 2008; Tricomi, Delgado, & Fiez, 2004). Tricomi et al. (2004) observed a specific activation in the caudate nucleus if an incentive outcome was expected following a response. There was no activation though if the outcome followed just a discriminative stimulus which required no response, thus suggesting that the activation in the nucleus caudate was modulated by R-O contingencies only, but not by S-O contingencies. Furthermore, Tanaka et al. (2008) showed that the activation in this brain region was modulated by objective R-O contingency. The activation increased in a high contingency condition and decreased for low contingency. In trial and error learning experiments Delgado et al. (2005) demonstrated that neural activation in caudate nucleus depended on acquisition of operant associations. Subjects were asked to estimate the number value of cards from a card game in a gambling task *("is card value > or < 5?"*). Correct estimations were rewarded and incorrect estimations were punished. Prior to the subjects estimation one of five possible

cue stimuli was presented prompting the probability of a high or a low value. The task involved learning S-R-O mappings in order to maximize the reward. While there was a high initial activation in the nucleus caudate it decreased with the formation of S-R-O associations over the course of the experiment. Valentin et al. (2007) investigated neural correlates of goal-directed behavior in an outcome devaluation paradigm. In human studies, outcome devaluation is achieved by continuously administering the outcome to the subject up until the point of saturation in which the reward loses its incentive property. In a first training phase subjects were asked to randomly choose from one of two possible symbols. One symbol was paired with a high probability of a reward (chocolate milk) and the other one with a low probability of a reward. In another pair, one symbol was paired with a high probability of tomato juice and the other one with a low probability of orange juice. If the point of saturation for either chocolate milk or tomato juice was reached, the response, which was associated with the now devaluated outcome, was reduced while this was not the case for the response associated with the non-devaluated outcome. On the neural level, activation in the orbitofrontal cortex (OFC) varied for devaluated responses in contrast to non-devaluated responses and affected both lateral as well as central regions. Furthermore, there is some evidence that subregions of the OFC differ in function. Lateral regions seem to be associated with the encoding of differential S-R-O mappings while medial regions seem to be more sensitive to the incentive aspect of the outcome with no regard to differentiation (Noonan, Kolling, Walton, & Rushworth, 2012; Noonan et al., 2011). In the study of Noonan et al. (2011) subjects learned to memorize 12 different S-R mappings. In one group correct responses were rewarded. The lateral OFC showed stronger activation for consistent S-O and R-O mapping information (differential outcomes). On the contrary, activation in the medial OFC seemed to reflect the expected value of the outcome, apart from consistency of a certain R-O mapping.

2.2.2 Acquisition of goal-directed behavior according to ideomotor theory

2.2.2.1 Behavioral aspects

The basic principle of modern ideomotor theory has already been formulated by William James (1890) when he stated that intentional actions are controlled by its ensuing sensory effects. He postulated that this requires knowledge about which actions are followed by which outcome. The establishment of such response (R) - outcome (O) associations expresses the first phase in the *Two-Phase-model* of voluntary action control later proposed by Elsner and Hommel (2001). According to this model movements are represented by specific activation patters in an agent's motor system (see Figure 1 left). In the first phase movements are triggered on an arbitrary basis but are followed by distinct observable outcomes. These

outcomes are perceived via sensory organs and are as well represented in terms of specific activation patterns in the cognitive system. The temporal overlap of motor as well as sensory activation patterns now results in a connection of both representations. This connection gets strengthened the more often the action is contingently followed by the same outcome.

The second phase in the model describes the process of action selection in order to achieve specific outcomes (see Figure 1 right). R-O associations acquired in phase one are bidirectional according to Elsner and Hommel. Hence, the activation of a certain outcome, which is represented by a specific combination of sensory codes in the cognitive system (outcome code), will result in an activation of all motor representations associated with this specific effect. A motor representation reflects the exact motor program of the precise action which reliably led to the desired outcome in the past. As activation of the outcome code can occur through the means of observation or mere imagination of the outcome, this prompts a functional explanation for the fundamental axiom in ideomotor theory proclaiming that goal-directed actions are triggered solely by anticipation of the desired outcome.

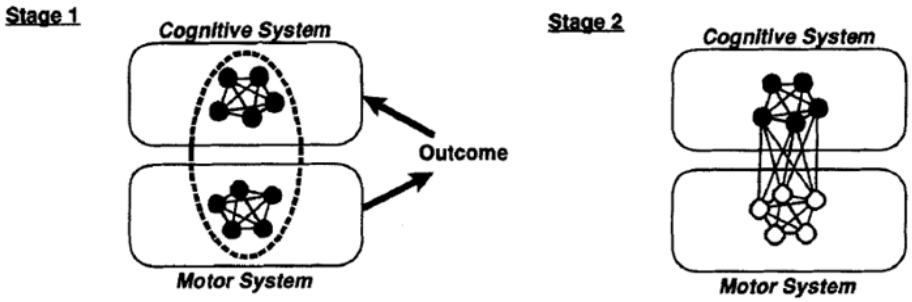

Figure 1: The Two-Phase-model of goal-directed action control according to Elsner and Hommel (2001).

Elsner and Hommel validated their assumptions in a series of experiments. In one experiment subjects were asked to push either a left or a right button on a keypad in the first phase (Elsner & Hommel, 2001, Experiment 1). Pushing the left button was followed by a high tone while pushing the right button was followed by a low tone. The subjects were told previously that those outcomes were irrelevant for the task. In the second phase of the experiment the subjects now had to react to a high or a low tone with either pushing the left or the right button. If the mapping of presented tone and consecutive action matched the previously established R-O association from the first phase subjects reacted faster compared to the incongruent mapping despite the fact that they were told that the outcome was irrelevant for the task. In a second experiment they were able to show that a previous presentation of

outcomes not only influences response times but also the selection of the following action. If the subjects had free choice of pushing either the left or the right button following a tone they chose the button which triggered the tone in phase 1 significantly more often. Both results strongly support the core assumption of ideomotor theory that actions and their ensuing effects are integrated automatically in the cognitive system and that actions are triggered automatically by mere presentation of its associated consequences.

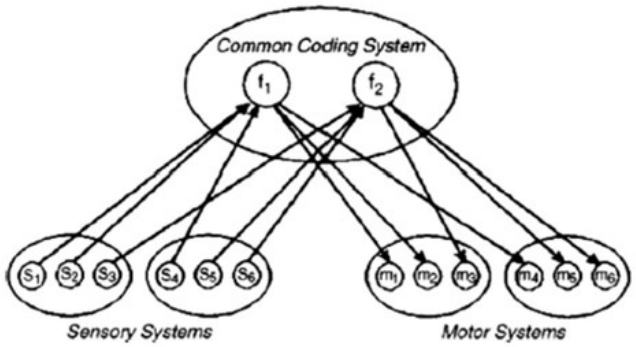

Figure 2: Graphic representation of the Common coding model (taken from Hommel et al., 2004).

One way of how perception and action initiation systems interact with each other to control human actions has been described in the *Theory of event coding* (TEC, B. Hommel et al., 2001). TEC assumes that all stimuli, which are relevant for action initiation, the action itself, as well as all ensuing effects, are stored in shared representations called *event files.* This *common coding* approach was first developed by Prinz (1990) and is displayed in Figure 2. The perception of an event (i.e. a certain consequence of an action) results in a specific neural activation pattern in designated areas of the cortex (sensory codes S_1-S_6). At the same time body movements are mapped as well in motor areas of the brain (motor codes m_1-m_6). Sensory codes are now translated into motor codes on a superficial level based on common feature codes (f_1 & f_2). Feature codes represent abstract properties of the perceived event, such as color, shape, etc. Thus, the feature codes with the label “right” would be activated by all sensory modes, may it be visual, auditory, or tactile, as long as they contain some kind of “right” information (an itch at the right hand, visual perception of a printed right arrow, someone whispering in ones right ear, etc.). Additionally, activation of feature codes results in priming of all actions somehow related with the feature “right” (lifting the right hand, pronouncing the word “right”, etc.). In this sense TEC answers the question how mental representations of goals and motor representations of actions achieving those goals can be linked to each other in a way that processes, which are required for planning and initiating an action are really the same. All body movements are exclusively represented based on their observable (and desired)

outcomes (Prinz, 1997). These response-outcome associations are the sole basis of voluntary actions according to ideomotor theory (Kunde, 2006).

Response-outcome associations as necessary and sufficient condition of goal-directed actions

The core assumption of ideomotor theory, which proclaims that goal-directed behavior is based on bidirectional associations between mental representations of actions and their ensuing effects (Greenwald, 1970; B. Hommel et al., 2001; W. James, 1890; Lotze, 1896), has been tested in two separate categories of paradigms (Kunde, 2006).

The first category focuses on research about the influence of perceived action consequences on action initiation. If motor actions are represented by means of their sensory effects, then perception of such effects should initiate those actions which typically produce them. Some research groups succeeded in showing that the presentation of effects, which had been triggered by a certain motor program over a period of years resulted in the activation of this specific motor program. For example, professional piano players hearing a certain chord primed the corresponding hand movements which would produce this chord on the piano (Drost, Rieger, Brass, Gunter, & Prinz, 2005). In another experiment similar findings were reported with secretaries for the execution of key presses on a keyboard (Rieger, 2007).

However, contingent R-O associations do not necessarily have to be trained over years in order to impact action initiation. There are a number of experiments showing strong evidence that outcome effects will trigger action initiation, even if they have not been associated with a specific action prior to the experiment (B. Hommel, 1996). These kinds of experiments mostly contain two separate phases. In the first acquisition phase actions are followed by a distinct outcome (i.e. left button → high frequency tone, right button → low frequency tone) in order to allow for the acquisition of R-O associations. In the second induction phase subjects are required to react to a stimulus (i.e. a color stimulus) with either a left or a right key press. Shortly after the presentation of the target stimulus one of the two outcomes from phase 1 is presented. It has been shown that reaction times and error rates are significantly decreased, if the outcome which is presented had also been produced in the learning phase by the action now required (high frequency tone → left button) (Elsner & Hommel, 2001; B. Hommel, 1996). Some studies even suggest that outcomes are represented in an analogous manner. Kunde (2003) showed that responses are slower if they produce a longer tone in comparison to responses which produce a shorter tone. Furthermore there is evidence that not only external stimuli but also internal affective states can be integrated as outcomes into an R-O association (Beckers, De Houwer, & Eelen, 2002). Interestingly, outcome induced action initiation is triggered, even if the corresponding outcomes are not perceived consciously (Kunde, 2004).

These results strongly suggest that actions can be integrated with different kinds of effects on a relatively short timescale and that those effect codes are able to activate the associated motor programs automatically.

This first research strand presented above, however, does not prove the central assumption of ideomotor theory that outcome anticipation is a necessary condition of goal-directed action (Pfister et al., 2010a). Since those kinds of studies merely require subjects to produce effects which already have been presented as sensory stimuli in advance to action initiation, they instead really only prove that outcome perception can influence action initiation. But they do not tip the core of goal-directed behavior, i.e. producing effects which are not yet present. In order to grasp this fundamental flaw it required a different study design which focused on investigating feedback loops between anticipated outcomes and action initiation without having presented the outcome already in advance.

This issue was dealt with in another strand of studies in ideomotor research focusing on response-outcome compatibility (Kunde, 2006; Zwosta, Ruge, & Wolfensteller, 2013). Kunde (2001b, Experiment 1) showed that a match between an action and its anticipated effect facilitated action initiation. In his experiment, subjects were required to react to a colored stimulus by either pushing a left or a right button on a keypad. Every key press led to a light bulb lighting up either to the left or to the right of the subject. If the action and the ensuing effect were compatible (pushing the left button led to lighting up the left light), subjects reacted faster in comparison to a non-compatible pairing of action and effect. Similar results of R-O compatibility were found with different modes of actions and effects, i.e. for different durations/pressure levels of key presses and tones varying in length and loudness (Kunde, 2001b, 2003; Kunde, Koch, & Hoffmann, 2004). Hence, this second research strand was able to prove that anticipated outcomes are able to influence action selection (Pfister, Kiesel, & Melcher, 2010).

Acquiring response-outcome associations as an automatized, associative learning process

In order for an agent to act according to ideomotor theory, response-outcome associations need to be acquired in the first place. According to Elsner and Hommel (2001), motor and effect codes are integrated automatically based on a temporal overlap in activation of motor as well as sensory systems, thus representing a necessary as well as sufficient condition for binding an outcome to its corresponding action. Indeed, it has been shown that outcomes can influence their preceding actions even if subjects were told not to pay attention to them (Elsner & Hommel, 2001). Additional parameters like contiguity as well as contingency of an outcome seem to modulate R-O learning, supporting the hypothesis of an associative learning process (Elsner & Hommel, 2004).

However, this view has also been challenged by several research groups. Specifically intentions of an agent seem to additionally modulate the acquisition of R-O associations, apart from R-O contingencies. Ziessler, Nattkemper and Frensch (2004a) showed in an experiment that key presses by subjects which are followed by intentional or non-intentional outcomes were distinctively associated with those outcomes which were produced intentionally. Furthermore, it has been shown that R-O learning only occurs if subjects are able to act intentionally in the acquisition phase and had free choice of whether or not they would press a key (Herwig, Prinz, & Waszak, 2007). If the key press was based on a forced choice, learning effects were significantly weaker. Another study from Haggard and Clark (2003) found evidence emphasizing the importance of intentionality on building R-O associations. In their experiment a key press was consistently followed by a tone. The key press, however, could be triggered either by a voluntary act of the subject or by a magnetic impulse in which no conscious intention of the subject was involved. Although in both conditions identical motor responses led to identical outcomes, it was only in the intentional condition that subjects reported a causal connection between their action and the ensuing effect, suggesting that intentionality has indeed great importance for outcome integration.

All the above studies prompt the conclusion that associative learning processes postulated by Hommel et al. (2001) play a role in the acquisition of response-outcome associations but are modulated by other variables, specifically volitional processes, as well. However, the underlying learning mechanisms of outcome anticipation still remain elusive (Hoffman, Butz, Herbort, Kiesel, & Lenhard, 2007).

Does outcome anticipation effect action selection or action initiation?

Cognitive approaches assume goal-directed behavior as a sequence of different sub processes which start with the mental representation of a stimulus and end with the perception of an outcome. The link between stimulus and outcome is mediated based on action selection, action initiation and action execution. Ideomotor-driven theories in contrary assume that mental activation patterns of outcome representations are not a consequence but instead a necessary condition for goal-directed action. The resulting spread in activation leads to selection and initiation of the action which in itself produces the outcome. Separate steps of action control merely represent different phases of the very same process of bidirectional activation of action and effect codes (Bernhard Hommel, 2009).

Kunde, Koch and Hoffmann (2004) proved the impact of anticipative outcome representations on different levels of goal-directed action control. Subjects were required to respond to different color stimuli with a gentle or a strong key press. Every key press was followed by a tone which could either be compatible with the response (gentle press → quite

tone, strong press → loud tone), incompatible (gentle press → loud tone, strong press → quite tone) or completely random regarding amplitude. In a first experiment Kunde et al. replicated the compatibility effect: subjects reacted faster if action and corresponding effect were compatible in comparison to an incompatible or random mapping.

In a second experiment they examined the impact of sensory outcome anticipation on different phases of action control. The experimental design was similar to the one from the first experiment but prior to the imperative colored stimuli, subjects now were additionally presented various cue stimuli which could either be neutral or correctly predicted the color of the following stimulus, hence prompting the correct response. The time range between cue and target stimulus varied between 200 and 1500 ms (Stimulus-Onset-Asynchrony, SOA). Using this type of design allowed the authors to contrast different phases of action production. Action selection starts as soon as the subject gets informed about the action required but still needs to wait for the final go-signal (the colored stimulus). Action initiation is characterized by the time range between the presentation of the go signal and the actual execution of the motor program. With regard to a possible impact of compatible or incompatible response-outcome mappings Kunde et al. derived several hypotheses. If R-O compatibility only affects action selection this should lead to a decrease of observable response time with increasing preparation time (longer SOA). If R-O compatibility only affects action initiation time differences in SOAs should not have any effect on response time. The results didn´t match any of the hypotheses above. Instead there were also highly significant compatibility effects in the condition with a long SOA of 1500 ms. This means even if the subjects had enough time to prepare the response they still reacted faster in the compatible compared to the incompatible condition. This suggests an impact of R-O associations on action initiation. However, with overall compatibility effects being stronger in the neutral cue condition (meaning both groups had to wait for the go signal in order to prepare and initiate the response) this suggests that they also impact action selection. Additionally, several parameters of action execution systematically varied with R-O compatibility, thus prompting the general conclusion that R-O associations impact all phases of goal-directed actions.

2.2.2.2 Neurophysiological correlates

Although there is no absolute separation of habitual and goal-directed action as human behavior mostly takes place on a continuum between those two extremes, they still differ with regard to stimulus- and outcome-based information that is taken into account in order to execute an action. Thus in ideomotor research it has been assumed that there are also two separate functional mechanisms for stimulus driven and goal-directed behavior and Waszak

and colleagues (Waszak et al., 2005) proposed two distinct neuroanatomical systems. According to their model, goal-directed actions are mediated by a network consisting of dorsolateral prefrontal cortex (DLPFC), anterior cingulate cortex (ACC) and the supplementary motor areal (SMA). Stimulus driven behavior on the other hand is generated by a different network consisting of lateral premotor as well as parietal regions. This assumption has been tested by Keller et al. (2006). Subjects were asked to equally separate the time span between two consecutive stimuli with a key press. In one condition (intention condition) the subjects had free choice of the button they would use while in the other condition the key was predefined (stimulus-based condition). Additionally, the key press was followed by a consistent outcome. In the stimulus-based condition this outcome determined which button subjects had to press in the subsequent trial. The induced intention-based actions (relying on response-outcome associations) and stimulus-based actions (relying on stimulus-response associations) could be separated in terms of electrical activity in the EEG. In line with their hypothesis, Keller et al. observed a stronger negativity in the intention condition compared to the stimulus based condition maximizing at frontocentral regions (close to SMA). They interpreted this result as evidence for differences in preparatory processes of stimulus-driven and goal-directed actions. Additionally, this increase in negativity was not only limited to motor and sensory regions, but instead involved the entire cortex prompting the conclusion that activation of the motor program corresponding to an action is always followed by the sensory representation of its consequence. Keller et al. found no difference in lateral potentials. Lateral potentials are thought to reflect the preparation of motor activity on a certain side of the body (in this case right hand fingers vs. left hand fingers). They interpreted this result as further evidence for the “Two Routes of Action” hypothesis (Waszak et al., 2005) in which stimulus driven and goal-directed behavior are processed via two separate neural circuits but eventually both terminate in the motor region in order to activate the necessary motor program.

Herwig and Waszak (2007) also focused specifically on outcome integration utilizing EEG. They showed that the execution of an action is indeed associated with the expectation of a corresponding outcome. In the first phase of their study subjects acquired R-O associations between key presses and presented tones. They were free to choose from two possible keys with the condition of pressing both keys approximately an equal number of times in a random fashion over the course of the learning phase. Every key press triggered either a high or a low frequency tone. The second phase of the experiment comprised a three tone oddball task in which presentations of sequences of repetitive stimuli were infrequently interrupted by a deviant stimulus. The reaction of the participant to this "oddball" stimulus was recorded. Every key press triggered one of three possible auditory stimuli with the standard tone (high frequency) and the deviant (low frequency) being exactly the same as in the learning

phase. The standard tone was presented with a probability of 75%; the deviant tone and the target stimulus (which had an even higher frequency than the standard tone) were presented with a probability of 12.5% each. Subjects were now asked to count and report the rate with which the target cue occurred. Herwig and Waszak found that deviant tones evoked a stronger positivity in the P3a component if the preceding response was associated with the standard tone. This effect most likely represents a stronger orientation reaction after a deviant outcome suggesting that sensory outcome processing is context-sensitive to outcomes which are associated with a certain response.

In fMRI research the overarching goal is to identify neural correlates of R-O learning in paradigms with non-incentive outcomes. Ruge and Wolfensteller (Ruge & Wolfensteller, 2013, 2015) used a paradigm in which R-O associations are formed in very few repetitions of distinct S-R-O mappings. In one study (Ruge & Wolfensteller, 2013) subjects were instructed a novel visuo-motor S-R mapping consisting of four distinct stimuli which were matched with two different responses (4:2 mapping) with the beginning of each block. The instruction was followed by an implementation phase in which the four different S-R mappings were repeated 8 times each. The experimental group was presented with distinct visual outcomes whereas in the control group correct responses were followed by non-contingent stimuli. Hence, for the experimental group it was possible to build up S-R-O associations. The functional connectivity analysis showed that contingent outcomes evoked an increase in functional coupling between the nucleus caudate and the lateral prefrontal cortex (LPFC) over the course of learning. However, this particular experimental design did not allow for a clear answer to the question on whether this effect was prompted by O-R associations themselves or rather by the active usage of these associations. In order to answer this question, in a follow up study (Ruge & Wolfensteller, 2015), the acquisition phase in which subjects learned 4:4:4 S-R-O mappings was followed by a test phase in which previous outcomes now served as imperative stimuli that required responses that could be either compatible or incompatible with the O-R associations acquired in the learning phase, yielding in a pure measure of O-R association strength. The results showed an increase in coupling between LPFC and putamen which was correlated with the response time compatibility measure prompting the interpretation that the putamen is relevant for stimulus driven S-R associations as well as highly automatized O-R associations. LPFC-caudate couplings on the other hand were correlated with response slowing between early and late learning stages (which was assumed to be a measure of active R-O usage) suggesting that the caudate is responsible for the online control of goal-directed action, even in instruction-based learning conditions. In a study of Melcher et al. (2013) one experimental group was presented with a contingent mapping between two responses and two non-incentive outcomes (tones) while the control group was presented with a non-contingent,

random R-O mapping. Subjects now performed a free choice response task over the course of 160 trials. This resulted in a stronger decrease in activation in the caudate in the contingent group compared to the random outcome group which has been interpreted as evidence for an increasing role of the caudate in early learning stages in the contingent group.

Additional to the networks mentioned above motor and sensory representations of outcomes seem to play a role in action selection and initiation as well (B. Hommel, 2013). Elsner et al. (2002) used Positron-Emission-Tomography (PET) to demonstrate that the perception of outcomes, triggered by a motor response, lead to reactivation of motor areas. If subjects were presented with a tone they learned to produce with a key press in a previous phase, it led to an increase in activation of the SMA and the Hippocampus. Similar results were found in an fMRI study by Melcher et al. (2008). Kühn, Seurinck, Fias and Waszak (2010) utilized fMRI to even demonstrate the reverse effect of increased activation in sensory areas after subjects executed a response associated with a consistent outcome.

2.3 Summary

Goal-directed behavior differs from mere habitual behavior by incorporating possible consequences of an action whereas habits are exclusively stimulus-driven. Anticipation of action consequences functions based on previously established response-outcome associations which can be even specific to distinct stimulus conditions. This has been proven in an abundance of studies, both, within the instrumental learning as well as the ideomotor research strand (Colwill & Rescorla, 1988, 1990; J. Hoffmann et al., 2007; Kunde, 2001b; Trapold, 1970; Ziessler et al., 2004a). Additionally, these kind of associations can be established in just a short amount of time (Ruge et al., 2012; Ruge & Wolfensteller, 2015; Wolfensteller & Ruge, 2011, 2014). According to both instrumental learning theory and ideomotor theory it is generally thought that goal-directed action is enabled on the basis of (differential) outcome integration via an S-O → O-R activation chain (Balleine & O'Doherty, 2010; Balleine & Ostlund, 2007; de Wit & Dickinson, 2009; Urcuioli, 2005).

However, both research fields differ substantially in the way of investigating outcome integration. In instrumental learning research most of the paradigms used involve trial-and-error learning utilizing incentive outcomes as feedback (de Wit et al., 2009; Delgado et al., 2005; Noonan et al., 2011; J. P. O'Doherty, 2011; Tanaka et al., 2008; Tricomi et al., 2004; Valentin et al., 2007). Those studies especially delivered evidence for the anterior caudate (J. P. O'Doherty, 2011; Tanaka et al., 2008; Tricomi et al., 2004) as well as the OFC (de Wit et

al., 2009; Noonan et al., 2011; J. P. O'Doherty, 2011) to play a key role in the acquisition of goal-directed behavior.

Ideomotor theory on the other hand assumes bidirectional associations between an action and its consequence. Ideomotor paradigms are characterized by non-incentive outcomes. Nevertheless neurophysiological studies in this field also showed evidence that the caudate and the OFC both seem to be involved in the formation of outcome integration processes (Melcher et al., 2013; Ruge & Wolfensteller, 2013). Furthermore, there are studies that suggest that additionally the SMA seems to be associated with goal-directed action selection (Elsner et al., 2002; Frimmel et al., 2016; Melcher et al., 2008; Melcher et al., 2013).

2.4 Methodological background

The two studies presented in this work were conducted utilizing both Electroencephalography (EEG) only as well as EEG and functional magnet resonance imaging (fMRI) in a combined study. In the following section both methods will be described briefly and contrasted against each other with respect to their features. Afterwards the method of co-registered EEG-fMRI will be introduced with a strong focus on how short comings of each individual method can be canceled out in a combination of both practices.

2.4.1 Electroencephalography (EEG)

The method of Electroencephalography (EEG) allows for the recording of modulations in electrical current directly on the skull surface of a test subject. These modulations in electrical activity originate in excitatory or inhibitory postsynaptic action potentials produced by cortical pyramid cells (Zschocke, 2002). The basic assumption is that active cognitive processes, related to a certain experimentally manipulated task, are represented by the firing of neurons or neuron clusters. The neural current is picked up by a network of EEG electrodes which are equally distributed in a cap and mostly laid out according to the so called 10-20 system (Jasper, 1958). The naming convention of electrodes is based on their position (frontal, central, parietal, occipital, temporal) and hemi sphericity (right hemisphere = even numbers, left hemisphere = odd numbers).

The method of Event Related Potentials (ERP) represents a frequently used approach of analyzing EEG data with respect to experimentally induced events. ERPs are changes in electrical activity which can occur prior, during, or after a sensory, motor, or even cognitive

incident (Rugg & Coles, 1995). However, event-related electrical currents are significantly weaker in terms of voltage compared to the noise in the raw EEG. Therefore segments belonging to the same kind of event are now averaged over a defined number of trials. The basic rationale is that event related ERP processes are identical over all trials while EEG noise is highly random and non-systematic. Averaging will cause reduction of noise while amplifying the true ERP signal correlated to the event in question (Jäncke, 2005). The extracted components can be measured in terms of amplitude or latency shift with regard to the triggering event. One of the major advantages of using ERPs is that they have a long history of research behind them and many components have been associated with distinct cognitive processes and even possible brain locations in terms of generation (Luck, 2005). The common view that ERPs are correlated on specific neural processes is based on two core assumptions: a) information processing in the brain is strictly serial with every component reflecting a certain sub process and b) these sub processes are mirrored in the peak amplitude of the component in question. These two assumptions, however, have more of a heuristic character as it has already been shown that human information processing is highly non-linear resulting in possible overlap of ERP components (Rüsseler & Münte, 2005). ERPs can be categorized into endogenous or exogenous components. Exogenous components are triggered by physical properties of an external stimulus (modality, intensity, duration, etc.). Endogenous components on the other hand are independent of physical stimulus properties but instead reflect higher cognitive brain processes (Jäncke, 2005). They usually occur after exogenous processes, usually in a range of 100 ms to 2000 ms with regard to event onset and are modulated by top-down processes like attention or memory retrieval.

One of the major advantages of EEG is its temporal resolution being in the range of milliseconds (ms). This feature allows EEG studies to even identify temporally fine grained processes which could not be revealed otherwise with a potential “online recording” capability of cognitive processes (Luck, 2005). However, this superb temporal resolution goes along with poor spatial resolution capability. It is not possible to locate the exact origin of a given ERP component, even if it is occurring only at specific electrodes. The number of electrodes (usually ranging between 32 and 128 electrode setups) simply does not allow for an even anywhere near satisfying localization procedure. This is not only due to the lack in sheer number of electrodes. Given the firing of a neuron cluster at a certain origin in the brain, it is highly possible for the nearest electrode to pick up most amount of the electrical current but in theory this current can be picked up by just any electrode on the scalp. Eventually, related to the prior point made, there is a substantial loss in information due to the fact that topological information from a three-dimensional object like the brain is trying to be mapped on a two-dimensional grid

of electrodes making an unambiguous inverse mathematical solution to this problem impossible (Luck, 2005).

2.4.2 Functional magnetic resonance imaging (fMRI)

FMRI has become one of the dominant methods in brain research (Huettel, Song, & McCarthy, 2009). Contrary to EEG, it uses an indirect measure of brain activity picking up changes of blood flow in brain tissue which is assumed to be a marker of neural activity. To this end fMRI scanners are equipped with various types of magnets. These include a superconducting multi tesla magnet (usually 1,5 up to 7 tesla) to generate the static field (b_0), smaller radiofrequency coils collecting the MR signal, as well as gradient coils to provide spatial information in the MR signal.

The fundamental parameter measured in fMRI studies is the so called Blood-Oxygen-Level-Dependent (BOLD, Menon et al., 1992; Ogawa, Lee, Kay, & Tank, 1990; Ogawa, Lee, Nayak, & Glynn, 1990; Ogawa et al., 1993; Ogawa et al., 1992). It is used based on the underlying assumption that cognitive load is correlated with increased blood flow as a result of providing nutrients such as oxygen and glucose to stressed brain tissues and allow them to function (*hemodynamic response*). As magnetic properties of oxygenated hemoglobin differ from deoxygenated hemoglobin this can be picked up by the fMRI radiofrequency coils. Oxygenated hemoglobin lacks unpaired electron pairs leaving it free of any magnetic momentum (*diamagnetic*). Deoxygenated hemoglobin on the other hand has unpaired electron pairs making it *paramagnetic* with a significant amount of magnetic momentum. This magnetic force induces an inhomogeneity in the scanners b_0 field which can be located by the head coil using specific magnet resonance (MR) pulse sequences. There are a number of sequences with a different tradeoff between contrast strength and acquisition speed. As it is impossible to simultaneously maximize both of these parameters, functional imaging techniques typically rely on sequences which emphasize speed of acquisition with the so called Echo planar imaging sequence (EPI, Mansfield & Maudsley, 1976) being used most frequently (Huettel et al., 2009). Increase in neural activity leads to an initial increase in oxygen consumption resulting in an increased cerebral blood flow after a delay of approximately two seconds. This causes an overcompensation of local oxygen consumption changing the balance of desoxyhemoglobin and oxyhemoglobin in favor of the later. These fundamental processes solely cause a change in the BOLD parameter which, due to the nature of its origin, is highly correlated with neural activity (Logothetis, Pauls, Augath, Trinath, & Oeltermann, 2001). Specific experimental designs involving only particular cognitive processes are designed to yield in increased blood flow only in brain regions specifically associated with the processing

of the experimental task. Hence, the BOLD signal is expected to be increased only in these regions. The signal itself has a very characteristic shape (Bandettini & Ungerleider, 2001; Boynton, Engel, Glover, & Heeger, 1996). The BOLD level increases approximately two seconds after increase in neural activity (i.e. triggered by the presentation of a stimulus). Prior to this main positive response there may be a short term decrease in signal strength below baseline (*initial dip*) most likely resulting from initial oxygen extraction before the later over-compensatory response. The BOLD level reaches its maximum after four to six seconds. Due to the combination of reduced blood flow and increased blood volume the BOLD amplitude then decreases below baseline over the course of seconds eight to eleven and takes another twenty to thirty seconds to recover from this *undershoot.*

Regarding advantages and disadvantages of fMRI it can be stated that it represents the exact complement to EEG in terms of its properties. FMRI is characterized by an immense spatial resolution capability in the range of mm. The exact resolution is defined by the predefined size of MR sampling units known as volume elements or *voxels.* Technically, it is even possible to decrease voxels even below 1 mm. However, there is always a trade-off as decreasing volume unit size goes along with a decreasing absolute amount of signal that can be detected within it. In contrast, the temporal resolution really is the limiting factor in fMRI research as it is naturally constrained by the inertia of the physiological changes that it seeks to measure. As described above the average BOLD signal phase prolongs over a time frame of over ten seconds.

2.4.3 Co-registered EEG-fMRI

EEG suffers from the so-called spatial inverse problem, whereby one cannot infer the spatial location of sources in the brain from electrical potentials on the scalp alone (Grech et al., 2008; Michel et al., 2004). Accordingly in fMRI, a map with regional activations does not necessarily permit inferences about the exact time and order in which these activations have occurred. This phenomenon is known as the *temporal inverse problem* (Logothetis, 2008). The main purpose and promise of combining EEG and fMRI lies in overcoming their individual disadvantages concerning temporal and spatial resolution. This however, is based on the underlying assumption that despite the differences in domain and signal content in both methods, that there exists a common neural basis that is described by both EEG activation patterns and fMRI BOLD response.

Data acquisition

In the early days of simultaneous EEG-fMRI, data acquisition was mostly performed via parallel recording where one subject was measured with the same experimental paradigm connected to the EEG and in the MR scanner on separate occasions. However, apart from introducing two completely different measurement environments, this kind of setup had to exclude situations where conducting the same experiment in succession led to memory or to learning effects or where some kind of unwanted habituation or sensitization was expected to occur. In recent years, concurrent sessions of simultaneous EEG-fMRI recording has become gold standard (Ullsperger & Debener, 2010). Nevertheless, this procedure casts several technical and safety related challenges which need to be accounted for.

In a concurrent EEG-fMRI scanning session EEG cap, electrodes, electrode leads, and even EEG signal amplifier (if placed inside the scanner room or even inside the scanner bore) are constantly exposed to the strong homogeneous static magnetic field of the scanner and, even more importantly, to the rapidly changing magnetic fields produced by gradient switching. Due to the nature of EEG signals, the electrodes used in EEG systems are made of electrically conducting materials, usually a Silver (Ag) or a Silver Chloride compound (AgCl). According to Faraday's law, changes in the magnetic field (induced by changes in the magnetic gradient, by head motion, by motion of electrode wires, or even by the heartbeat of the subject inside the scanner bore) induce electrical currents in the electrodes and electrode leads (Hill, Chiappa, Huang-Hellinger, & Jenkins, 1995; Lemieux, Allen, Franconi, Symms, & Fish, 1997). These electrical currents are picked up by the electrodes and result in artifacts that superimpose the spontaneous EEG with amplitudes of up to two orders of the underlying EEG signal and equally fast rates of change that are often three times faster than those of the EEG acquired (Allen, Josephs, & Turner, 2000; Krakow et al., 2000). Dealing with these technical changes will be discussed in more detail later in chapter 5.2.

Regarding safety, the most imminent risk for the subject is caused by radio frequency (RF) energy being deposited onto the electrodes during slice excitation. This RF energy could become a danger to the subject if coupled onto closed electrode cable loops. Those would dissipate the energy through heat emitted, eventually resulting in potential burning of subject body tissue. It is therefore of most importance when placing the subject inside the scanner bore to avoid creating closed cable loops at all cost (Dempsey & Condon, 2001; Dempsey, Condon, & Hadley, 2001). This effect is not limited only to cable loops. In fact, any cable can act as an RF antenna and therefore potentially cause severe burning. This effect is dependent on a variety of parameters, such as scanner field strength and frequency, cable length, cable shape, and orientation (Konings, Bartels, Smits, & Bakker, 2000; Nitz et al., 2001; Pictet, Meuli,

Wicky, & van der Klink, 2002). It is therefore important to verify that the setup used does not induce any heating. If these critical points are taken into consideration and are dealt with in a proper manner, then concurrent EEG-fMRI recording will not pose any risk to subjects.

Data analysis

Generally, data analysis methods for simultaneously acquired EEG-fMRI can be categorized into asymmetric and symmetric data integration methods (Huster et al., 2011). As the name implies, in asymmetric approaches information from both modalities are not used in an equally weighted manner. Instead, information of one modality is used to guide the analysis of the other. The most prominent of these approaches are fMRI-informed EEG and EEG-informed fMRI analysis. The method of fMRI-informed EEG is specifically designed to provide a solution to the spatial EEG inverse problem by guiding EEG source imaging using information obtained from fMRI (Babiloni et al., 2002; Babiloni et al., 2000; Heinze et al., 1994). To this end, the subjects head geometry and other important features of the brain are first estimated to build a forward model from which the path of currents from a prior simulated neural event to the scalp can be calculated. In order to derive spatiotemporal information from the EEG data using additional information from the fMRI, one possible method relies on inferring the number of potential EEG current dipoles from the pattern of activations in fMRI BOLD maps. These dipoles can then be seeded to specific brain locations correlating with local fMRI maxima. In a final step the time course of neural activity in each of these locations can be estimated (Hamalainen & Ilmoniemi, 1994). Recently there have also been alternative approaches in which so called distributed source models reconstruct neuro-electric activity at each point in a 3D grid of possible current sources. These statistical maps are further used to compute the source space by providing the probability of a particular region as a possible origin of the signal (Dale et al., 2000; Ou et al., 2010).

Being another prominent approach of asymmetric data integration, EEG-informed fMRI analysis considers associations of changes over time at a within-subject level. This however, is based on a strong assumption of a direct coupling between EEG and fMRI features (Ullsperger & Debener, 2010). For this method a distinct EEG parameter of interest is extracted over the time course of the experimental session. Potential features include ERP amplitudes (Debener, Ullsperger, Siegel, et al., 2005), ERP latencies (C. G. Benar et al., 2007), EEG synchronization and phase coherence (Jann et al., 2009; Mizuhara, Wang, Kobayashi, & Yamaguchi, 2005) or the power within specific EEG frequency bands (Scheeringa et al., 2009). Whatever parameters are used, the core assumption in any case is that feature fluctuations over time co-vary with fluctuations in the fMRI signal over the course of the experimental session. FMRI processing follows standard procedures up to first-level analysis. When setting

up the regressors for single subject statistics, however, these regressors are not derived from the timing of stimulus onsets convolved with a modeled hemodynamic response function (HRF) alone. Rather, these HRFs are additionally parameterized using the trial-wise extracted EEG parameter in a way that an increased potential amplitude in the single-trial EEG causes an up-scaling of the HRF for a given event and vice versa. Likewise to conventional fMRI analysis, the resulting level one beta estimates are then tested at the group level either against other conditions or against zero to reveal areas in the brain involved with putative significant co-variations between electrophysiological and hemodynamic responses. EEG-informed fMRI analysis relies on the assumption that underlying neural processes recorded by both modalities are at least partially correlated in a linear manner. No specific assumption is made about the spatial organization of activation patterns. This on the other hand implies that this method technically could yield activation in brain regions that are not necessarily the generators of the complementary EEG feature recorded at the scalp (Debener, Ullsperger, Siegel, et al., 2005; Minati et al., 2008). Eventually, one has to keep in mind that single trial EEG data can contain extremely high levels of noise which is increased by potential residual MR artifacts. Hence, one might have to rely on techniques that increase the signal-to-noise ratio of individual trials (C. J. James & Hesse, 2005; Onton, Westerfield, Townsend, & Makeig, 2006).

Symmetric data fusion methods of co-registered EEG-fMRI data avoid an a priori bias of either modality (Riera & Sumiyoshi, 2010; Rosa, Daunizeau, & Friston, 2010; Valdes-Sosa et al., 2009). Relevant methods all differ in assumptions as well as requirement of prior information. One exemplary method presented here relies on Independent component analysis (ICA) in which it is assumed that the observed data originate from a linear mixture of the underlying independent components identified. In this joint ICA approach (Calhoun, Adali, Pearlson, & Kiehl, 2006; Calhoun, Liu, & Adali, 2009) EEG and fMRI signal modalities are first processed separately. In the following, fMRI analysis statistical maps and EEG data of all subjects are merged into one single matrix which is then processed by a joint ICA. The ICA analysis results in a joint spatiotemporal decomposition with joint independent components corresponding to measured responses together with correlated clusters of active brain regions. Contrary to the unimodal approach in which only either temporally or spatially independent components can be identified, the multimodal approach delivers joint spatiotemporal independent components associated with electrophysiological responses, correlated with clusters of active regions (Eichele, Calhoun, et al., 2008; Eichele, Rachakonda, Brakedal, Eikeland, & Calhoun, 2011; Eichele, Rachakonda, & Calhoun, 2008; Moosmann, Eichele, Nordby, Hugdahl, & Calhoun, 2008). Multimodal approaches, although long established in computer science, are fairly new in its application to neuroscientific problems. Due to the

heterogeneity of these algorithms it might still be difficult to derive a tailored solution to a specific research question (Huster, Debener, Eichele, & Herrmann, 2012).

3 General objectives and research questions

Study 1 mainly served two distinct purposes. For one, the EEG data was generated to provide a blue print in terms of quality to be compared with the EEG data acquired in the latter co-registered EEG-fMRI study. The idea was to have a baseline of clean MR-artifact free EEG data which later could be utilized for comparison with the MR-artifact polluted EEG data. Comparing both data sets would allow to derive information about how much loss in terms of data quality and signal to noise ratio (SNR) to expect on both the averaged as well as on the single trial level. Second and more importantly the study was an exploratory study to answer the question on what kinds of EEG effects to expect in the first place. While fMRI correlates of both S-R learning as well as O-R outcome integration processes have already been examined using this paradigm (Ruge & Wolfensteller, 2015), there has been no information if those two processes are reflected in the EEG and if so which specific EEG parameters are modulated by them. This reasoning led to the formulation of the first central research question.

Research question 1: *Can ERP patterns associated with the initial learning of bi-directional R-O associations under forced choice conditions be identified?*

O-R outcome integration specific EEG correlates further served as regressors in a unified GLM (EEG-informed fMRI analysis) in the later co-registered EEG-fMRI study. This study as well utilized the exact same paradigm as study 1. By doing so it was secured that the data generated could be aligned to the data that was produced previously. Hence, epoched and single trial EEG data could be directly compared to the EEG data produced in study 1, both in terms of data quality as well as possible ERP correlates of S-R learning or O-R outcome integration. The overarching goal of study 2 was to assess various methods of EEG and fMRI data fusion and the results that could be produced by them with regards to outcome-response learning. The main focus lied in an asymmetric data fusion approach, namely EEG-informed fMRI analysis. The main reason for using this method was to make optimal use of the previously generated knowledge about learning-related ERP markers from study 1. If putative markers could be replicated in study 2 in terms of latency and amplitude one would have a stable and valid ERP foundation for disentangling within trial information of the fMRI BOLD signal.

By adding a specific ERP parameter (i.e. a marker of O-R outcome integration) as additional regressor into the fMRI analysis it is possible to extract a BOLD signal specifically correlated with that parameter cleansing it from variance related to other sub processes. One of the key questions in this study was if the EEG signal could help to differentiate between BOLD activation associated with processes related to response preparation or initiation and activation associated with post-response outcome integration processes.

Research question 2a: *Can a putative pre-response ERP marker of O-R learning predict distinct activation in the brain?*

Research question 2b: *Can a brain region be identified that is distinctly correlated with an ERP marker of post-response O-R outcome integration?*

One major advantage of the EEG-informed analysis is that it does not necessarily rely on single trial data since EEG information can be concatenated into event related epochs first before sent to the fMRI analysis. Hence, this method is likely to deliver interpretable results also in the case of not perfectly clean single trial EEG data. Further, in order to assess to which extent fMRI-EEG data could be used in a symmetric analysis approach, it was tested to generate independent components (IC) from single trial EEG data. If proven feasible, both EEG and fMRI data could be used in an exemplary Joint Independent Component Analysis (JICA).

4 Study 1 – Learning-related brain-electrical activity dynamics associated with the subsequent impact of learnt action-outcome associations

4.1 Introduction

Behavior is considered goal-directed when the actor integrates information about the anticipated outcome (Dickinson & Balleine, 1994). This requires the prior acquisition of knowledge about the current contingencies between behavioral responses (R) and their outcomes (O) under certain stimulus conditions (S). Knowledge about S-R-O contingencies can be acquired via trial and error where learning relies on evaluating retrospectively whether a behavioral response yielded a desirable outcome. However, acquisition can be accelerated by using explicit instructions which specify prospectively how to yield intended outcomes under the appropriate stimulus conditions (Doll, Jacobs, Sanfey, & Frank, 2009b; Ruge & Wolfensteller, 2016; Wolfensteller & Ruge, 2012). In two earlier functional MRI studies, Ruge and Wolfensteller have examined the neural activation dynamics associated with the rapid acquisition of novel S-R-O contingencies via explicit instruction procedures (Ruge & Wolfensteller, 2013, 2015). The present EEG study aimed to examine the neural activation dynamics with higher temporal precision not only across learning trials but also within learning trials. Within a trial, stimulus-locked and response-locked event-related potential (ERP) dynamics were inspected in order to identify both pre-response and post-response outcome integration processes. Importantly, while previous EEG studies have identified neural markers of outcome integration (Hughes, Desantis, & Waszak, 2013a, 2013b; Hughes & Waszak, 2011; Mifsud et al., 2016; Roussel, Hughes, & Waszak, 2013, 2014; Sanmiguel, Todd, & Schroger, 2013; Waszak, Cardoso-Leite, & Hughes, 2012; Waszak et al., 2005), there are virtually no data on the initial acquisition processes that enable outcome integration in the first place.

The experimental design was based on a modified version of the differential outcome paradigm (Colwill & Rescorla, 1985; Noonan et al., 2011; Shin et al., 2010; Trapold, 1970; Urcuioli, 2005) where differential auditory response outcomes were presented during instruction-based visuo-motor learning (Ruge & Wolfensteller, 2015; Wolfensteller & Ruge, 2014). Specifically, each distinct link between a visual stimulus and a manual response was predictably followed by a distinct auditory outcome. To obtain sufficient data for initial learning trials, each subject worked through ten different learning episodes each comprising a novel and unique set of visual stimuli and auditory outcomes. Successful acquisition of novel S-R-O contingencies enables goal-directed action selection through an S-O → O-R activation chain (Balleine & Ostlund, 2007; de Wit & Dickinson, 2009; Trapold, 1970; Urcuioli, 2005). According

to ideomotor theory, O-R associations in this chain are conceptualized as bidirectional associations between an action´s motor code and the ensuing sensory effects (Elsner & Hommel, 2001; Greenwald, 1970; Herwig et al., 2007; Prinz, 1997; Shin et al., 2010; Urcuioli, 2005; Waszak et al., 2012).

Behaviorally, the strength of acquired O-R associations can be analyzed via O-R compatibility effects measured in a subsequent outcome-priming test phase (Greenwald, 1970). In this test phase a previously learned outcome becomes an imperative stimulus that requires either the response which produced that outcome in the preceding learning phase (O-R compatible) or a response which produced a different outcome (O-R incompatible). Such compatibility effects, expressed in shortened response times and decreased error rates in compatible trials compared to incompatible trials, are commonly observed and indicate that the perception and even the anticipation of a previous outcome automatically activates the action it was previously produced by (Elsner & Hommel, 2001; Janczyk, Skirde, Weigelt, & Kunde, 2009; Keller & Koch, 2006; Kunde, 2001b; Pfister et al., 2010; Pfister & Kunde, 2013; Rieger, 2007) even after very short acquisition periods (Ruge et al., 2012; Wolfensteller & Ruge, 2011, 2014).

Besides such O-R compatibility effects another marker of outcome integration is the action-induced sensory attenuation effect which refers to the observation that stimuli that are predicted and triggered by human actions (i.e. action outcomes) are perceived to be attenuated compared to stimuli that are unpredicted or predicted by another stimulus, which might in fact be the reason why it is hard to tickle oneself (Blakemore, Wolpert, & Frith, 2000; Blakemore, Wolpert, & Frith, 1998). Action-induced sensory attenuation is a widespread phenomenon that has been assessed behaviorally (Bays & Wolpert, 2007a, 2007b; Miall & Wolpert, 1996) and neuro-physiologically using EEG or fMRI (Aliu, Houde, & Nagarajan, 2009; Martikainen, Kaneko, & Hari, 2005; McCarthy & Donchin, 1976; Schafer & Marcus, 1973).

Previous EEG studies have shown that action-triggered sounds as compared to externally triggered sounds elicited a reduced anterior negativity within and subsequent to the auditory N1 latency range, suggesting that cortical activity was attenuated for the action-triggered sounds due to anticipation of the forthcoming effect (Baess, Jacobsen, & Schroger, 2008; Hughes & Waszak, 2011; Mifsud et al., 2016). The present study examined whether such findings are reproducible in the instructed rapid learning paradigm employed in this study when action selection depends on antecedent stimuli. In particular, it aimed to examine how sensory attenuation ERP effects might evolve across the first few learning trials. More specifically, if the attenuation of the anterior negativity is indeed due to outcome anticipation based on acquired O-R associations, this attenuation effect should be increasing from early to

late in learning. Furthermore, the experimental design allowed for an additional exploration of possible learning-related ERP modulations associated with pre-response outcome integration processes triggered by the antecedent stimulus.

Importantly, however, a learning-related increase in outcome integration processes might potentially be confounded with a different process of perceptual learning due to the mere repetition of the O (auditory stimuli) alone which is known to be associated with an increased anterior negativity within a similar time-window as the sensory attenuation effect (Alain, Snyder, He, & Reinke, 2007; Atienza, Cantero, & Dominguez-Marin, 2002; Mishra, Rolle, & Gazzaley, 2015). Hence, due to their similar spatio-temporal distribution, a learning-related decrease of the anterior negativity associated with outcome integration processes might be over-shadowed by an increase of the anterior negativity associated with perceptual learning processes. The same possible confound applies to learning-related stimulus-locked ERP modulations. Perceptual learning processes due to repeated exposure to the S (visual stimuli) are known to be associated with an increase of the visual N1 component (Clark, Appelbaum, van den Berg, Mitroff, & Woldorff, 2015; Mishra et al., 2015), especially with non-familiar (Brem et al., 2005) and complex (Song et al., 2005) stimuli as used in this study. Again, these perceptual learning processes might overshadow ERP correlates of stimulus-triggered outcome anticipation processes or S-R learning processes which are of primary interest in this study. Note that learning-related ERP modulations due to repetition priming should be negligible in the present paradigm as the re-occurrence of a specific sound outcome or a specific visual stimulus is on average several seconds apart, which is too long for the typical ERP suppression effects to be observed (Budd, Barry, Gordon, Rennie, & Michie, 1998; Henson, Rylands, Ross, Vuilleumeir, & Rugg, 2004; Naatanen & Picton, 1987).

Fortunately, there is a way to disentangle these inherently confounded processes by using behavioral markers. Specifically, outcome priming tests after each S-R-O learning episode were implemented in order to determine O-R association strength via the O-R compatibility effect as described above. Learning-related ERP modulations that are related to outcome integration processes rather than perceptual learning should be correlated with independently measured behavioral markers of O-R association strength. Similarly, learning-related ERP modulations related to the early instruction-based formation of novel S-R links should be correlated with performance accuracy following explicit S-R instruction.

4.2 Methods

Subjects

Thirty-five subjects participated in this study. Six of them were excluded due to error rates greater than 25% in the first unguided implementation trial (SRO repetition 4). High error rates in this particular trial suggest that those subjects proceeded not according to instructions resulting in an undesired trial-and-error effect. The mean age of the resulting 29 subjects was 24.1 years, ranging from 18 to 33 years with 18 being female and eleven male. All subjects were treated in accordance with the Declaration of Helsinki and gave written informed consent in advance of taking part in the experiment and were paid €8 per hour or received course credit.

Experimental procedure

S-R-O acquisition phase

Instructions were delivered via a 'guided implementation' procedure in which the instruction is embedded within the first three behavioral implementation trials that also comprised the presentation of differential outcomes following correct responses (see Figure 3).

The guided implementation phase comprised twelve correct trials (three repetitions of four different stimuli, responses and outcomes). Stimuli were four abstract visual patterns that differed for each block. In the acquisition phase each trial started with the presentation of a visual stimulus *S* in the center of the screen for 500ms. Following 250 ms after *S* onset an additional instruction stimulus (*IS*) was displayed which remained on screen until a response was made or until timeout after 1750 ms. The *IS* was a yellow square highlighting one of four constantly displayed empty boxes. Manual responses (left middle finger, left index finger, right index finger, and right middle finger) were mapped in a spatially compatible manner to the *IS* position. After a 150 ms gap, correct responses were followed by a naturalistic sound effect which lasted for 500 ms, differing for each *S* (differential outcome). This guided implementation phase was followed by an unguided implementation phase where the *IS* was omitted and comprised another 20 correct trials (i.e., five repetitions of the four distinct S-R-O triples). Thus, starting from the fourth S-R-O repetition (SRO-rep), the correct response had to be retrieved from memory as it was not indicated by the IS anymore. In case of erroneous responses, error feedback was displayed and the trial was immediately repeated. The experiment comprised ten different S-R-O learning blocks each with novel visual stimuli and novel outcome sounds.

The inter-trial interval (ITI) was randomly selected from a geometric distribution including interval durations of 800 ms (24 trials per block), 2350 ms (five trials per block), and 4700 ms (3 trials per block). Analyses of learning-related changes in behavior and brain activation were based on correct trials ranging from SRO-rep 1 to SRO-rep 8.

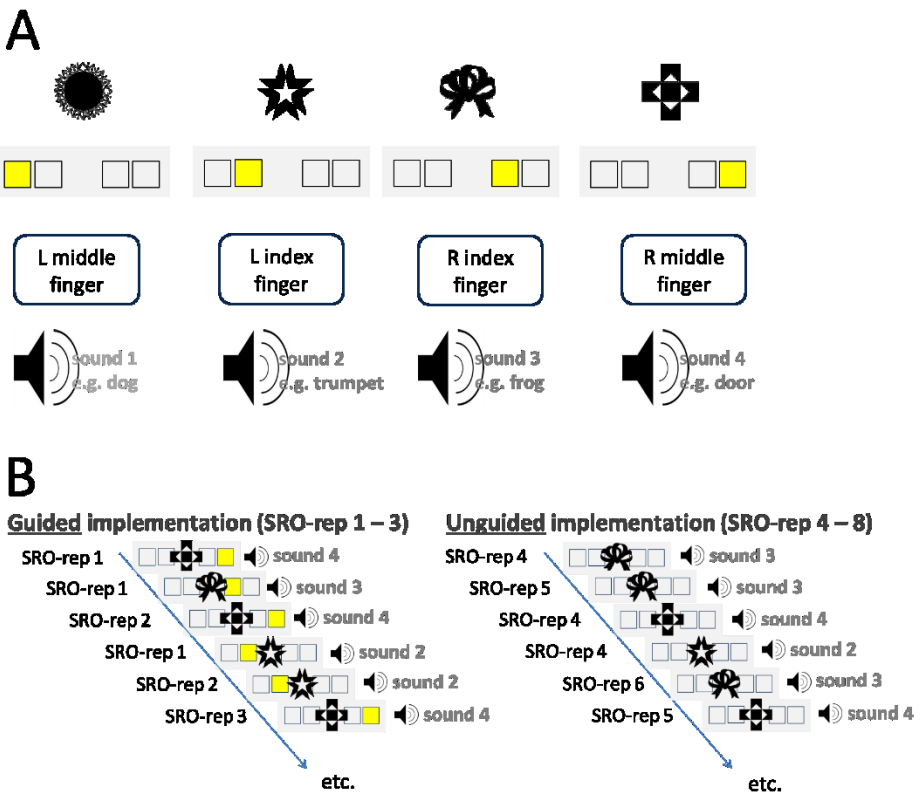

Figure 3: Schematic representation of the S-R-O acquisition phase for an exemplary set of visual antecedent stimuli and auditory differential outcomes. Over the course of the experiment subjects had to learn ten such S-R-O mappings each comprising a novel and distinct set of four visual stimuli and four auditory outcomes. (A) Exemplary mapping between visual stimuli, instruction cues, responses and auditory outcomes. (B) Novel S-R-O mappings were learned in the 'guided implementation phase' via explicit instruction cues presented for the first three repetitions of each distinct S-R-O triple (SRO-rep 1 – 3). Afterwards, in the 'unguided implementation phase' (SRO-rep 4 – 8) instruction cues were omitted and the correct response had to be retrieved from memory.

O-R test phase

Each of the ten S-R-O learning blocks was followed by a test phase probing the strength of the previously acquired O-R associations. Subjects were now required to react to the previous effect sounds of the acquisition phase with one out of the four responses (see Figure 4). The response keys were the same as during the preceding S-R-O learning phase. Two

outcome sounds were mapped to the response that produced that sound in the preceding phase (compatible trials) whereas the two remaining outcome sounds were mapped to responses that had produced another sound before (incompatible trials). According to ideomotor theory, previously learnt O-R associations should prime the correct response in compatible trials but the incorrect response in incompatible trials. As in the preceding S-R-O acquisition phase, also the test phase was divided into twelve guided and 20 unguided trials. The instruction stimuli (IS) were now the letters 'D', 'F', 'J', 'K' presented centrally on the screen and mapped onto left middle finger, left index finger, right index finger, and right middle finger, respectively. A trial started with a fixation cross displayed for 500 ms followed by the sound lasting 500 ms. In the guided phase the IS was presented 150 ms after sound onset and lasted until the response or timeout after 1500 ms. Accuracy feedback was displayed for 650 ms indicating correct, wrong, or too slow responses. The ITI distribution was the same as in the S-R-O learning phase.

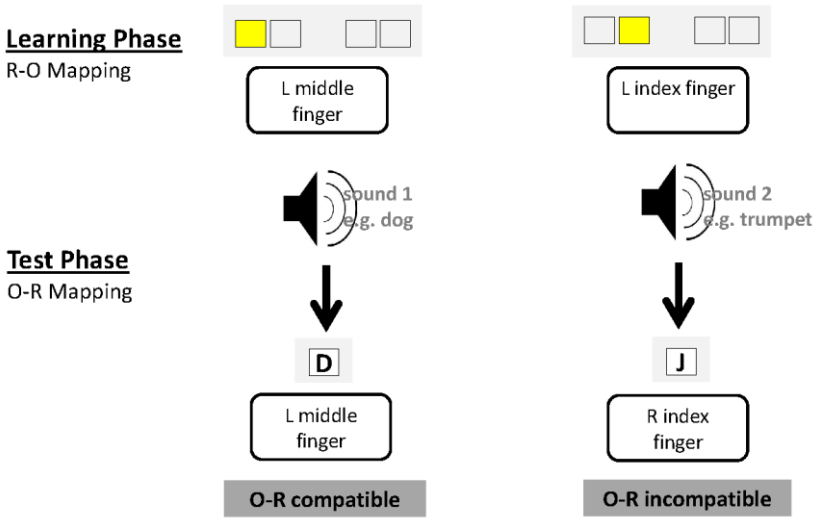

Figure 4: Schematic representation of the O-R test phase. The four sound stimuli that had been produced by correct responses to the antecedent visual stimulus in the learning phase serve as antecedent stimuli in the test phase. The required response to these stimuli could be the same (compatible) or different (incompatible) regarding the response that produced the sound before. The correct response was indicated by instruction cues (letter D, F, J, K) in the "guided implementation phase" (SRO repetitions 1 – 3). As in the learning phase, starting from SRO repetition 4 up to 8 the correct response had to be retrieved from memory. Test phase data were exclusively used to compute the size of the behavioral O-R compatibility effect, which was later correlated with EEG activity during the preceding S-R-O learning phase in a linear regression.

EEG recording

EEG was recorded using 64 sintered AG/AgCl electrodes which were distributed on the electrode cap according to the 10-20 System (Klem, Luders, Jasper, & Elger, 1999), using the AFz electrode as reference. Impedance at each electrode was kept below 5kΩ. Two additional electrodes were used to identify eye blinks and saccades. One was placed under the lower eye lid and the other 1 cm lateral to the right eye. EEG data were digitized using a 64-channel amplifier (www.brainproducts.com) with a sampling rate of 1000 Hz.

EEG Preprocessing

All EEG data was imported and preprocessed using Brain Vision Analyzer 2.0 (www.brainproducts.com). Continuous EEG data were down-sampled to 250 Hz and band pass filtered from 0.2 – 30 Hz. All EEG Channels except horizontal and vertical EOG channel contributed to an average-based new reference. Ocular correction was performed using the regression based implementation by Gratton and Coles (Gratton, Coles, & Donchin, 1983). Electrode-specific artifact rejection sorted out segments exhibiting a gradient in electrical activity greater than 50 µV/ms as well as segments exhibiting absolute differences of more than 200 µV within a 200 ms interval. EEG data were segmented time-locked to both the response and the stimulus, respectively. Response-locked epochs contained the manual response ranging from 750 ms pre-response to 700 ms post-response. Stimulus-locked epochs contained the stimulus *S* ranging from 250 ms pre-stimulus to 1500 ms post-stimulus. Note that a baseline-correction for the segmented EEG data was not applied.

Analysis of performance data

For statistical evaluation of the behavioral performance data the R environment (R Core Team, 2012) and *lme4* (Bates, 2012) were used to compute two separate linear mixed-effect models for mean response times (RTs) as well as mean error rates with the factor SRO repetition (SRO-rep 1 to SRO-rep 8) being fixed effect and the factor subject being random effect. Linear mixed-effects models were chosen since they provide post-hoc tests regarding individual SRO repetitions which are, in contrast to those of the general linear model, corrected for dependencies within the data points of the response variable (Bretz, Hothorn, & Westfall, 2011). Additional post-hoc significance tests were realized and Bonferroni-corrected for multiple comparisons with the Multcomp package (Hothorn, Bretz, & Westfall, 2008). This package provides *p* values for post-hoc comparisons between factor levels tested on a z

distribution. Deviance of the model was tested for significance against the deviance of the so called null model. This hypothetical model only contains the intercept and therefore has no explanatory power whatsoever. This procedure is equivalent to an omnibus test of significance in a conventional GLM.

ERP main analysis

Response-locked and stimulus-locked epochs of EEG activity were averaged for each SRO repetition containing 40 correct trials per SRO repetition excluding trials rejected by artifact rejection. The analysis of rapid learning dynamics associated with initial instruction encoding processes compared ERPs between SRO-rep 1 and SRO-rep 3. The analysis of slower learning dynamics associated with more gradual changes in association strength compared ERPs between early SRO repetitions (collapsed across SRO-rep 2 and 3, further called SRO-rep 23) and late SRO repetitions (collapsed across SRO-rep 7 and 8, further called SRO-rep 78). For this latter analysis SRO-rep 1 was excluded to avoid a dominant contribution of initial instruction encoding.

To deal with the expected spatiotemporal overlap of ERP modulations due to the learning processes of interest (R-O and S-R) with purely perceptual learning processes of no interest I assessed correlations between learning-related ERP modulations and specific behavioral markers. Thereby, I aimed to disentangle three distinct sub-processes. First, learning-related changes of post-response O-R integration can be revealed by correlating the behavioral index of O-R strength (O-R compatibility effect) with response-locked ERP amplitude changes from SRO-rep 23 to SRO-rep 78 and with ERP amplitude changes from SRO-rep 1 to SRO-rep 3. Second, learning-related changes of pre-response stimulus-based outcome integration processes can be revealed by correlating the behavioral index of O-R strength (O-R compatibility effect) with stimulus-locked ERP amplitude changes from SRO-rep 23 to SRO-rep 78 and with changes from SRO-rep 1 to SRO-rep 3. Third, I aimed to identify ERP correlates of initial instructed S-R learning by correlating amplitude differences in stimulus-locked and response-locked ERPs between SRO-rep 1 and SRO-rep 3 with the subsequent error rate at SRO-rep 4 (assuming that good S-R learners should achieve low error rates).

Correlational relationships between ERPs and behavioral indices of interest (O-R compatibility effect and error rate at SRO-rep 4) were determined based on multiple linear regression models. These multiple regressions included additional nuisance regressors to control for possible confounds assessed by additional behavioral markers, as detailed next.

Importantly, inter-individual differences in the size of the O-R compatibility effect might in part not only reflect differences in acquired O-R association strength but additionally also differences in dealing with response competition in incompatible trials as a result of previously acquired O-R associations. Similarly, inter-individual differences in learning-related changes from SRO-rep 23 to SRO-rep 78 might in part also reflect inter-individual differences in dealing with increasing response competition between multiple response options from the guided learning phase (competition low) to the unguided phase (competition high) as might be indicated by increased error rates and relatively increased response times. In order to control for this, differences in error rates and response times were included as two additional learning-related predictors in the linear regression. Thereby, possible covariance components, associated with response competition during the learning phase, that might drive the correlation with the O-R compatibility effect rather than inter-individual differences in O-R association strength, could be regressed out.

The experimental approach was different from the typical sensory attenuation procedure which compares ERPs elicited by internally vs. externally triggered sounds and does not focus on learning-related dynamics of the identified attenuation effects. Hence, the analysis of ERPs was divided into a hypothesis-driven part focusing on known effects reported in earlier sensory attenuation studies and an exploratory part to identify additional effects that might be specific for the present paradigm.

Literature-based hypothesis-driven ERP analysis

The hypothesis-driven analysis was performed for the expected post-response attenuation of the anterior negativity. The previous literature assessing auditory sensory attenuation effects suggests maximal effects at FCz or Cz electrodes (Baess et al., 2008; Baess, Widmann, Roye, Schroger, & Jacobsen, 2009; Hughes & Waszak, 2011; Lange, 2011; Sanmiguel et al., 2013). The reported time when sensory attenuation reached its maximum was somewhat variable across studies but most studies suggest that the effect reaches its maximum clearly after the N1 peak. This study employed more complex sounds than previous studies with longer duration (500ms) which implies prolonged sensory analysis of these sounds. Hence, ERP effects associated with sensory attenuation (and perceptual learning for that matter) might be prolonged and/or delayed compared to previous studies. Due to this temporal fuzziness I searched for significant effects in a time window between the mean post-response auditory N1 peak (260 ms, i.e., 110 ms after sound onset) and the offset of the auditory outcome (650 ms). Note, that I explicitly searched for maximal ERP differences

pointing in both directions due to the already mentioned possible overlap of the sensory attenuation effect and the antagonistic perceptual learning effect. Statistical significance was determined via paired t-tests for the averaged signal within a +/- 24 ms time window around the time point in which the learning-related modulation of electrical activity was maximal. I then determined the correlation between this amplitude difference and the behavioral O-R compatibility effect regardless of the direction of the difference identified (e.g., either in the direction of sensory attenuation or opposite to it) in order to clearly relate the observed ERP difference to O-R integration processes. Additionally, I performed an analysis covering the whole post-response time range (260 ms to 650 ms) to determine the maximal correlation between learning-related modulations of electrical activity and the behavioral O-R compatibility effect not biased by pre-selecting time windows exhibiting maximal ERP differences.

Exploratory ERP analysis

As just described, for the analysis of post-response auditory sensory attenuation effects I could exploit prior knowledge about the likely spatio-temporal profile of the expected learning-related ERP modulations. To reveal possible additional ERP modulations specific to the present paradigm I pursued a more exploratory analysis style not relying on prior knowledge about the specific spatiotemporal nature of ERP effects. To protect against false positive results I exploited the relatively large sample size and implemented a multi-step analysis procedure with a split-half replication approach at its core based on two subsamples of 14 (Sample 1) and 15 subjects (Sample 2). Subjects were randomly assigned to either sample 1 or sample 2. Thereby I avoided circular analysis problems that arise when using the same data set for selection and selective analysis, potentially yielding distorted descriptive statistics and invalid statistical interference (Kriegeskorte, Simmons, Bellgowan, & Baker, 2009). Furthermore this allowed us to test the reliability of the identified activation effects. I first used sample 1 to determine spatiotemporal maxima regarding the difference between SRO-rep 23 and 78 and between SRO-rep 1 and 3, respectively. In order to reduce data complexity I created averaged topographical maps for a series of 48 ms time windows covering the entire ERP segment and identified spatiotemporal local maxima regarding the absolute value of the amplitude differences of interest (either SRO-rep 23-78 or SRO-rep 1-3). Note, that within a time window several electrodes could be identified. In order to define the time window of maximal amplitude differences at each of the identified electrodes more precisely, I determined the maximum amplitude difference within the identified 48 ms time window and defined a final time window of interest within a +/- 24 ms range around this peak. Note that this procedure could result in exactly the same time window for different electrodes (e.g., as depicted in Figure

4). Both stimulus-locked and response-locked ERPs were measured as the mean voltage amplitude within each time window and electrode, which were selected as described above.

Following this initial step of selecting the spatiotemporal regions of interest (ROIs) based on sample 1 alone, I then proceeded with the statistical evaluation of these regions of interest. Specifically, I performed paired t-tests of amplitude differences between SRO repetitions separately for both sample 1 (two-tailed) and sample 2 (one-tailed). Importantly, a certain amplitude difference was only accepted as statistically significant if it passed significance tests in both sub-samples. In this case I applied simple t-tests (as opposed to linear mixed-effect models applied in other place in this study) as I performed only one test per dependent variable.

In a final step I used the complete dataset to perform correlation analyses between amplitude differences that passed the split-half significance test and the behavioral indices of interest (O-R compatibility effect or error rate at SRO-rep 4). Pre-selecting spatiotemporal regions of interest based on amplitude differences alone would not bias correlations with entirely independently determined behavioral indices.

Supplementary ERP control analyses

To further exclude the possibility that ERP amplitude differences may reflect confounds related to the presence vs. absence of visual instruction cues rather than early vs. late learning processes I performed an additional control analysis where I separately assessed the abrupt transition from guided to unguided learning trials (SRO-rep 23 vs. SRO-rep 45) and learning dynamics across *unguided* learning trials only (SRO-rep 45 vs. SRO-rep 78). I used the exact same time windows and electrodes as in the main analysis which yielded significant correlations between the ERP difference between SRO-rep 23 vs. SRO-rep 78 and the behavioral marker of O-R association strength. If I could replicate overall learning effects (SRO-rep 23 vs. SRO-rep 78) also for unguided learning trials (SRO-rep 45 vs. SRO-rep 78) this would clearly rule out any possible confound introduced by contrasting guided and unguided learning conditions. By contrast, if the overall learning effects (SRO-rep 23 vs. SRO-rep 78) were primarily replicated for the transition from guided to unguided trials (SRO-rep 23 vs. SRO-rep 45) this would imply a more cautious interpretation of the original results. Specifically, such a pattern of results would either indicate faster R-O learning dynamics primarily reflected by ERP modulations between SRO-rep 23 vs. SRO-rep 45 or it might reflect a confound related to the transition from guided to unguided learning trials.

To conduct proper post-hoc tests in the context of repeated measurements, I set up a linear mixed-effect model using R (R Core Team, 2012) and *lme4* (Bates, 2012) for mean electrical activity with the factor SRO repetition (SRO-reps 23, 45, 78) being fixed effect and the factor subject being random effect. Differences in mean ERP amplitudes were assessed based on this linear mixed-effect model. Additional post-hoc significance tests were realized and Bonferroni-corrected for multiple comparisons with the Multcomp package (Hothorn et al., 2008). I then again correlated ERP differences with the O-R compatibility effect in a linear regression. Since the correlation effects were expected to be in the same direction as the original correlations, significance tests were one-tailed. As for the main analysis I also included differences in response time and accuracy as additional regressors to control for nuisance variance components.

4.3 Results

Behavioral results

S-R-O learning phase

Figure 5Figure 5A displays the learning curve over all SRO repetitions. On the descriptive level, increasing SRO repetitions were associated with a drop of response times (RT) paralleled by an increase in error rates. The guided learning phase was characterized by a rapid gain in performance speed from SRO-rep 1 to SRO-rep 3. At SRO-rep 4 RT briefly increased due to the transition to the unguided phase before RT continued to decrease gradually. Unsurprisingly, error rates were low during the guided phase, jumped up at SRO-rep 4 (i.e. the first unguided trials) before gradually decreasing again across the unguided phase (see Figure 5B). The analysis resulted in highly significant effects in the factor *SRO repetition* within the saturated model compared to the null model for both error rates [$F(7,196) = 15.35$, $p < .001$] as well as RTs [$F(7,196) = 90.94$, $p < .001$]. The response time drop of 125 ms within the guided implementation phase (from 759 ms in SRO-rep 1 down to 633 ms in SRO-rep 3) exceeded significance threshold applying post-hoc Tukey-test corrected for multiple comparisons [$p < .001$]. The RT decrease from SRO-rep 1 to SRO-rep 3 predicted smaller error rates in SRO-rep 4 [$r(27) = -0.38$, $p < .04$] suggesting that the RT decrease during the guided instruction phase is an index of S-R associations formation and usage (see Figure 5C). In order to statistically assess RT differences on the slower timescale I collapsed SRO repetitions 2 and 3 (SRO-rep 23) as well as 7 and 8 (SRO-rep 78) to compute another post-

hoc Tukey-test corrected for multiple comparisons which yielded a significant result [$p < .001$]. Regarding error rates, a post-hoc Tukey-test revealed a highly significant increase in error rates from 2% at SRO-rep 1 to 13% at SRO-rep 4 [$p < .001$, Bonferroni-corrected for multiple comparisons]. This indicates the transition from the guided to the unguided implementation phase in which responses now had to be selected according to memorized S-R associations from the preceding three guided trials. However, given a chance error rate level of 75%, a mean error rate of 13% at SRO-rep 4 suggests that the newly instructed S-R mappings were well memorized. Following this initial error rate increase it than decreased again down to 6% at SRO-rep 8 [$p < .001$].

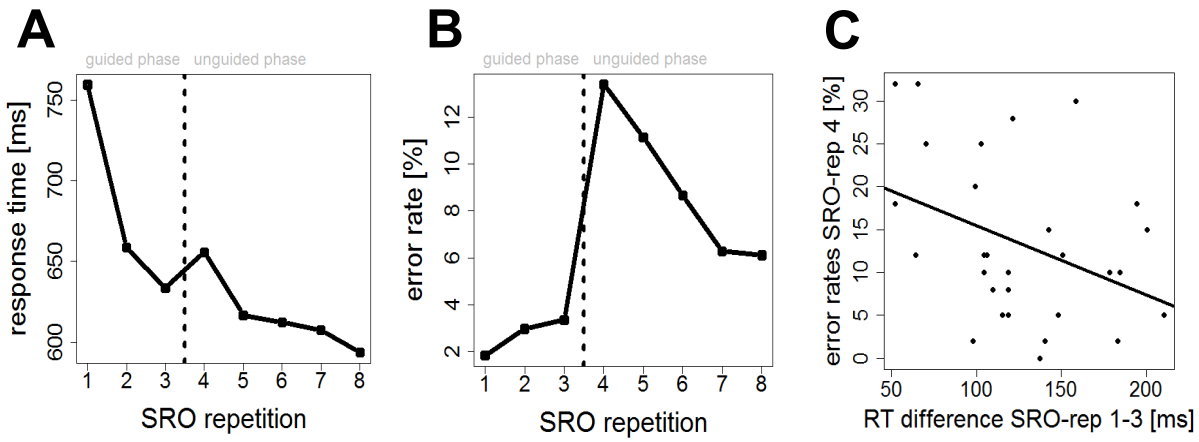

Figure 5: Behavioral data from the S-R-O acquisition phase with mean (A) response times (RT) and (B) mean error rates (%) throughout the course of all eight SRO repetitions. (C) Correlation between the difference in response times between SRO-rep 1 and SRO-rep 3 and error rates in SRO-rep 4.

O-R test phase

I computed two separate linear mixed-effect models for accuracy und response time with factors compatibility and SRO repetition as fixed effect and variance over all trials within each subject being random effect. The analysis resulted in highly significant O-R compatibility effects for both error rates [$F(1,224) = 34.03$, $p < .001$] with an average of 11% error trials in the compatible condition and 16% error trials in the incompatible condition as well as response times [$F(1,224) = 18.33$, $p < .001$] with an average of 553 ms in the compatible condition and 574 ms in the incompatible condition. Additionally, there was a significant interaction effect between SRO repetition and compatibility in error rates [$F(1,224) = 3.19$, $p = .003$, see Figure 6A]. Regarding response times no such interaction effect between these two factors was found [$F(1,224) = .66$, $p = .704$, see Figure 6B]. The subject-wise behavioral index of O-R encoding strength which was later used for correlation with ERP difference measures was defined as the individual O-R compatibility effect in RT, providing a more consistent measure over all SRO repetitions compared to the compatibility effect in error rates.

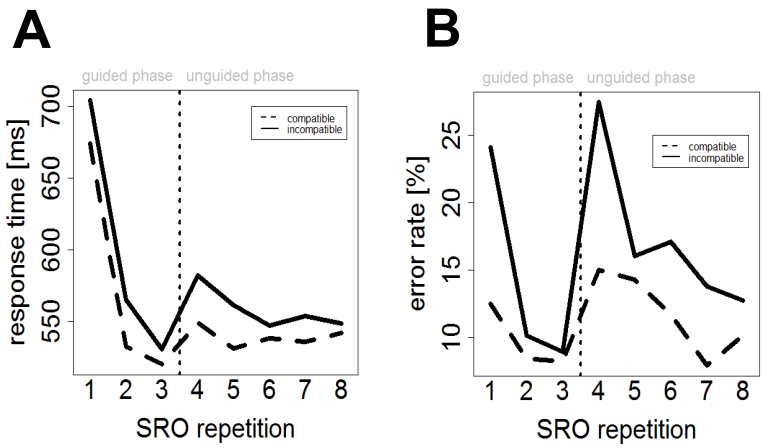

Figure 6: Behavioral data from the S-R-O test phase (A) mean response times (RT) and (B) mean error rates (%) throughout the course of all eight SRO repetitions.

EEG results

Response-locked ERPs

Literature-based spatio-temporal ROIs: Learning-related amplitude modulations on the slower timescale

I expected effects of sensory attenuation in a time window following the auditory N1 peak at anterior electrodes. Typically, attenuation effects are evaluated for the electrode exhibiting the largest overall N1 amplitude (typically Cz or FCz). I focused on the analysis on FCz which exhibited the maximal overall N1 amplitude (see Figre 7 and

Table 1). While the N1 component itself peaked at 260 ms (110 ms past onset of auditory outcome) the maximum amplitude difference between SRO-rep 23 and 78 was found at 328 ms (178 ms past onset of auditory outcome). Note that this effect was due to an *increased* learning-related negativity which suggests a dominant contribution of perceptual learning. However, in a slightly later, yet overlapping time window between 336 ms to 384 ms (186 ms to 234 ms past onset of auditory outcome) I observed a significant *negative* correlation between amplitude difference and the O-R compatibility effect (i.e., the smaller the increase in negativity the bigger the compatibility effect). This strongly suggests that a relative attenuation of the anterior negativity associated with increasing outcome integration is embedded within an overall mean increase in negativity associated with perceptual learning.

Table 1: Statistical analysis of the response-locked ERP difference SRO-rep 23-78 at electrode FCz.

Time window	**Electrode *FCz***		
	Paired t-test for ERP difference	**Correlation with O-R compatibility effect in Linear Regression**	
		Overall regression model	*predictor O-R compatibility*
SRO-rep 23 – 78 maximal (304 – 352 ms)	$t(28) = 3.38$, $p = .002$	$R^2_{adj.} = .07$, $F(3, 25) = 1.73$, $p = .185$, *n.s.*	$b = -.012$, $t(25) = -2.12$, $p = .044$
Correlation with O-R compatibility maximal (336 – 384 ms)	$t(28) = 2.4$, $p = .023$	$R^2_{adj.} = .24$, $F(3, 25) = 3.89$, $p = .021$	$b = -.016$, $t(25) = -3.11$, $p = .005$

Since at SRO-rep 23 response selection was guided by an instruction stimulus, whereas at SRO-rep 78 it was not, I conducted an additional control analysis which included collapsed unguided SRO repetitions 4 and 5 (SRO-rep 45). Thereby I could quantify the extent to which the original finding was due to the transition from the guided into the unguided implementation phase. I found a significant main effect for the factor SRO repetition including the three levels SRO-rep23, SRO-rep 45, and SRO-rep 78 for both time windows identified before at electrode FCz ([$F(4,112) = 15.62$, $p(F) < .001$] for the early time window, [$F(4,112) = 12.3$, $p(F) < .001$] for the later time window). Post-hoc test for the relevant ERP differences (SRO-rep 23 vs. SRO-rep 45 and SRO-rep 45 vs. SRO-rep 78) and the corresponding correlation with the O-R compatibility effect are listed in Table 2. Most importantly, the results of this analysis suggest that correlations with the O-R compatibility effect were primarily driven by the transition from SRO-rep 23 to SRO-rep 45. This indicates either faster R-O learning dynamics primarily reflected by ERP modulations between SRO-rep 23 vs. SRO-rep 45. Alternatively, it might reflect possible confounds related to the transition from guided to unguided learning trials.

Table 2: Statistical analysis at electrode FCz for the response-locked ERP differences SRO-rep 23-45 and SRO-rep 45-78.

Electrode and time window	SRO-rep 23 vs. SRO-rep 45			SRO-rep 45 vs. SRO-rep 78		
	Post Hoc test for ERP difference	**Correlation with O-R compatibility effect in Linear Regression**		**Post Hoc test for ERP difference**	**Correlation with O-R compatibility effect in Linear Regression**	
		Overall regression model	*predictor O-R compatibility*		*Overall regression model*	*predictor O-R compatibility*
304 – 352 ms (from main analysis)	z = -2.04, p = .075,	R^2_{adj} = .33, F(3, 25) = 5.54, p = .005	b = -.014, t(25) = -3.17, p = .002	z = -5.53, p < .001	$R^2_{adj.}$ = .05, F(3, 25) = 1.54, p = .228, *n.s.*	b = .001, t(25) = .15, p = .558, *n.s.*
336 – 384 ms (from main analysis)	z = -2.46, p < .027	R^2_{adj} = .32, F(3, 25) = 5.31, p = .006	b = -.013, t(25) = -2.93, p = .004	z = 4.96, p < .001	$R^2_{adj.}$ = .02, F(3, 25) = 1.17, p = .34, *n.s.*	b = -.002, t(25) = -.5, p = .312, *n.s.*

Literature-based spatio-temporal ROIs: Learning-related amplitude modulations on the rapid timescale

To assess whether sensory attenuation ERP effects would already be expressed by learning-related changes on the rapid timescale I compared ERPs for SRO-rep 1 and SRO-rep 3. I identified a time window in which the difference between SRO-rep 1 and 3 was significant for the FCz electrode. However, this difference was not associated with a significant correlation with the O-R compatibility effect (see Table 3). I also failed to identify any other time window were the correlation effect reached significance.

Table 3: Statistical analysis of the response-locked ERP difference SRO-rep 1-3 at electrode FCz.

Time window	Electrode *FCz*		
	Paired t-test for ERP difference	**Correlation with O-R compatibility effect in Linear Regression**	
		Overall regression model	predictor O-R compatibility
SRO-rep 1 – 3 maximal (554 – 602 ms)	t(28) = 5.99, p < .001	$R^2_{adj.}$ =.05, F(3, 25) = .24, p = .745, *n.s.*	b = -.011, t(25) = -.01, p = .945, *n.s.*

Spatio-temporal ROIs determined via exploratory split-half analysis procedure: Learning-related amplitude modulations on the slower timescale

Regarding amplitude modulations in response-locked potentials associated with learning across SRO-rep 23 and SRO-rep 78, I identified three spatiotemporal ROIs that survived the statistical evaluation. The complete statistical evaluation is summarized in Table 4. Specifically, I observed an increased negativity from SRO-rep 23 to SRO-rep 78 at electrode F1 in a time window (192 ms – 240 ms) slightly prior to the auditory N1 peak, and another increased negativity at FCz in a later time window (628 ms – 676 ms). Additionally, I found a decreased negativity at Oz in a time window between 284 ms and 332 ms. One time window identified in sample 1 was omitted from further analysis since significance could not be replicated in sample 2. Only the early ERP amplitude difference at F1 correlated significantly with the O-R compatibility effect, as depicted in Figure 7. Additionally, I took the time window identified in the literature-based ROI analysis at electrode FCz (304 ms – 352 ms) and re-applied it also to F1 in order to assess whether the effects observed at FCz would spread to the nearby F1 electrode. This resulted in both a significant effect for the amplitude difference between SRO-rep 23 and 78 as well as a significant correlation with the RT compatibility effect (but clearly weaker than the one originally found for FCz).

Table 4: Statistical analysis of spatiotemporal ROIs identified for the response-locked ERP difference SRO-rep 23-78.

Time window, electrode	**SRO-rep 23 – 78 Sample 1**	**SRO-rep 23 – 78 Sample 2**	**Prediction of amplitude difference by O-R compatibility effect (complete dataset)**	
			Overall regression model	*Predictor O-R compatibility*
192 – 240 ms, F1	$t(13) = 2.94$, $p = .014$	$t(14) = 5.66$, $p < .001$	$R^2_{adj.} = .28$, $F(3, 25) = 4.69$, $p = .018$	$b = -.012$, $t(25) = -3.24$, $p = .003$
304 – 352 ms, F1	$t(13) = 3.2$, $p = .007$	$t(14) = 4.62$, $p < .001$	$R^2_{adj.} = .21$, $F(3, 25) = 3.54$, $p = .03$	$b = -.011$, $t(25) = -2.37$, $p = .026$
284 – 332 ms, Oz	$t(13) = -2.4$, $p = .003$	$t(14) = -5.81$, $p < .001$	$R^2_{adj.} = .01$, $F(3, 25) = 0.15$, $p = .931$, *n.s.*	$b = .001$, $t(25) = 0.18$, $p = .858$, *n.s*
628 – 676 ms, FCz	$t(13) = 3.31$, $p = .006$	$t(14) = 3.53$, $p = .001$	$R^2_{adj.} = .1$, $F(3, 25) = 0.15$, $p = .929$, *n.s.*	$b = .002$, $t(25) = 0.32$, $p = .749$, *n.s*

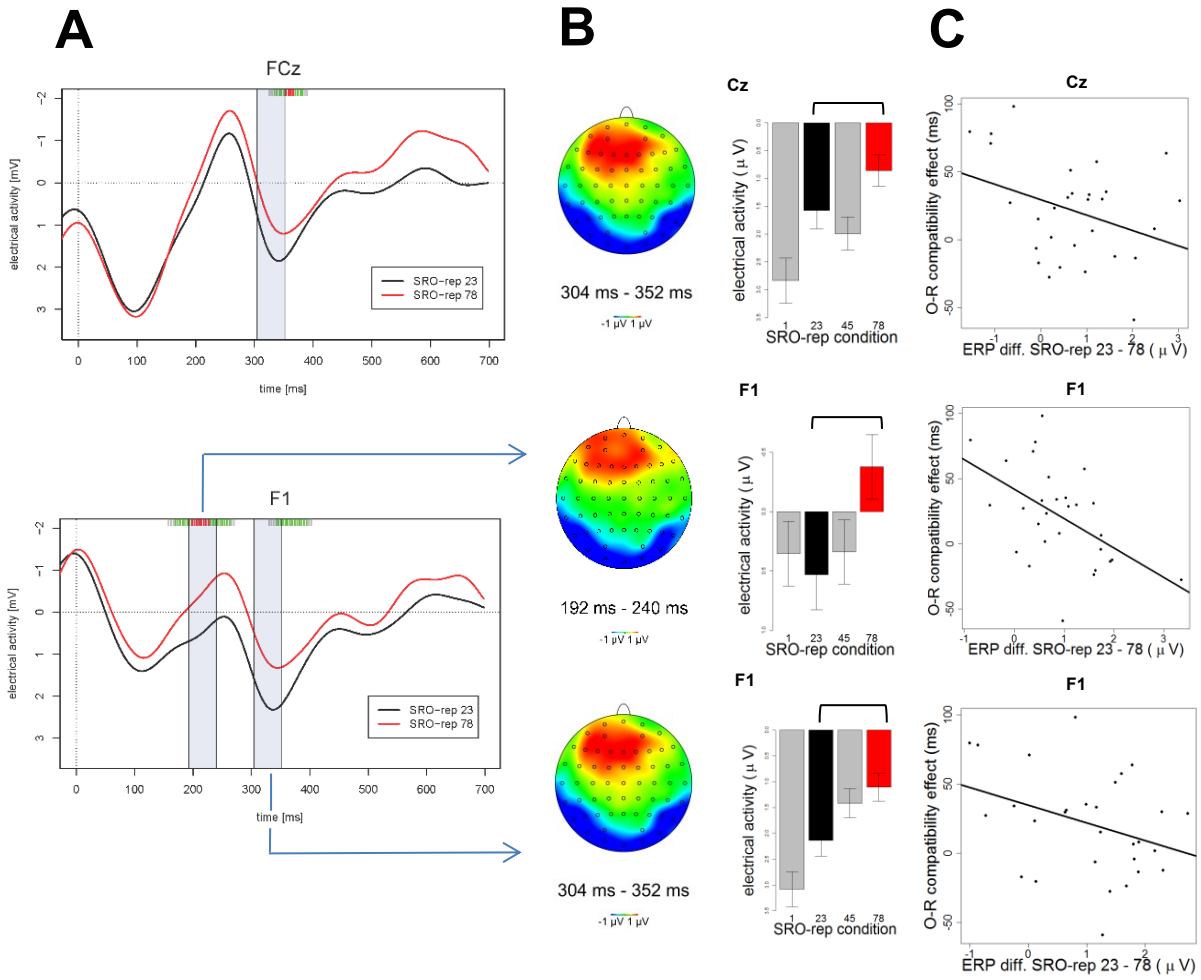

Figure 7: (A) Response-locked grand average waveforms exhibiting significant learning-related effects across SRO-rep 23 and SRO-rep 78. The interval highlighted in light blue represents the time interval which was used for statistical analysis following a split-half approach. The upper border of the plot displays time points at which the difference in electrical activity between SRO-rep 23 and 78 showed a significant correlation with the compatibility effect (gray: p <. 1, green: p < .05, red: p <.01). Time point zero indicates the time of responding. The onset of the auditory outcome was at 150 ms. (B) Averaged topographical map of the difference in electrical activity between SRO-rep 23 and 78 within the specified time windows. Bar graphs for average electrical activity within the extracted time window are plotted for all factor levels that were used in both main and control analysis with the two levels depicted in ERP plots highlighted in black and red. (C) Scatter plots of electrical activity difference (for the time window in which the ERP difference was maximal) in relation to the O-R compatibility effect.

In order to test whether the findings at F1 regarding the difference between SRO-rep 23 and SRO-rep 78 were merely due to the transition from the guided to the unguided learning phase I conducted a control analysis additionally considering SRO-rep 45 as an intermediate

level for the originally identified time window (192 – 240 ms) as well as for the time window re-applied from the literature-based FCz analysis (304 – 352 ms). I found a significant main effect for the factor SRO repetition including the three levels SRO-rep 23, SRO-rep 45, and SRO-rep 78 ([$F(4,112) = 17.93$, $p(F) < .001$] for the early time window, [$F(4,112) = 17.30$, $p(F) < .001$] for the latter time window). Post-hoc tests for the relevant ERP differences (SRO-rep 23 vs. SRO-rep 45 and SRO-rep 45 vs. SRO-rep 78) and the corresponding correlations with the O-R compatibility effect are listed in Table 5. Most importantly, the results of this analysis suggest that correlations with the O-R compatibility effect were driven by different sources for the early vs. late time window. In the early time window the correlation was strongest for the SRO-rep 45 vs. SRO-rep 78 comparison suggesting that the original results were *not* driven by possible confounds associated with the transition from the guided to the unguided phase (i.e., SRO-rep 23 vs. SRO-rep 45). By contrast, in the later time window the correlation was indeed primarily driven by the transition from SRO-rep 23 to SRO-rep 45 confirming the FCz results in the same time window reported earlier in Table 2. This latter finding either indicates faster R-O learning dynamics reflected by ERP modulations between SRO-rep 23 vs. SRO-rep 45 or it might be due to possible confounds related to the transition from guided to unguided learning trials.

Table 5: Statistical analysis at electrode F1 for the response-locked ERP differences SRO-rep 23-45 and SRO-rep 45-78.

Electrode and time window	**SRO-rep 23 vs. SRO-rep 45**			**SRO-rep 45 vs. SRO-rep 78**		
	Post Hoc test for ERP difference	**Correlation with compatibility effect in Linear Regression**		**Post Hoc test for ERP difference**	**Correlation with compatibility effect in Linear Regression**	
		Overall regression model	predictor O-R compatibility		*Overall regression model*	predictor O-R compatibility
F1, 192 – 240 ms	$z = -1.22$, $p = .442$, *n.s.*	$R^2_{adj.} = .15$, $F(3, 25) = 2.71$, $p = .062$, *n.s.*	$b = -.006$, $t(25) = -1.5$, $p = .072$, *n.s.*	$z = 7.26$, $p < .001$	$R^2_{adj.} = .21$, $F(3, 25) = 3.56$, $p = .003$	$b = -.007$, $t(25) = -1.9$, $p = .031$
F1, 304 – 352 ms	$z = .98$, $p = .518$, *n.s.*	$R^2_{adj.} = .34$, $F(3, 25) = 5.84$, $p = .004$	$b = -.01$, $t(25) = -2.24$, $p = .017$	$z = 4.54$, $p < .001$	$R^2_{adj.} = .05$, $F(3, 25) = 1.48$, $p = .245$, *n.s.*	$b = -.002$, $t(25) = -.4$, $p = .346$

Spatio-temporal ROIs determined via exploratory split-half analysis procedure: Learning-related amplitude modulations on the rapid timescale

Concerning initial rapid learning processes occurring between SRO-rep 1 and SRO-rep 3 I identified three spatiotemporal ROIs in the response-locked ERPs that survived the statistical evaluation. The complete statistical evaluation is summarized in Table 6. However, these amplitude modulations were neither significantly correlated with the O-R compatibility effect nor with error rates at SRO-rep 4.

Table 6: Statistical analysis of spatiotemporal ROIs identified for the response-locked ERP difference SRO-rep 1-3.

Time window, electrode	**SRO-rep 1 – 3 Sample 1**	**SRO-rep 1 – 3 Sample 2**	**Prediction of amplitude difference by [1] O-R compatibility effect and [2] error rates in SRO Rep-4 (complete dataset)**	
			Overall regression model	*Specific predictors*
90 – 138 ms, FCz	$t(13) = -3.41$, $p < .005$	$t(14) = -5.03$, $p < .001$	[1] $R^2_{adj.} = .01$, $F_{(3, 25)} = .47$, $p = .706$, *n.s.* [2] $R^2_{adj.} = .01$, $F_{(2, 26)} = .85$, $p = .439$, *n.s.*	[1] $b = -.006$, $t(25) = -0.86$, $p = .398$, *n.s.* [2] $b = .029$, $t(26) = -0.01$, $p = .993$, *n.s.*
482 – 530 ms, FCz	$t(13) = 4.84$, $p < .001$	$t(14) = 3.81$, $p < .001$	[1] $R^2_{adj.} = .02$, $F(3, 25) = 0.825$, $p = .493$ *n.s.* [2] $R^2_{adj.} = .05$, $F(2, 26) = 0.38$, $p = .69$, *n.s.*	[1] $b = -.005$, $t(25) = -1.3$, $p = .207$, *n.s.* [2] $b = 4.122$, $t(26) = 0.87$, $p = .393$, *n.s.*
482 – 530 ms, Oz	$t(13) = -3.16$, $p = .008$	$t(14) = -3.6$, $p = .002$	[1] $R^2_{adj.} = -.07$, $F(3, 25) = 0.43$, $p = .734$ *n.s.* [2] $R^2_{adj.} = .03$, $F(2, 26) = .63$, $p = .539$, *n.s.*	[1] $b = .006$, $t(25) = 0.98$, $p = .335$, *n.s.* [2] $b = -1.61$, $t(26) = -0.28$, $p = .785$, *n.s.*

Stimulus-locked ERPs

Spatio-temporal ROIs determined via exploratory split-half analysis procedure: Learning-related amplitude modulations on the slower timescale

I identified three spatiotemporal ROIs with significant amplitude differences between SRO-rep 23 and SRO-rep 78. The complete statistical evaluation is summarized in Table 7. Spatiotemporal ROIs which additionally showed a significant correlation with the O-R compatibility effect are depicted in Figure 8. Two ROIs were identified within the N1-range. I found an increased positivity from SRO-rep 23 to SRO-rep 78 at Fz (128 – 176 ms) which was paralleled by an increased negativity at Oz (128 – 176 ms). A third ROI was identified in a later time window (580 to 628 ms) at Oz reflecting an increased learning-related negativity. Only the two earlier amplitude differences were significantly associated with the O-R compatibility effect.

Notably, I found for both correlation effects that *smaller* absolute amplitude differences were associated with bigger O-R compatibility effects. This strongly suggests that stimulus-based outcome integration processes associated with the O-R compatibility effect are reflected by ERP amplitude modulations that are pointing in exactly the opposite direction as the mean amplitude difference itself. Hence, learning-related increased stimulus-based outcome integration is in fact reflected by a *reduced* positivity at frontal electrodes accompanied by a *reduced* negativity at occipital electrodes in the N1 latency range. This pattern is consistent with the superposition of two antagonistic ERP modulations as outlined in the Introduction. One (on average weaker) process is associated with stimulus-based outcome integration (indicated by correlations with the O-R compatibility effect) and the other (on average stronger) process is associated with the perceptual learning induced by the mere repetition of the visual stimulus itself (indicated by the overall mean amplitude difference).

Table 7: Statistical analysis of spatiotemporal ROIs identified for the stimulus-locked ERP difference SRO-rep 23-78.

Time window, electrode	**SRO-rep 23-78 Sample 1**	**SRO-rep 23-78 Sample 2**	**Prediction of amplitude difference by O-R compatibility effect (complete dataset)**	
			Overall regression model	*predictor O-R compatibility*
128 – 176 ms, FZ	$t(13) = -5.19$, $p < .001$	$t(14) = -5.19$, $p < .001$	$R^2_{adj.} = .34$, $F(3, 25) = 5.85$, $p < .005$	$b = .013$, $t(25) = 4.03$, $p < .001$
128 – 176 ms, Oz	$t(13) = 4.99$, $p < .001$	$t(14) = 4.29$, $p < .001$	$R^2_{adj.} = .31$, $F(3, 25) = 5.15$, $p = .007$	$b = -.016$, $t(25) = -3.9$, $p < .001$
580 – 628 ms, Oz	$t(13) = -5.65$, $p < .001$	$t(14) = 4.76$, $p < .001$	$R^2_{adj.} = .01$, $F(3, 25) = .60$, $p = .662$, *n.s.*	$b = .004$, $t(25) = 0.86$, $p = .446$, *n.s.*

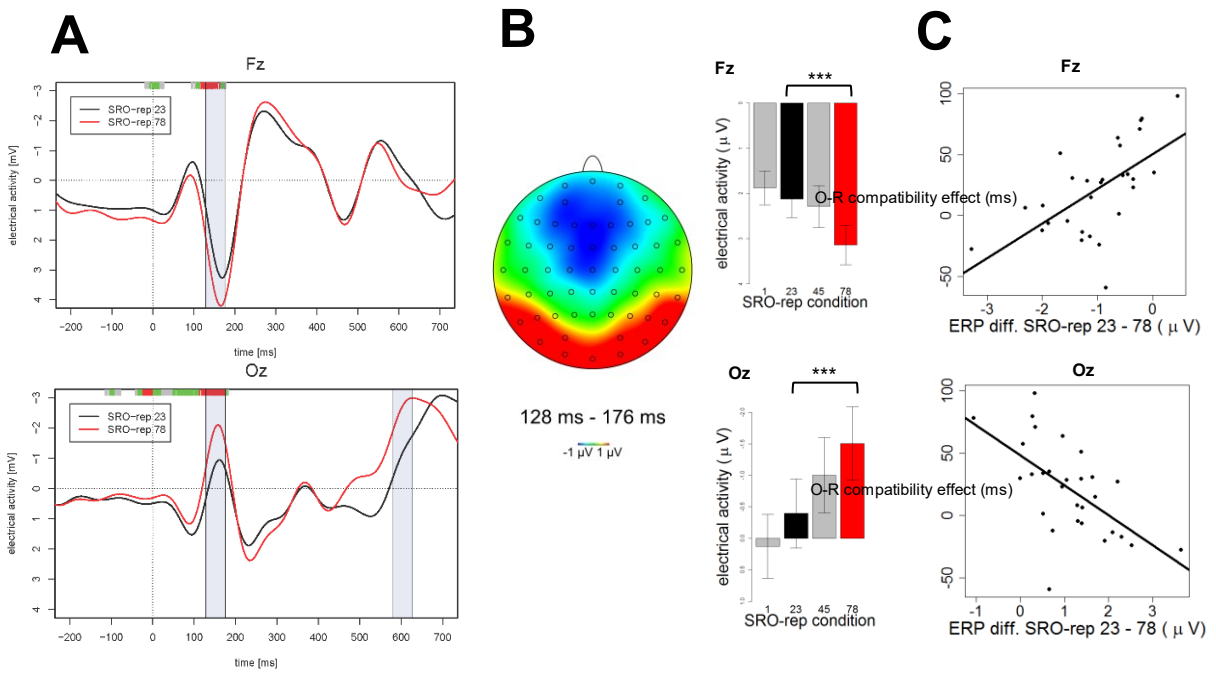

Figure 8: (A) Stimulus-locked grand average waveforms exhibiting significant learning-related effects across SRO-rep 23 and 78 at frontal electrode FZ and occipital electrode Oz. The intervals highlighted in light blue represent the time intervals which were used for statistical analysis following a split-half approach. The upper border of the plot displays time points at which the difference in electrical activity between SRO-rep 23 and 78 showed a significant correlation with the compatibility effect (gray: p <. 1, green: p < .05, red: p <.01). Time point zero indicates the time of visual stimulus onset. (B) Averaged topographical map of the difference in electrical activity between SRO-rep 23 and 78 within the specified time window (128 ms – 176 ms). Bar graphs for average electrical activity within the extracted time window are plotted for all factor levels that were used in both main and control analysis with the two levels depicted in ERP plots highlighted in black and red. (C) Scatter plots of electrical activity difference in relation to the O-R compatibility effect (for the time window in which the ERP difference was maximal).

Again, as for the analysis of response-locked ERPs, I quantified the extent to which the original finding was due to the transition from the guided into the unguided implementation phase. Therefore, I conducted a control analysis additionally considering ERP activity at SRO-rep 45. For both spatiotemporal ROIs in which amplitude modulations between SRO-rep 23 and SRO-rep 78 were correlated with the RT compatibility effect (Fz, 128 – 176 ms; Oz, 128 – 176 ms) there was a highly significant main effect for amplitude differences between all three SRO repetition levels SRO-rep 23, SRO-rep 45, and SRO-rep 78 ([$F(4,112) = 10.2$, $p(F) < .0001$] for FZ, [$F(4,112) = 14.83$, $p(F) < .001$] for Oz). Post-hoc tests for the relevant ERP differences (SRO-rep 23 vs. SRO-rep 45 and SRO-rep 45 vs. SRO-rep 78) and the corresponding correlation with the O-R compatibility effect are listed in Table 8. At both

electrodes I found that the correlation effect was strongest for the SRO-rep 45 vs. SRO-rep 78 comparison suggesting that the original results were not primarily driven by the transition from the guided to the unguided phase (i.e., SRO-rep 23 vs. SRO-rep 45).

Table 8: Statistical analysis at electrode Fz and Oz for the stimulus-locked ERP difference SRO-rep 23-45 and SRO-rep 45-78.

	SRO-rep 23 vs. SRO-rep 45			**SRO-rep 45 vs. SRO-rep 78**		
Time window and electrode	**Post Hoc test for ERP difference**	**Correlation with compatibility effect in Linear Regression** *Overall regression model*	*predictor O-R compatibility*	**Post Hoc test for ERP difference**	**Correlation with compatibility effect in Linear Regression** *Overall regression model*	*predictor O-R compatibility*
128 – 176 ms, Fz	z = -0.88, p = .832, *n.s.*	$R^2_{adj.}$ = .08, F(3, 25) = 0.3, p = .821, *n.s.*	b = -.003, t(25) = 0.57, p = .29, *n.s.*	z = -4.62, p < .001	$R^2_{adj.}$ = .11, F(3, 25) = 2.1, p = .134, *n.s.*	b = .008, t(25) = 1.48, p = .071, *n.s.*
128 – 176 ms, Oz	z = 3.8, p < .001	$R^2_{adj.}$ = .05, F(3, 25) = 1.53, p < .234, *n.s.*	b = -.004, t(25) = -0.98, p = .171, *n.s.*	z = 3.16, p < .005	$R^2_{adj.}$ = .23, F(3, 25) = 3.76, p = .002	b = -.012, t(25) = -1.98, p = .023

Spatio-temporal ROIs determined via exploratory split-half analysis procedure: Learning-related amplitude modulations on the rapid timescale

Concerning initial learning processes occurring between SRO-rep 1 and SRO-rep 3, I identified three spatiotemporal ROIs: F3 (416 to 464 ms), Oz (596 to 644 ms) and FCz (632 to 680 ms). Table 9 summarizes the complete statistical evaluation. While there were no significant correlations with the O-R compatibility effect, the F3 amplitude difference was significantly associated with error rates at SRO-rep 4 (see Figure 9). More specifically, smaller absolute amplitude differences between SRO-rep 1 and 3 were associated with fewer errors at SRO repetition 4.

Table 9: Statistical analysis of spatiotemporal ROIs identified for the stimulus-locked ERP difference SRO-rep 1-3.

Time window, electrode	**SRO-rep 1-3 Sample 1**	**SRO-rep 1-3 Sample 2**	**Prediction of amplitude difference by O-R compatibility effect [1] and error rates in SRO-rep 4 [2] (complete dataset)**	
			Overall regression model	*specific predictors*
416 – 464 ms, F3	$t(13) = -3.82$, $p = .002$	$t(14) = -3.37$, $p = .002$	[1] $R^2_{adj.} = .21$, $F(3, 25) = 3.49$, $p = .03$, *n.s* [2] $R^2_{adj.} = .17$, $F(2, 26) = 3.91$, $p < .05$	[1] $b = .005$, $t(25) = 1.59$, $p = .125$, *n.s.* [2] $b = -8.084$, $t(26) = -2.8$, $p < .001$
596 – 644 ms, Oz	$t(13) = 4.99$, $p < .001$	$t(14) = 4.29$, $p < .001$	[1] $R^2_{adj.} = .05$, $F(3, 25) = 0.59$, $p = .631$, *n.s* [2] $R^2_{adj.} = .02$, $F(2, 26) = 1.21$, $p = .316$, *n.s*	[1] $b = .004$, $t(25) = -0.51$, $p = .614$, *n.s.* [2] $b = 5.153$, $t(26) = 1.2$, $p = .258$, *n.s.*
632 – 680 ms, FCz	$t(13) = -8.80$, $p < .001$	$t(14) = 5.57$, $p < .001$	[1] $R^2_{adj.} = .04$, $F(3, 25) = 1.42$, $p = .261$, *n.s* [2] $R^2_{adj.} = .01$, $F(2, 26) = .23$, $p = .796$, *n.s*	[1] $b = .001$, $t(25) = 0.08$, $p = .941$, *n.s.* [2] $b = -2.338$, $t(26) = -0.54$, $p = .595$, *n.s.*

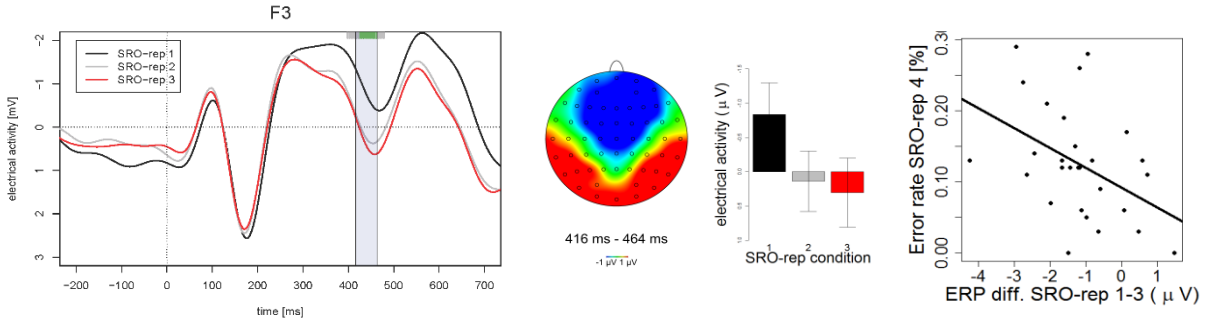

Figure 9: (A) Stimulus-locked grand average waveforms exhibiting significant learning-related effects across SRO-rep 1 and 3. The interval highlighted in blue represents the time interval which was used for statistical analysis following a split-half approach. The upper border of the plot displays time points at which the difference in electrical activity between SRO-rep 23 and 78 showed a significant correlation with the compatibility effect (gray: p <. 1, green: p < .05, red: p <.01). Time point zero indicates the time of visual stimulus onset. (B) Averaged topographical map of the difference in electrical activity between SRO-rep 1 and 3 within the specified time window (416 ms – 464 ms). Bar graphs of average electrical activity in all three guided SRO repetitions. (C) Scatter plots of electrical activity difference in relation to error rates at SRO-rep 4 (for the time window in which the ERP difference was maximal).

4.4 Discussion

This study was designed to investigate the rapidly evolving dynamics of instruction-based learning of novel goal-directed actions with high temporal precision by using EEG recording. I primarily focused on identifying EEG correlates of both pre-response stimulus-based outcome integration and post-response outcome integration as they unfold across learning. I assessed ERPs with regard to possible effects of outcome integration on a rapid timescale during the initial instruction phase (SRO repetition 1 to 3) as well as on a slower timescale across the entire learning episode (SRO repetitions 23 to 78). Learning-related changes in ERPs were considered to be associated with outcome integration processes if they exhibited a significant correlation with the behavioural O-R compatibility effect as an index of the acquired strength of O-R associations. Generally, I observed both pre-response as well as post-response ERP effects of outcome integration, but on the slower timescale only. In contrast, learning-related ERP changes on the rapid timescale were unrelated to outcome integration processes, but were instead associated with instructed S-R learning.

Post-response outcome integration processes

Previous EEG studies have demonstrated a post-response reduction of an anterior negativity within the auditory N1 range as a likely marker of action-induced sensory attenuation effects due to previously acquired action-outcome associations in the context of voluntarily chosen actions (Baess et al., 2008; Baess et al., 2009; Hughes et al., 2013a, 2013b; Hughes & Waszak, 2011; Lange, 2011; Martikainen et al., 2005; Sanmiguel et al., 2013; Waszak et al., 2012). However, so far no data existed regarding the acquisition processes that enable outcome integration in the first place. The results suggest that previously reported effects of sensory attenuation can be established within very few repetitions of specific S-R-O pairings. Furthermore, the results highlight that such attenuation effects generalize to situations in which stimulus-based actions are learned rapidly by explicit instruction. Indeed, I found such a sensory attenuation effect at anterior electrodes with a maximum at the FCz electrode. This attenuation effect was revealed by correlation with the behavioral O-R compatibility effect and was embedded within an overall mean *increase* of the anterior negativity. Specifically, a *smaller* learning-related increase of the anterior negativity was associated with a *larger* compatibility effect. Hence, strong O-R integration shown in behavior was associated with a relative attenuation of the negative ERP amplitude across learning. The overall learning-related increase of the anterior negativity, however, was likely due to a superimposed ERP modulation associated with perceptual learning based on mere repetition of auditory outcomes (Alain et al., 2007; Atienza et al., 2002; Mishra et al., 2015), completely unrelated to O-R learning.

Notably, the attenuation effect I observed was maximal clearly after the auditory N1 peak. Even though a number of previous studies observed maximal effects of action-induced sensory attenuation after the auditory N1 peak (Baess et al., 2008; Sanmiguel et al., 2013), the maximum of the attenuation effect was shifted even further in this study. This is most likely due to the different nature of the presented auditory stimuli. Previous studies typically used pure sine tones with short durations (50 – 140 ms) whereas this study employed relatively complex natural sounds with a rather long duration of 500 ms. This might imply longer perceptual analysis times which might translate into rather late attenuation effects. By contrast, it seems rather unlikely that this temporal shift was due to the relatively long 150 ms interval between response execution and outcome onset as a few earlier studies suggested that the attenuation effect was unaffected by response-outcome delays up to 1000 ms, regardless of whether the onset of outcome presentation was predictable or not (Baess et al., 2008; Sanmiguel et al., 2013).

I was able to rule out that the correlation effect between the post-N1 anterior negativity and the behavioural O-R compatibility was contaminated by learning-related changes in error rates and RTs as possible indicators of changing levels of response competition during the learning phase. However, the correlational effect was primarily driven by the transition from the guided instruction phase (SRO-rep 23) to the unguided implementation phase (SRO-rep 45) as revealed by post-hoc tests separately assessing learning-related changes from SRO-rep 23 to SRO-rep 45 and from SRO-rep 45 to SRO-rep 78. This finding indicates that the post-N1 attenuation reflects either fast R-O learning dynamics or alternatively it might reflect possible confounds related to the transition from guided to unguided learning trials.

This latter caveat does not hold for an additional pre-N1 (but still post-response) attenuation effect that I observed maximally at the F1 electrode. This effect likely reflects an anticipatory component of the action-induced sensory attenuation effect. Different from the post-N1 attenuation effect at FCz, this pre-N1 effect was primarily reflected by ERP modulations between SRO-rep 45 vs. SRO-rep 78. Hence, I can exclude possible confounds related to the transition from guided to unguided learning trials and it is safe to interpret this effect as a relatively slowly evolving anticipatory attenuation component as R-O learning proceeds.

Pre-response stimulus-based outcome integration processes

With respect to pre-response learning processes I found an ERP modulation within the N1 range in response to the antecedent stimulus which was again inversely correlated with the O-R compatibility effect. I found this effect at fronto-central electrode sites with a maximum at Fz as well as at occipital sites with a maximum at Oz. Having the exact same temporal time course it seems likely that those effects were generated by the same dipole, hence reflecting the same brain process. Analogously to the post-response effects, a relative learning-related attenuation of the ERP amplitude difference was associated with stronger O-R association strength shown in behavior. Again, this suggests that this outcome integration effect was superimposed onto a larger general *increase* of the visual N1 which is likely reflecting perceptual learning as a result of repeated presentation of the visual stimulus alone (Clark et al., 2015; Mishra et al., 2015), especially with the visual material being rather complex (Song et al., 2005) and non-familiar (Brem et al., 2005). Next, I am discussing possible explanations of this ERP marker of stimulus-based outcome integration which occurred surprisingly early within a trial during an early stimulus processing stage.

Employing different modalities as imperative stimulus (visual) and outcome (auditory) in this study pre-response stimulus-based outcome integration processes might be revealed by neural markers typically associated with multi-sensory (here, visuo-auditory) integration processes (Murray et al., 2015). Multi-sensory integration processes, that is, interaction between different sensory modalities have been identified even in very early stages of stimulus processing (Talsma, Doty, & Woldorff, 2007). Giard and colleagues found that the processing of a stimulus containing redundant bimodal information (e.g. seeing and hearing a barking dog) is more rapid than that of either unimodal stimulus alone (Giard & Peronnet, 1999). This finding was complemented by EEG studies which reported modulations of the visual N1 in response to the bimodal stimulus in comparison to visual modality only (Fort, Delpuech, Pemier, & Giard, 2002; Molholm, Ritter, Javitt, & Foxe, 2004).

Importantly, in the present study the putative multi-sensory integration effect revealed by N1 attenuation can only be due to S-O integration, i.e. associating the visual stimulus with the auditory outcome. However, the N1 attenuation effect was revealed by a significant correlation with a behavioral marker of O-R integration processes. This suggests that S-O processes (measured by visual N1 attenuation) and O-R processes (measured in behavior) are closely related to each other at least in the present context. But how is this relationship mediated? My working hypothesis is that outcome anticipation triggered by visual stimulus onset (based on learned S-O associations) will amplify the strengthening of O-R associations after response execution. In other words, the earlier an outcome is anticipated (based on S-O)

the better it will be associated with R (leading to stronger O-R compatibility effects later on). This account is consistent with the general notion that more salient events (here outcomes that are pre-activated sooner) will be associated more easily and more rapidly (Le Pelley & McLaren, 2003; Mackintosh, 1975).

Pre-response instruction-based S-R learning processes

In addition to outcome integration processes discussed above the study also made an effort in characterizing potential ERP markers associated with the initial learning of instructed S-R associations. The analysis identified such markers by correlating ERP amplitude changes across the instruction phase (SRO-rep 1 to SRO-rep 3) with error rates at SRO-rep 4 (as a behavioral marker of S-R encoding quality during the preceding instruction phase). I found that an increased learning-related frontal positivity in the mid-latency range between 416 and 464 ms post-stimulus was associated with higher error rates later on. That is, weak S-R learners exhibited a stronger frontal positivity increase whereas good S-R learners exhibited a weaker increase in frontal positivity. Assuming that better performance is due to better S-R encoding beforehand, this observation implies that good S-R learners engage in learning processes at a relatively steady level during the instruction phase. By contrast, weak learners who are characterized by a stronger learning-related ERP modulation are less steadily engaged in learning across the instruction phase. There are two possible scenarios explaining this relationship. According to the first scenario, weak learners start out with a strong engagement at SRO-rep 1 (similar to good learners) and just fail to keeping up this high level of learning engagement (unlike good learners). According to the alternative scenario, weak learners fail to properly engage in S-R learning at SRO-rep 1 (maybe because they are more strongly distracted by stimulus novelty) and simply do not have sufficient opportunity to compensate this initial failure even though they try hard in the remaining two SRO repetitions of the guided instruction phase. Notably, a recent study by Luque et al. (2015) also investigated ERP modulations related to S-R learning, yet after a period of extensive practice had been completed. In contrast to the results present in this study they found an ERP modulation in a much earlier time window suggesting, maybe not surprisingly, that S-R-related processes are reflected differently depending on the stage of automatization and that more automatized S-R translation is taking place earlier in the processing stream.

5 Study 2 - Within trial distinction of O-R learning-related BOLD activity with the means of co-registered EEG information

5.1 Introduction

This study built up on the results produced in study 1 (see chapter 4.3). It utilized the exact same paradigm except for the fact that it was set up as a simultaneous EEG-fMRI experiment this time. Again participants had to learn novel 4:4:4 stimulus-response-outcome (SRO) mappings by instruction in 10 different learning blocks. These SRO repetitions were unique for each block and were each repeated eight times (8 SRO repetitions). Acquired O-R association strength was probed in a test phase following each learning block. Subjects had to respond to the previous outcomes with the same set of 4 responses used during the acquisition phase, which could either be compatible or incompatible to the response that produced that outcome during acquisition (O-R compatibility).

Using the same paradigm in this study gave us the advantage of having strong hypotheses on the expected EEG activation patterns. Study 1 identified two main findings of EEG modulations which can be summarized as follows:

1. A post-response reduction of fronto-central response-locked ERP amplitudes in the auditory N1 range following the onset of the outcome which was significantly associated with stronger O-R compatibility effects.
2. A reduced stimulus-locked negativity within the visual N1 range in response to the visual antecedent stimulus across learning which also was positively correlated with O-R compatibility effect strength.

If reproduced, those parameters were to be utilized in the latter joint EEG-fMRI analysis. Following the 'EEG-informed fMRI analysis' approach (Debener, Ullsperger, Fiehler, von Cramon, & Engel, 2005; Debener, Ullsperger, Siegel, & Engel, 2006) the temporally highly resolved ERP activation maps are taken and utilized as an additional parameter in the analysis of simultaneously recorded fMRI data. By doing so, it technically enables an analysis approach in which it is possible to disentangle distinct sub processes within the fMRI signal. Due to the sluggish nature of the BOLD response this was rather difficult to assess in fMRI only studies dealing with the evolution of R-O integration processes across learning trials on multiple time scales of learning that have been conducted so far (Melcher et al., 2013; Mohr, Wolfensteller, Frimmel, & Ruge, 2015; Ruge & Wolfensteller, 2013, 2015).

By entering the response-locked post-response N1 modulation as an additional regressor into the fMRI brain regions that are especially associated with post-response O-R

outcome integration can be identified. Several brain regions have been associated with outcome integration processes in both instrumental learning and ideomotor contexts. A number of studies have reported relevant SMA activation when perceiving outcome stimuli following extensive phases of R-O learning (Bonini et al., 2014; Elsner et al., 2002; Melcher et al., 2008; Melcher et al., 2013). Frimmel et al. (2016) were able to demonstrate that these findings could be replicated in the context of only few presentations of S-R-O mappings (likewise to this study). In this study the SMA was specifically associated with the acquisition of contingencies regarding the entire association chain. It is reasonable to expect activation in this region in this study as well. Even more, SMA activation should be predicted by a potential EEG marker of O-R outcome integration. In contrary to the experimental design of Frimmel and colleagues, this setup includes an O-R test phase which makes it possible to even relate potential functional brain activation directly to O-R encoding processes.

Correspondingly, by using the stimulus-locked pre-response visual N1 ERP modulations in the EEG-informed analysis brain regions related to the multi-sensory integration processes already discussed in section 4.4 could be revealed. Numerous neuro-imaging studies have documented auditory-visual convergence within primary sensory cortices (Haxby et al., 1994; Kawashima, O'Sullivan, & Roland, 1995; Laurienti et al., 2002; Mozolic, Hugenschmidt, Peiffer, & Laurienti, 2008), even in the absence of external stimuli or tasks (Eckert et al., 2008). It has also been shown repeatedly that sounds are able to activate visual cortices as a function of prior multisensory experiences (Matusz et al., 2015; Meylan & Murray, 2007; Murray, Foxe, & Wylie, 2005; Murray et al., 2004; Thelen, Cappe, & Murray, 2012; Thelen, Matusz, & Murray, 2014; Zangenehpour & Zatorre, 2010). However, there is still an ongoing debate if early multisensory audio-visual effects emanate from nominally visual (Fort, Delpuech, Pemier, et al., 2002; Molholm et al., 2002) or nominally auditory cortices (Vidal, Giard, Roux, Barthelemy, & Bruneau, 2008) or both (Raij et al., 2010; Senkowski, Saint-Amour, Hofle, & Foxe, 2011; Teder-Salejarvi, McDonald, Di Russo, & Hillyard, 2002). Hence, if early N1 multisensory attenuation effects are replicated in this study, one might expect to see a coupling with increased activation in either the primary auditory or visual cortex, or both. To summarize, the great advantage of this study lies in its ability to temporarily discriminate brain responses within a trial, i.e. to assign functional activation in specific brain regions to events prior or subsequent to the response. This would have not been possible in isolated EEG or fMRI setups alone.

Study 1 analyses primarily paid attention to EEG correlates associated with the behavioral marker of O-R encoding strength, namely the O-R compatibility effect. In this study, potential coupling effects between ERP parameters and fMRI BOLD activation will additionally focus on its correlation with response time differences between late and early learning stages.

I am assuming that these markers, possibly denoting a putative marker of O-R usage, could predict activity in brain regions that are involved into monitoring processes in goal-directed action. For example, Ruge and Wolfensteller (2015) found that the active usage of O-R associations correlated with LPFC-caudate coupling. They concluded that the caudate therefore seemed to act as a control instance for goal-directed actions, especially in an instruction-based learning environment.

On a more minor note this study would also serve as a duplicate of the study mentioned above (Ruge & Wolfensteller, 2015) to answer the question if the prior findings regarding response-outcome relations could be replicated. Additionally to the identified LPFC-caudate couplings the study revealed that O-R encoding strength is associated with LPFC-putamen coupling prompting that this particular brain region is involved into the formation O-R associations.

5.2 Methods

Experimental procedure

This study utilized the exact same experimental paradigm as study 1 (see chapter 4.2).

Subjects

This study comprised 30 subjects. I excluded four subjects due to error rates greater than 25% in the first unguided implementation trial (SRO Repetition level 4). Again, this was done because high error rates in this particular trial suggest that those subjects proceeded not according to instructions resulting in an undesired trial-and-error effect. Three subjects with insufficient EEG had to be excluded in EEG-informed fMRI analyses involving response-locked ERPs (resulting in a total of 23 subjects). Only two subjects had to be excluded for this reason in the stimulus-locked EEG-informed fMRI analyses (resulting in a total of 25 subjects for these analyses). The mean age of the resulting subjects was 27.9 years, ranging from 21 to 36 years. All subjects were treated in accordance with the Declaration of Helsinki and gave written informed consent in advance of taking part in the experiment and were paid €8 per hour or received course credit.

Study 2 - Within trial distinction of O-R learning-related BOLD activity with the means of co-registered EEG information

EEG-fMRI Recording

Whole-brain images were acquired on a Siemens 3-T whole-body Trio System (Erlangen, Germany) with a 16-channel circularly polarized head coil. MR-Confon headphones were used for sound presentation and additionally reduced scanner noise. For each subject structural and functional images were acquired. High-resolution structural images (1.0 x 1.0 x 1.0 mm) were acquired using a MP-RAGE T1-weighted imaging sequence (TR = 1900 ms, TE = 2.26 ms, TI = 900 ms, flip = 9°). Functional images were acquired utilizing a gradient echo planar imaging sequence (EPI, TR = 2000 ms, TE = 30 ms, flip = 80°). Each volume contained 32 4.0 mm-thick slices (in-plane resolution 4.0 x 4.0 mm) plus 0.8 mm gap which were oriented parallel to the AC-PC plane. The paradigm itself was programmed in E-Prime 2.0 software running on a Windows XP computer. Visual stimuli were displayed by an LCD projector on a back-projection screen mounted behind the magnet, which was viewed at by subjects through mirror glasses. Behavioral responses were locked via a fiber-optic, light-sensitive keypress device. Continuous EEG data were collected from 64 standard scalp sites using the 64Ch BrainAmp MR+ system, a high-input impedance amplifier specifically designed for recordings in high magnetic fields (Brain Products, Munich, Germany, www.brainproducts.com). The system used sintered AG/AgCl ring electrodes with built-in 5 kΩ resistors. The electrodes were mounted into an electrode cap according to the 10-20 system (Klem et al., 1999) with electrode Cz used as reference. Additional two electrodes were used to identify eye blinks and to record electrocardiographic activity. The ocular electrode was placed under the lower eye lid. The ECG electrode was attached medially on the back of the subject along the paravertebral line. Electrode impedances were kept below 10 kΩ before recordings. The nonmagnetic EEG amplifier was fixed just behind the scanner bore and powered by a rechargeable power pack. The subject´s head was fixed using vacuum cushions and sponge pads. The amplified EEG signal was transmitted to a recording computer outside the scanner room via fiber optic cable. A SyncBox (Brain Products, Munich, Germany) was used in order to synchronize the sampling rate of the amplifier with the internal scanner clock system. The aim was to achieve phase synchronicity between the two clock systems, subsequently ensuring optimum correction of scanner-induced EEG artifacts. EEG data was recorded with a passband filter of 0.01 – 250 Hz and digitized with 5000 samples per second at 16 bit with 0.5 µV resolution.

FMRI Preprocessing

The fMRI data was analyzed with SPM8 running under MATLAB 8.1.0.604. Preprocessing steps included slice-time correction, rigid body movement correction (three

translation, three rotation parameters), and normalization of the functional images by directly registering the mean functional image to the standard Montreal Neurological Institute (MNI) echo-planar-imaging template image provided by SPM8, with a resulting interpolated spatial resolution of 3 x 3 x 3 mm. in a final step, images were spatially smoothed (Gaussian kernel, full width at half maximum = 8 mm). A temporal high-pass filter with a cutoff of 1/256 Hz was applied during model estimation.

Analysis of behavioral data

Likewise to study 1 the behavioral performance data were analyzed using R (R Core Team, 2012) and *lme4* (Bates, 2012) to compute two separate linear mixed-effect models for mean response times (RTs) as well as mean error rates with the factor SRO repetition (SRO-rep 1 to SRO-rep 8) being fixed effect and the factor subject being random effect. Omnibus tests of significance for main effects again were calculated by comparing the deviance of the tested model to the deviance of the null model. Post-hoc significance tests were employed and Bonferroni-corrected for multiple comparisons using the Multcomp package (Hothorn et al., 2008).

FMRI only replication analysis

The sole purpose of analyzing the fMRI only data was to replicate fMRI findings by Ruge and Wolfensteller (2015) using the same paradigm as implemented in this study. To this end, the analysis approach presented there will be completely followed here.

First level analysis

The psychophysiological interaction (PPI) framework implemented in SPM8 (Friston et al., 1997; Gitelman, Penny, Ashburner, & Friston, 2003) was used in its generalized form proposed by McLaren et al. (McLaren, Ries, Xu, & Johnson, 2012) in order to analyze functional coupling between LPFC and any other voxel in the brain. PPI is a method of assessing functional neuro-connectivity by predicting the blood-oxygenation-level-dependent (BOLD) signal time course in target voxels anywhere in the brain, on the basis of the BOLD signal time course in a predefined seed voxel. Mathematically this is not simply done by correlating these two signal time courses, but instead it is implemented as the difference in the slopes of the regression function of varying paradigm-specific psychophysiological states

associated with two different experimental conditions. The generalized form of the PPI used in this study accommodates situations in which the two contrasted conditions are occurring in the context of additional experimental conditions intermixed with the conditions of interest. For each experimental condition two regressors were defined for the generalized linear model (GLM), first regressor being a standard event-related regressor obtained by convolving a canonical BOLD response model with a stick function representing repeated occurrences of that condition. This so called task regressor picks up average event-related BOLD action associated with that condition. The second regressor is built by multiplying the task regressor with the seed voxel activation time course in a threefold process. First, the seed voxel activation time course is de-convolved, then multiplied with the task-related stick function, and then re-convolved with the canonical BOLD response (Gitelman et al., 2003). Being combined with the task regressor in a linear fashion, this PPI regressor accumulates any inter-trial deviation from the mean task-related activation that is common between seed voxel and target voxel. Thus, the PPI regressor measures task-related synchrony between the seed-voxel and target-voxel activation time courses. This process defines the term “functional coupling” as it will be used in this study, following the nomenclature of Ruge and Wolfensteller (Ruge & Wolfensteller, 2015). The GLM comprises the seed voxel time course as an additional predictor to catch up unspecific sources of covariance between seed voxel and target voxel. PPI repressor estimates are assessed for early learning trials (SRO-rep 2 and 3) as well as late learning trials (SRO-rep 7 and 8). Again, as in study 1 as well as also done in the previous fMRI study (Ruge & Wolfensteller, 2015), SRO-rep 1 was not included as a potential instance of early learning as it was considered a special condition comprising strong perceptual novelty components as visual stimuli and sounds were perceived for the very first time. Thus, SRO-rep 2 and 3 were considered to be more neutral instances of early learning.

Second level analysis

In a first step, general couplings between the LPFC seed to other brain regions were assessed from early (SRO-rep 23) to late learning stages (SRO-rep 78). Furthermore, this analysis intended to replicate correlations between predefined behavioral covariates and the functional coupling between lateral PFC as well as other brain regions as first reported by Ruge and Wolfensteller (2015). The behavioral markers used were namely the response time O-R compatibility effect (named “O-R encoding strength” in the original paper) and the difference in response time between SRO-rep 23 and SRO-rep 78 (“O-R usage”). Both behavioral markers were therefore included as covariates in the second level analysis of PPI effects. They were included simultaneously in order to ensure that a possible correlation between PPI effect

and a covariate was exclusively driven by a covariance component that was orthogonal to the other covariate. By doing so, the potential influence of the other covariate was being regressed out. Additionally, group-level analysis were also performed only comprising one of the two covariates in order to not miss any significant correlation which might be due to covariance components shared by both covariates. When only including one of the two markers into the model differences in error rates between SRO-rep 23 and SRO-rep 78 were also added as covariate to control for potential confounds between the two behavioral markers of interest (O-R compatibility and RT difference) and error rate differences across the S-R-O learning period. According to the first step (where no behavioral covariates were added) this time the intention was to identify significant correlations between each of the covariates with the PPI effect defined by the difference in functional couplings in late learning relative to early learning. Significant correlations were only taken into account if they exceeded a family-wise-error (FWE) threshold of $p < .05$, adjusted for the volume of each selected region of interest (ROI) either on the voxel level or on the cluster level at a cluster-forming threshold of $p < .001$. Finally, the PPI was additionally computed FWE-corrected on the whole-brain level to search for global effects outside of the predefined ROIs.

Seed region and regions of interest

Analogously to prior studies of Ruge and Wolfensteller (2013, 2015) as well as other studies on instruction-based learning (Dumontheil, Thompson, & Duncan, 2011; Hartstra, Kuhn, Verguts, & Brass, 2011), the left posterior LPFC was selected as a seed region. Being a literal replication with regard to the paradigm and methodology this study utilized the same seed voxel as Ruge and Wolfensteller (2015, MNI coordinates: - 42 8 32). Likewise, this study utilized the same three ROIs that were used previously to look for significant PPI effects. The left and right basal ganglia were chosen to be of primary theoretical interest. Ruge and Wolfensteller additionally included the left and right hippocampus as it has been reported in previous studies on instruction-based control (Li, Delgado, & Phelps, 2011; Ruge & Wolfensteller, 2013) and suggested to play a crucial role regarding these processes in a formal neurocomputational model (Huang, Hazy, Herd, & O'Reilly, 2013). Finally, the orbitofrontal cortex (OFC), more precisely Brodmann areas BA 11 and BA 47, was chosen as a third ROI since its importance in goal-directed action had been stressed by a number of studies (Noonan et al., 2012; Ruge & Wolfensteller, 2013; Valentin et al., 2007). Anatomical information was taken from the automatic anatomic labeling atlas (AAL) for the basal ganglia as well as the hippocampus (Tzourio-Mazoyer et al., 2002). The OFC ROI was defined using the Brodmann parcellation as implemented in the MRICRON software (Rorden, Karnath, & Bonilha, 2007).

FMRI induced EEG artifacts and EEG preprocessing

EEG data derived from combined EEG-fMRI acquisition sessions are contaminated by additional artifacts of various sources, adding a huge amount of noise to the recorded data. This makes additional preprocessing steps necessary dealing with these kinds of disturbances. These artifacts can be categorized as motion-related, MR imaging-related (Allen et al., 2000; Felblinger, Slotboom, Kreis, Jung, & Boesch, 1999) and cardiac related (Allen, Polizzi, Krakow, Fish, & Lemieux, 1998; Bonmassar et al., 2002). From these three categories, the following three artifacts are the most severe and must be removed or ruled out from recordings before further analysis: the gradient artifact, the cardioballistic artifact as well as the Helium pump artifact. In the following I will explain the source and the nature of each of these artifacts and additionally describe various ways how to deal with them and how they were dealt with in this study.

Gradient artifact

The Gradient artifact (GA) is an exogenous technical artifact reflecting the imaging slice acquisition (see Figure 10). It is produced by the switching of magnetic gradients which are necessary for MRI image acquisition. Hence, the subsequent distortions in the EEG signal cannot be avoided. In an echo planar imaging sequence (EPI) which was used in this study, gradient switching is resumed every time a new slice is acquired, leading to artifacts that repeatedly occur with the collection of each new fMRI slice. Its intensity can be 10 to 100 times larger than the actual EEG signal with very steep peaks in the order of millivolts per millisecond (Allen et al., 2000; Felblinger et al., 1999). Artifact strength can vary from one EEG channel to another depending on the location of the electrode and wire connections (Anami et al., 2003; Garreffa et al., 2003; A. Hoffmann et al., 2000). Additionally, its frequency range is most likely to overlap that of the EEG, thus it cannot simply be filtered out. Although having extremely large amplitudes of up to more than 25000 µV/s with low pass filters preventing the signal from drifting into saturation, the recorded distorted EEG signal will contain the normal EEG signal lying on top of the GA making statistical removal of the GA possible.

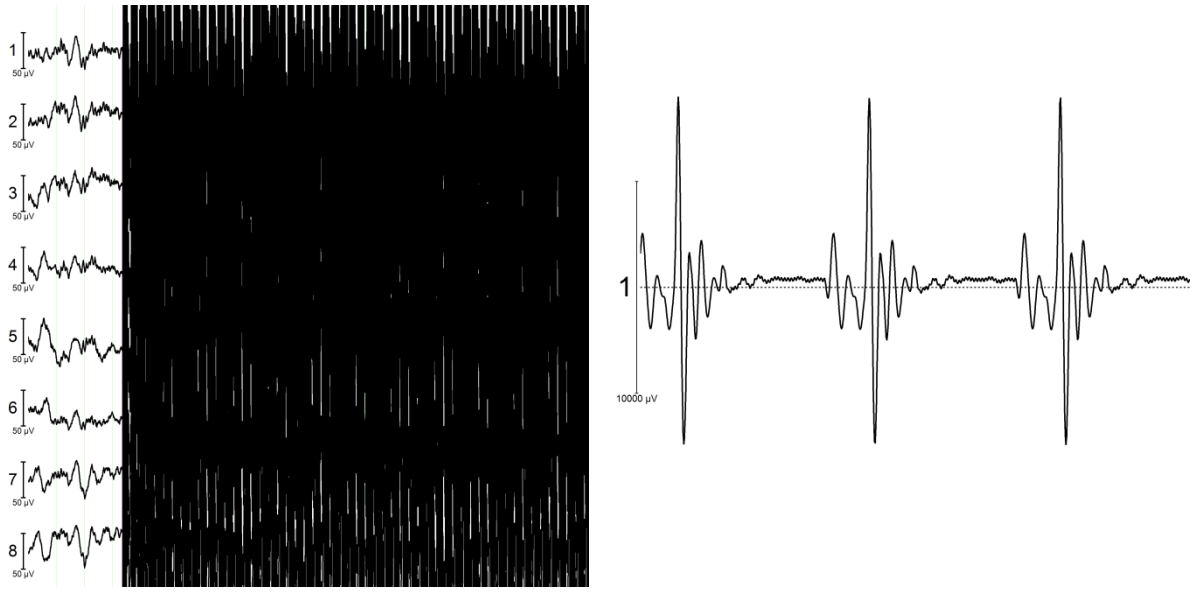

Figure 10: (Left) Raw EEG data recorded inside an MR scanner containing MR induced EEG artifacts. (Right) Characteristic shape of the MR induced gradient artifact with peaks of 2000 µV amplitude.

There are various methods of separating the gradient artifact from signals produced by the subject inside the scanner during an fMRI session including procedures like adaptive filtering (Sijbers et al., 1999) or frequency domain techniques (A. Hoffmann et al., 2000). The most prominent one is the method of average artifact subtraction (AAS, Allen et al., 2000; C. Benar et al., 2003) which takes advantage of the assumption that the artifact is invariant over all slices, given the circumstance that gradient fields and radio frequency (RF) pulses are put out with extreme temporal accuracy regarding magnitude. Thus, it can be expected that the GA will lead to similar distortions in the EEG signal every time it occurs. This invariability is used to form a template of the average gradient artifact which is then subtracted from the EEG data. Doing so requires that the consecutive onsets of RF pulses are recorded with the same precision and temporal invariance by the EEG amplifier with which they are delivered with. The artifact template will differ systematically for each channel due to different positions and orientations of the EEG electrodes with respect to the gradient. For this to happen in the first place requires a signal sent by the MR scanner whenever changes in the gradient field occur. This is done via output of a Transistor-transistor logic (TTL) signal at the exact onset time of a new slice or volume acquisition. I will call this signal the volume trigger from now on. This volume trigger is then sent to the EEG recording device and will appear together with the recorded EEG data in the recording software. Together with the pre-set MR sampling rate (TR) of 2000 ms technically all information necessary to model and eventually withdraw the GA are provided.

However, there are two major challenges which have to be met concerning removal of the GA artifact. First, it is possible and quite common and actually also occurred in this EEG-fMRI setup that the volume trigger is actually not set correctly at the very same time point across the entire time course of the volume. Even more, the trigger signal was not only delayed in relation to the actual onset but the delay itself was jittered in the range of ms over all volume onsets. Hence, the volume trigger was not a valid indicator regarding the onset of the GA and was not further used for artifact correction. Instead, the gradient onset and frequency were estimated using a solution implemented in Brain Vision Analyzer. Secondly, the GA is not exactly invariant over the entire course of the session. Instead, it fluctuates over time which is mostly due to head movement of the subject changing the position and orientation of the electrodes on the electrode cap. There can be two types of head movements: slow, involuntary movement happening over a longer course of time or fast, voluntary and temporally restricted movement. To compensate for the former Allen et al. (2000) proposed to only use events which are correlated with an initial GA template with over $r = 0.975$, effectively rejecting outliers. Additionally, the GA template will be calculated based on a moving average of adjacent volumes. Doing so accounts for involuntary head movements over time. However, this procedure will not work for abrupt head movements, dramatically altering the geometry of electrodes and cables in the magnetic field and consequently the induced GA properties. In this case, having only one GA mean template may not be sufficient. This problem can be solved by not defining only one but several GA templates over time. One template is then used only for the consecutive GA events until a severe head movement occurs, while those events followed by the head movement will be cleansed by a new defined GA template based on the new parameters of the gradient field. In the present study one fMRI session comprised three separate runs. Thus, three different templates had to be computed per subject and session. More recent approaches take the head movement parameters from the fMRI preprocessing into account to estimate improved artifact templates (Moosmann et al., 2009; Sun & Hinrichs, 2009).

The GA artifact in this study was removed using the implemented AAS algorithm in Brain Vision Analyzer (Brain Products, Munich, Germany, www.brainproducts.com). Instead of using the volume trigger it utilized an implemented function which estimated the gradient threshold and frequency. Figure 11 shows a snippet of continuous EEG data cleansed of the GA artifact. As clearly visible, the EEG data now looks more like the typical data (acquired outside the MR scanner). It is now possible to identify some other characteristic patterns which are part of another motion-related MR artifact: the cardiobalistic artifact.

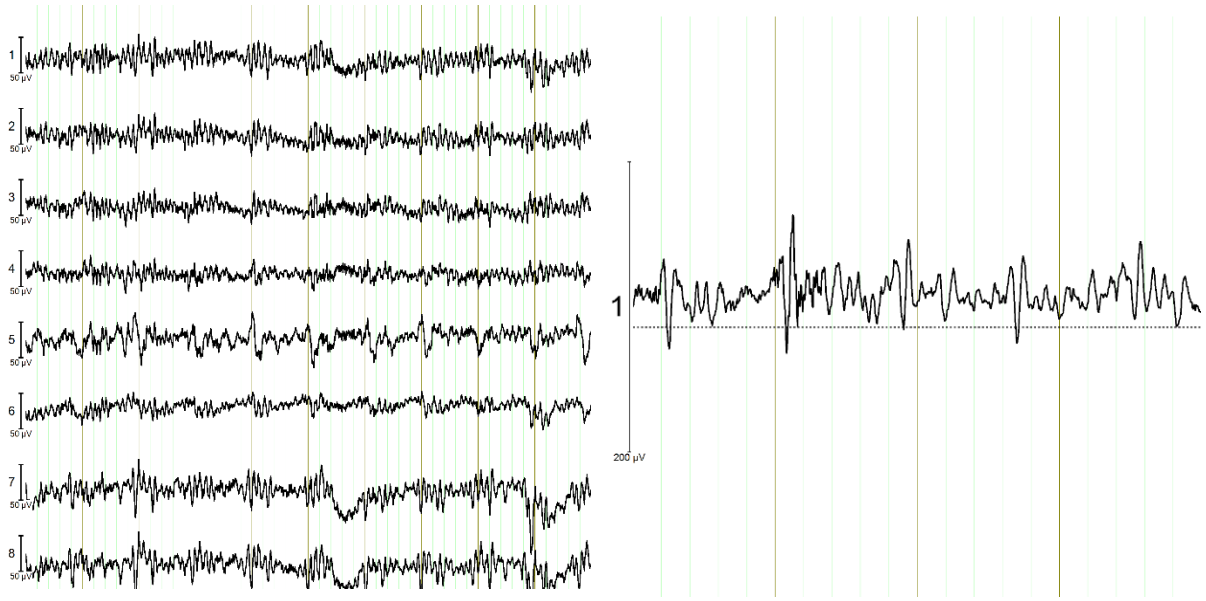

Figure 11: Gradient artifact-free EEG data.

Cardiobalistic artifact

Other than the GA, which occurs only in and as a result of slice and volume acquisition periods, the cardiobalistic artifact (BCG, see Figure 12) is always present in the magnetic field of the scanner, contributing substantially to the lower frequency spectrum smaller than 15 Hz (Srivastava, Crottaz-Herbette, Lau, Glover, & Menon, 2005). Although its exact origin still remains unclear, there are several possible explanations. Some of them include EEG electrodes or cables over, or adjacent to, pulsatile blood vessels which are in constant motion, or the acceleration of the electrically conductive blood to be the source of current induction that is registered in the EEG. But most likely above all is that the pulsatile flow of blood associated with the cardiac cycle induces a head motion which than itself is picked up by the electrodes, thus constituting the BCG artifact (Anami, Saitoh, & Yamoto, 2002). It can be called a mesogenous artifact (Eichele, Moosmann, Wu, Gutberlet, & Debener, 2010) comprising contributions from the subject´s cardiovascular system (endogenous component) which interacts with the scanner´s b_0 field (exogenous component). This has to be kept in mind as potential variability within the BCG may have its source in the MRI environment (e.g. variability in scanner field strength) or in cardiovascular parameters, such as heart rate variability. As with the GA, the BCG also is present in all EEG channels with the degree of artifact varying between the channels. Generally spoken, the sereneness of the BCG artifact is reduced with increasing distance of the EEG channel from the EEG reference electrode. Additionally, a high field MRI scanner causes larger BCG amplitudes than a lower field scanner (Debener,

Mullinger, Mazy, & Bowtell, 2008) with the BCG amplitude being proportional to the scanners b_0 field (Tenforde, Gaffey, Moyer, & Budinger, 1983). The timeline of the artifact itself is coupled to the cardiac cycle of the subject with a delay of approximately 200 ms between the ECG R peak and the corresponding BCG artifact peak in the EEG channels (Allen et al., 1998). This strong relationship to the cardiac cycle makes correcting the artifact quite challenging as fluctuations in the subject´s heart rate or any other cardiovascular parameter are directly reflected in the BCG and, in case of a higher heart rate, having the possibility of two cardiac adjacent cardiac cycles overlapping to some extent (Vincent, Larson-Prior, Zempel, & Snyder, 2007). As discussed above, the BCG represents a rather complex and dynamic contribution to the EEG and needs to be addressed (Nakamura et al., 2006).

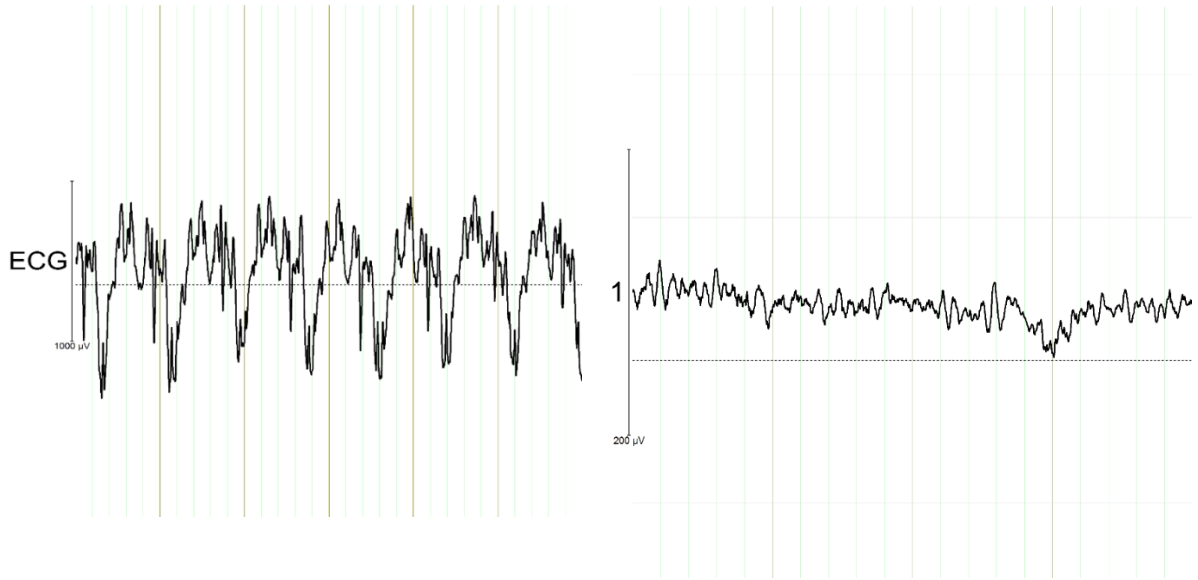

Figure 12: (Left) Characteristic shape of the pure MR induced cardiobalistic artifact recorded in the ECG channel. (Right) Sample of an EEG time series cleansed from the cardiobalistic artifact.

Again there is a variety of different correction methods with the AAS (Allen et al., 1998) being the most frequently used and influential. Similar as in the AAS approach with the GA, the basic principle is that a template of a prototypical BCG artifact is computed and then withdrawn from the recorded EEG signal leaving only true EEG contributions. Due to the temporal as well as topographical variability of the artifact, some additional parameters need to be taken into account in order to properly construct a template. First, estimates of the onset of each cardiac-cycle from the concurrently recorded ECG are required. The artifact template

itself is then calculated based on a moving average for each EEG channel separately through averaging the EEG time-locked to each cardiac cycle onset and then withdrawn from each EEG epoch. The AAS method has been found to generally deliver satisfying results (Hamandi et al., 2008; Sammer et al., 2005). However, two major pitfalls have to be kept in mind when dealing with the AAS method. First of all, the ECG channel itself also contains the GA and BCG artifact and therefore detecting the R peak might not always be so easy using automatized algorithms. This can lead to inaccurate positioning of R peak event markers, eventually resulting in a bad BCG template (Debener et al., 2008). This problem is already addressed in some software solutions such as the Brain Vision Analyzer where jitter information are already taken into account in a way that markers are aligned statistically such that the overall jitter is minimalized before the AAS algorithm is applied. The second major issue is the problematic assumption of similarity between adjacent BCG occurrences. In the chosen moving average window approach, it is assumed that the BCG artifact contribution to each EEG channel is very similar between adjacent cardiac cycles with changes occurring only slowly over time. This assumption may not always be met. Although there are some solutions with alternative template constructions based on weighted averages (Goldman, Stern, Engel, & Cohen, 2000) or median values (Sijbers, Van Audekerke, Verhoye, Van der Linden, & Van Dyck, 2000), they still rely on the problematic assumption of local BCG similarity and assume that the template is fully sufficient for each BCG epoch. A different approach that takes these latter problems into account comes from Niazy and colleagues (Niazy, Beckmann, Iannetti, Brady, & Smith, 2005), as well as by Negishi et al. (Negishi, Abildgaard, Nixon, & Constable, 2004). These two groups suggested constructing the BCG artifact template based on a channel-wise temporal principal component analysis (PCA), thereby avoiding the assumption of any local BCG similarity. Niazy named his method the optimal basis set (OBS) method, referring to the view that the first few principal components represent several distinct BCG templates and explain most of the BCG variance in any EEG channel. These templates are in the following jointly regressed out of the polluted EEG data, leaving only the true EEG signal. This procedure has received wide acclaim in the EEG-fMRI community since it does not assume that adjacent BCGs are more similar to each other than distant ones. Further, it additionally accounts for the possibility of different artifact shapes. Apart from template-based correction methods there are also spatial pattern removal approaches in which the BCG is characterized by a number of prototypical topographies. Among these, principal components (PCA) or independent component (ICA) algorithms are the most common (C. Benar et al., 2003). For these methods exact knowledge about the onset of each cardiac cycle is not necessarily required, which is a major advantage over template based approaches. However, current evidence shows that spatial filtering is not as efficient as template methods, especially in scanners with higher field strength (Debener et al., 2007). The optimal strategy possibly lies

in the combination of ICA or PCA based algorithms with a template-based method such as AAS or OBS, combining the best of two worlds and even yielding good results even at higher field strengths (Debener et al., 2006).

Helium pump artifact

As the name already suggests the Helium pump (He) artifact results from kinetic activity of the scanner Helium pump. The pump causes vibrations that are transmitted from the compressor unit of the pump to the scanner bore. These vibrations generate large artifacts on the EEG signal, which can occur almost in the entire frequency range varying across different scanner types (Nierhaus et al., 2013). Specifically for the scanner used in this study (Siemens Trio) the He-pump induces additional broadband frequency power starting at 20 Hz (see Figure 13). This type of artifact was completely avoided in the study by switching the Helium pump off during scanning sessions.

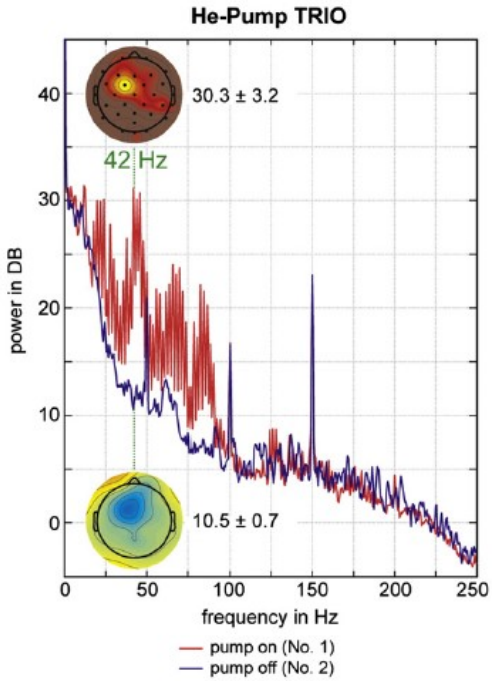

Figure 13: Impact of the Helium pump artifact to the EEG spectrum during co-registered EEG-fMRI in a SIEMENS Trio scanner in comparison to EEG data in which the artifact is avoided by switching off the Helium pump. Taken from: Nierhaus, T., Gundlach, C., Goltz, D., Thiel, S.D., Pleger, B., Villringer, Arno, 2013. Internal ventilation system of MR scanners induces specific EEG artifact during simultaneous EEG–fMRI. NeuroImage 74, 70–76.

Study 2 - Within trial distinction of O-R learning-related BOLD activity with the means of co-registered EEG information

Further EEG preprocessing

The session-wise segmented EEG data were down-sampled to 250 Hz and band pass filtered from 0.2 – 30 Hz. All EEG channels except the EOG and the ECG channel contributed to an average-based new reference. Ocular correction was performed using the regression-based implementation by Gratton and Coles (Gratton, Coles, & Donchin, 1983). Electrode-specific artifact rejection sorted out segments exhibiting a gradient in electrical activity greater than 50 µV/ms as well as segments exhibiting absolute differences of more than 200 µV within a 200 ms interval. EEG data were segmented time-locked to both the response and the stimulus, respectively. Response-locked epochs contained the manual response ranging from 750 ms pre-response to 700 ms post-response. Stimulus-locked epochs contained the stimulus S ranging from 250 ms pre-stimulus to 1500 ms post-stimulus. I did not apply a baseline-correction for the segmented EEG data.

In the following, response-locked and stimulus-locked epochs of EEG activity were averaged for each SRO repetition containing 40 correct trials per SRO repetition excluding trials rejected by artifact rejection. Likewise to study 1, for this latter analysis SRO-rep 1 was excluded to avoid a dominant contribution of initial instruction encoding. The segmented condition-wise (SRO-rep 1 to 8) single trial EEG data were then exported to Matlab for further statistical analysis.

Derivation of EEG parameters

Since study 1 already provided information about potential EEG correlates on both the rapid as well as the slower timescale with respect to S-R learning and O-R outcome related processes there was no need to rely on a purely exploratory analysis approach in this study. Instead, I assessed if the spatiotemporal ROIs identified in study 1 could be replicated on the EEG level. In case of a successful replication those ROIs were then used later as potential regressor in the EEG-informed analysis.

I specifically tried to replicate the three main findings of study 1. On the slower timescale (SRO-rep 23 – SRO-rep 78) these included the modulation of the post-response anterior negativity within the visual N1 latency range. Response locked effects were found prior to the any across the slower time scale as well as an ERP marker of stimulus-triggered pre-response outcome integration negativity maximizing at F1 (192 – 240 ms) and after the anterior negativity maximizing at FCz (304 – 352 ms). Modulations of the visual N1 were observed in both frontal sites maximizing at Fz as well as posterior sites with a maximum at Oz in a time range of

128 – 176 ms. On the rapid timescale (SRO-rep 1 – SRO-rep 3) I found an ERP marker associated with the initial encoding of newly instructed S-R associations at electrode F3 (416 – 464 ms) in study 1, which I also now looked for in study 2. To this end I again compared ERPs between SRO-rep 1 and SRO-rep 3. For the analysis of slower learning dynamics associated with more gradual changes in association strength I compared ERPs between early SRO repetitions (collapsed across SRO-rep 2 and 3, further called SRO-rep 23) and late SRO repetitions (collapsed across SRO-rep 7 and 8, further called SRO-rep 78). Likewise to the analysis procedure implemented in the pilot study, statistical significance was determined via paired t-tests for the averaged signal within a +/- 24 ms time window around the time point in which the learning-related modulation of electrical activity was maximized. Further, correlation analyses between amplitude differences confirmed in the replication statistics and the behavioral indices of interest (O-R compatibility, RT difference between SRO-rep 23 and 78, or error rates at SRO-rep 4) were performed.

Additionally to these predefined EEG markers I also did an explorative analysis with different EEG regressors varying in terms of combining electrodes to clusters or using a different time window. When varying time windows I only used other local maxima that were already present in study 1 regarding the difference in EEG activation between the two SRO-rep conditions of interest.

When replicating the previously found effects I was faced with two major issues, one regarding temporal and one regarding spatial concerns. For one, I experienced a time delay of about 40 ms when comparing the averaged ERP data of study 1 with the data of study 2, regardless of the fact that in both cases exactly the same design (including the exact same presentation durations and interval) was used (see example Figure 14). This temporal delay occurred in both, stimulus-locked and response-locked components and is most likely due to different hardware setups used in both studies.

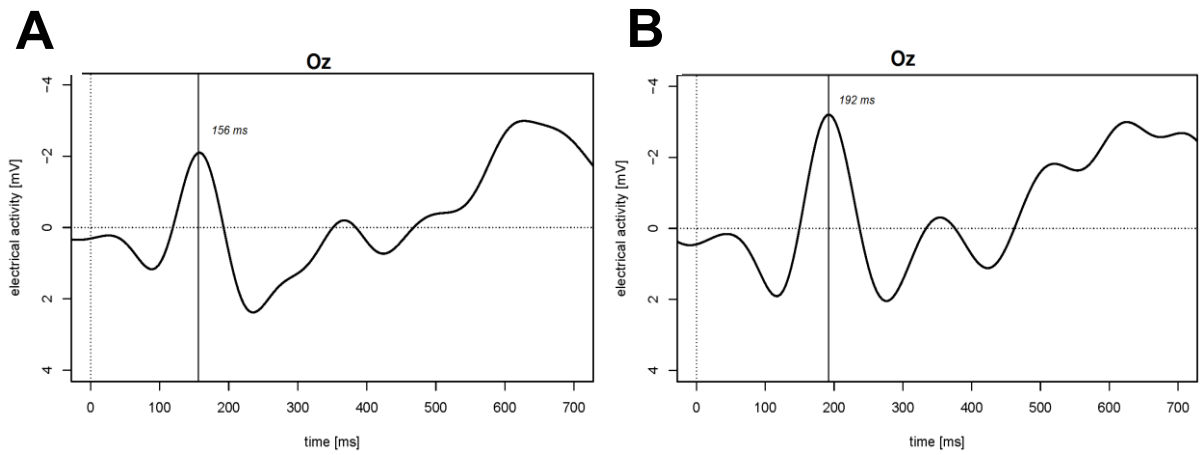

Figure 14: Averaged stimulus-locked N1 peaks at electrode OZ in (A) study 1 and (B) study 2 displaying the time delay of around 40 ms in study 2 with regard to study 1.

The second issue in comparing both datasets resulted from the fact that the actual electrode setup on the EEG caps was different in both studies. Although both caps were arranged based on the 10-20 System (Klem et al., 1999) there are slight differences in the electrode layout which lead to the fact that corresponding electrodes are not exactly superimposed to each other (see Figure 15).

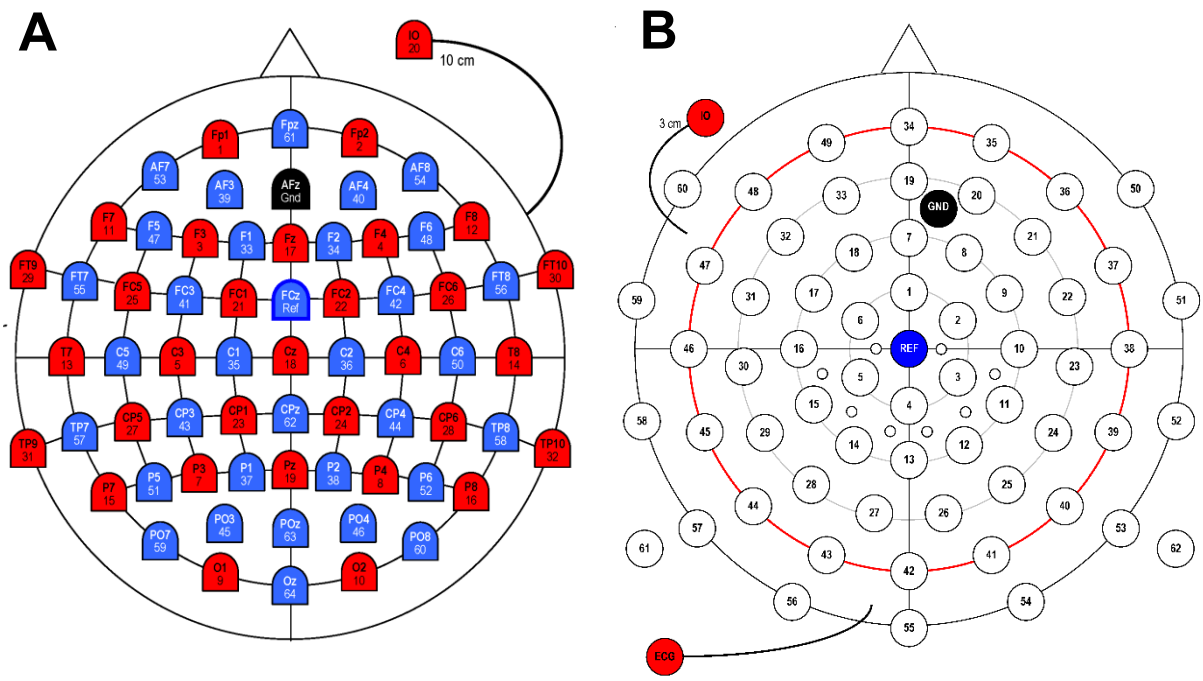

Figure 15: Different electrode cap layouts used in (A) study 1 and (B) study 2.

Those two circumstances had to be accounted for in the replication of the EEG effects identified in study 1. Specifically two measures were taken to avoid null findings that purely resulted from one of the two issues discussed above. First, since there is no exact electrode correspondence in both EEG cap setups, for the replication analysis I took the electrode identified in study 1, assigned the nearest electrode in the cap layout used in study 2 and allowed for a deviance of one neighboring electrode position. Secondly, due to the 40 ms time delay introduced in study 2 I also allowed for a 40 ms shift of time windows between study 1 and study 2.

EEG informed fMRI analysis

First level analysis

The main analysis in this study focused on the fusion of both EEG data as well as fMRI data in a combined GLM in which a predefined EEG parameter serves as additional regressor in order to modulate BOLD activation. To this extend the extracted EEG Parameters (stimulus-locked and response-locked instances of SRO repetition 1 to 8) were imported into Matlab and fused with the fMRI onsets with a module called *parametric modulation* implemented in SPM

8. Via parametric modulation, it is possible to alter the stick function representing the fMRI onsets. In the SPM design matrix these stick functions are used to model the occurrence or absence of a specific event indicated in a specific (task) regressor. There are only two values possible, 0 (for absence of the event) and 1 (for presence of the event). The parametric modulation adds a new regressor for every event type. Regressors have indicator functions for events or epochs that are modulated in amplitude by some variable, in this case the preselected EEG parameter. Convolution with the hemodynamic response function (HRF) results in an EEG-weighted BOLD regressor that contains information on the strength of the correlation between the EEG parameter and the observed BOLD activation in each single trial (see Figure 16 left). Depending on the nature of the correlation, the additional information of the EEG parameter will lead to either an increase or a decrease of the predicted BOLD response in a specific voxel (see Figure 16 right). Eventually, the EEG-informed analysis is predestined to reveal only activation in those brain regions that highly correlate with activation in the predefined EEG parameter of interest used in the joint analysis.

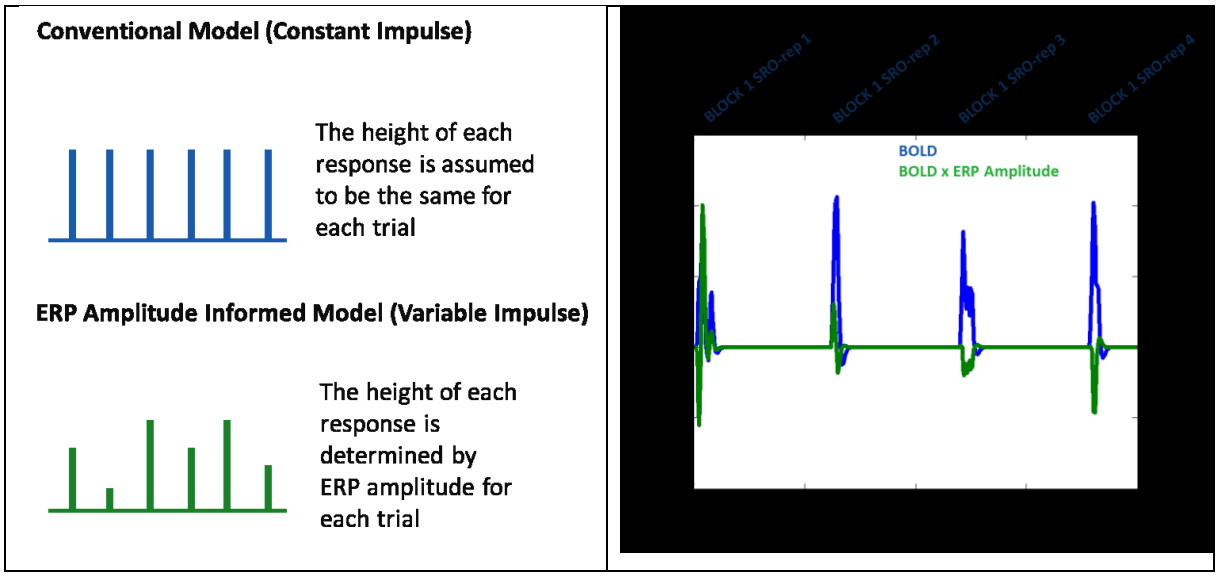

Figure 16: (Left) Convolution of fMRI onsets with the additional EEG regressor. Stick functions are modulated individually varying from trial to trial. (Right) Negative correlation of the ERP regressor with the BOLD response may lead to attenuation of the fMRI signal.

The additional EEG regressor was added to the GLM condition-wise (SRO-rep 1 to 8) and contained the average value of electrical activity per SRO repetition over the entire time window (48 ms), resulting in eight additional EEG regressors convoluted with the HRF. I then used two separate one-sample t-tests to assess the correlation of the EEG parameters with

the BOLD signal. First for both rapid time scale as well as slower timescale, I contrasted all conditions of interest (either SRO-rep 1 to 3 or SRO-rep 1 to 8) against baseline to get a general idea of the strength of the effects. Furthermore, I then calculated one-sample t-tests between either SRO-rep 1 and 3 to access specific neural changes on the rapid timescale. Analogously, one-sample t-tests to compare the concatenated conditions SRO-rep 23 and SRO-rep 78 to access changes on the slower time scale.

Second Level analysis

The second level GLM utilized the EEG-modulated fMRI regressors to calculate t-statistics on the group level. The model also contained behavioral markers O-R outcome integration (RT compatibility, RT difference between SRO-rep 23 and 78) in the analysis of the slower time scale. O-R learning markers were included simultaneously in order to ensure that a possible correlation between EEG-informed fMRI effect and a covariate was exclusively determined by a covariance component that was orthogonal to the other covariate. Thus, the potential influence of the other covariate was being regressed out. On the rapid time scale, contrasts were defined using the EEG-modulated fMRI regressors between SRO-rep 1 and SRO-rep 3. This model additionally contained error rates at SRO-rep 4 as behavioral covariate. Significant correlations were only taken into account if they exceeded a family-wise-error (FWE) threshold $p < .05$, either on the voxel level or on the cluster level at a cluster-forming threshold of $p < .001$. T-values reported in the results section (see 5.3) represent the behavioral marker-adjusted BOLD activation.

Figure 17 depicts the entire preprocessing pipeline of both the EEG as well as the fMRI data down to their final shape in which they are unified in an EEG-informed fMRI GLM.

Study 2 - Within trial distinction of O-R learning-related BOLD activity with the means of co-registered EEG information

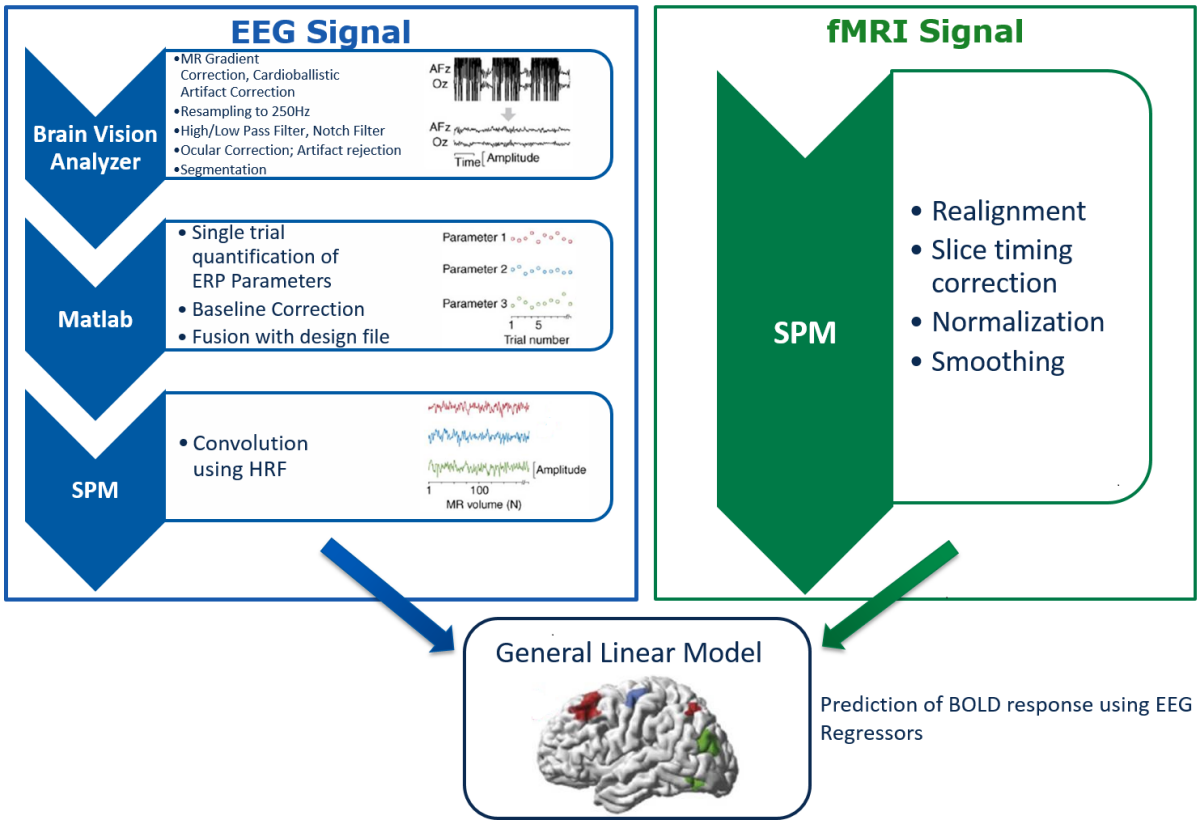

Figure 17: Preprocessing stream for EEG-fMRI analysis.

Feasibility analysis

In a first step, I wanted to asses if the fundamental process of extracting and correlating EEG parameters with the BOLD response would produce plausible results. Therefore, I utilized three distinct and to my reasoning isolated mean EEG parameters averaged over all SRO repetition levels to predict the mean BOLD signal against baseline accumulated over all SRO repetition levels. Namely, I used the EEG motor signal at the time of the response (+/- 25 ms), derived from a cluster of centro-parietal electrodes (CP1, CPz, CP2, P1, P2). I hypothesized that the EEG motor response signal would be highly associated with corresponding activation in motor areas of the brain. Accordingly, I used the stimulus-locked visual N1 peak amplitude (192 ms +/- 25 ms) at posterior sites (O1, OZ, O2, POz) to check if it would predict activation in visual areas of the brain. Finally, I assumed that the response-locked auditory N1 peak amplitude (268 ms +/- 25 ms) at central sites (Cz, C1, C2, CPz) would predict activation in auditory areas of the brain.

5.3 Results

Behavioral results

S-R-O learning phase

The general pattern regarding response times and error rates that was already present in study 1 was confirmed in study 2. Increasing SRO repetitions were associated with a drop of response times (RT) paralleled by an increase in error rates also in this study. The guided learning phase was characterized by a rapid gain in performance speed from SRO-rep 1 to SRO-rep 3. At SRO-rep 4 RT briefly increased due to the transition from the guided to the unguided phase before it continued to decrease gradually (see Figure 18a). The error rate curve was shaped similar to the one in study 1 with the typical peak at SRO-rep 4 (again due to the transition from unguided to guided learning phase) before gradually decreasing again across the unguided phase (see Figure 18b). The analysis resulted in highly significant effects in the factor *SRO repetition* within the saturated model compared to the null model for both error rates [$F(7,175) = 12.59$, $p < .001$] as well as RTs [$F(7,175) = 47.63$, $p < .001$]. The response time drop of 82 ms within the guided implementation phase (from 848 ms in SRO-rep 1 down to 766 ms in SRO-rep 3) exceeded significance threshold applying post-hoc Tukey-test corrected for multiple comparisons [$p < .001$]. The RT decrease from SRO-rep 1 to SRO-rep 3 predicted smaller error rates in SRO-rep 4 [$r(24) = -0.31$, $p < .03$], being a marker of early formation of S-R associations formation and usage during the guided instruction phase (see Figure 18c). Again for the purpose of assessing RT differences on the slower timescale accordingly to the later EEG analysis I collapsed SRO repetitions 2 and 3 (SRO-rep 23) as well as 7 and 8 (SRO-rep 78) to compute another post-hoc Tukey-test corrected for multiple comparisons which yielded a significant result [$p < .001$]. Regarding error rates, a post-hoc Tukey-test revealed a highly significant increase in error rates from 3% at SRO-rep 1 to 14% at SRO-rep 4 [$p < .001$, Bonferroni-corrected for multiple comparisons], again indicating the transition from the guided to the unguided implementation phase in which responses now had to be selected according to memorized S-R associations from the preceding three guided trials. Following this initial error rate increase it than decreased again down to 6% at SRO-rep 8 [$p < .001$].

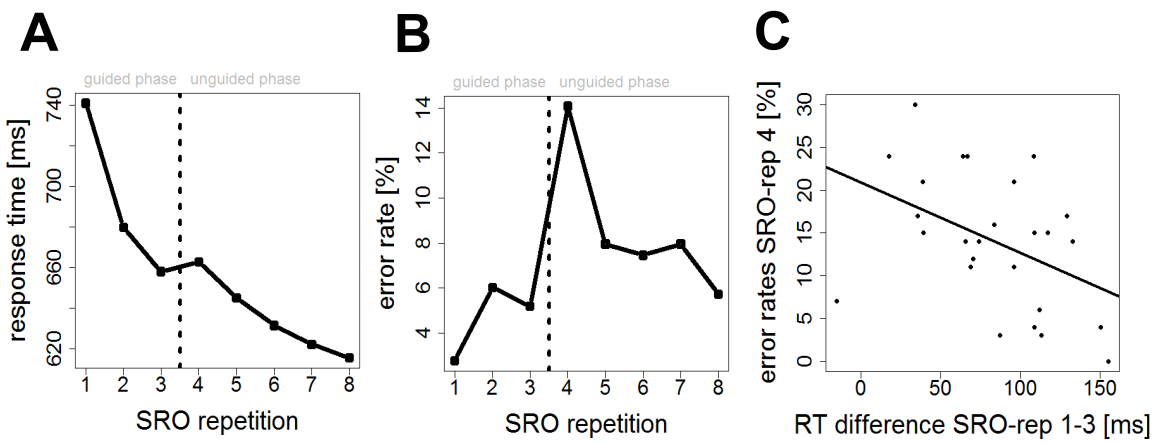

Figure 18: Behavioral data from the S-R-O acquisition phase with (A) mean response times (RT) and (B) mean error rates (%) throughout the course of all eight SRO repetitions. (C) Correlation between the difference in response times between SRO-rep 1 and SRO-rep 3 and error rates in SRO-rep 4. A sharper response time decrease from SRO-rep 1 to SRO-rep 3 predicted lower error rates in SRO-rep 4.

O-R test phase

I again computed two separate linear mixed-effect models for accuracy und response time with factors compatibility and SRO repetition as fixed effect and variance over all trials within each subject being random effect. The analysis resulted in highly significant O-R compatibility effects for both, error rate [$F(1,200) = 9.96$, $p = .002$] with an average of 12% error trials in the compatible condition and 14% error trials in the incompatible condition as well as response times [$F(1,200) = 8.61$, $p = .004$] with an average of 592 ms in the compatible condition and 609 ms in the incompatible condition. There was no significant interaction effect between SRO repetition and compatibility in both error rates as well as response times. The subject-wise behavioral index of O-R encoding strength which was later used for correlation with ERP difference measures was defined as the individual O-R compatibility effect in RT, following the rationale of study 1. Additionally, I verified if subjects exhibited an effect of response slowing as reported already in previous studies. To this end I correlated response time differences between SRO-rep 23 and 78 with the O-R compatibility effect from the test phase. The analysis resulted in an inverse correlation [$r(24) = -0.48$, $p = .014$]. Thus, high R-O learners were characterized by smaller absolute differences in response times between early and late stages of learning (see Figure 19).

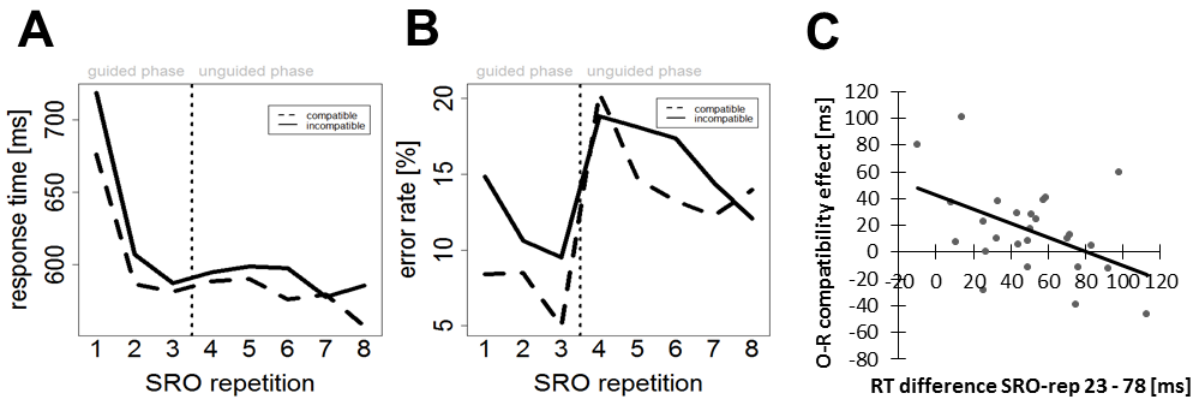

Figure 19: Behavioral data from the S-R-O test phase with (A) mean response times (RT) and (B) mean error rates (%) throughout the course of all eight SRO repetitions. (C) Correlation between O-R compatibility effect from the test phase and response time differences between SRO-rep 23 and SRO-rep 78 in the learning phase.

FMRI PPI analysis

As far as step 1 of the analysis procedure (as described above) is concerned general changes in functional coupling with the LPFC seed from early to late learning were observed. In accordance with previous findings (Ruge & Wolfensteller, 2013, 2015) I observed increasing functional couplings between LPFC and anterior caudate, as well as between LPFC and OFC (see Table 10).

However, I could not replicate significant correlations between each of the two behavioral covariates (O-R compatibility and R-O usage) and changes in fronto-striatal couplings as reported in earlier studies. More specifically, I did neither observe a correlation between O-R compatibility and LPFC-Putamen coupling strength nor a correlation between active R-O usage and LPFC-Caudate coupling. Regarding the control analysis there was also no significant correlation when entering the difference in error rates into the model.

Table 10: Functional coupling with LPFC during S-R-O learning (late-early, based on predefined ROIs).

Region of Interest		**MNI coordinates**			**coupling at late - early**				
	Sub-region	x	y	z	*t*	*z*	*p* Voxel (FWE-corr.)	Cluster Size	*p* Cluster (FWE-corr.)
Left basal ganglia	anterior Caudate	**-9**	**23**	**-5**	**5.73**	**4.43**	**.00**	**12**	**.02**
		21	5	22	3.69	3.22	.07	3	.05
Right basal ganglia	anterior Caudate	**8**	**17**	**13**	**4.88**	**3.98**	**.01**	**24**	**.01**
Left orbitofrontal cortex	anterior lat. OFC	**-39**	**29**	**1**	**4.71**	**3.88**	**.016**	**106**	**.039**
		-9	**23**	**-8**	**4.73**	**3.89**	**.03**	**210**	**.01**
		-15	**35**	**-11**	**4.42**	**3.70**	**.05**	**210**	**.01**

Additionally, there was an increased functional coupling between LPFC and the Supplementary Motor Area (SMA) which was significant on the whole brain level (see Table 11).

Table 11: Functional coupling with LPFC during S-R-O learning (late-early, whole brain).

Brain region	**MNI coordinates**			**coupling late - early**				
	x	y	z	*t*	*z*	*p* Voxel (FWE-corr.)	Cluster Size	*p* (FWE-corr.)
SMA	**-3**	**14**	**67**	**5.75**	**4.45**	**0.11**	**121**	**0.01**

ERP parameters

EEG data quality

When comparing EEG data quality between EEG recorded outside the scanner (study 1) and EEG data acquired in a co-registered EEG-fMRI session it is important to differentiate between two levels of data inspection: The averaged event-related response (ERP) data level and the single trial EEG data level.

ERP data level

On the averaged ERP level there is already a visible difference in data quality between the data of study 1 (EEG only) and study 2 (co-registered EEG-fMRI). Both ERP plots show strongly expressed stimulus-locked ERP components (see Figure 20). However, especially the first 125 time points (representing the first 500 ms), including the baseline period and the visual P1-N1 complex, are considerably noisier in the EEG data of study 2. Additionally, from time point 200 to 250 there seems to be also a greater variance in the EEG data of study 2, presumably as a result of a lower Signal-to-Noise ratio. This holds true for both of the collapsed conditions, SRO-rep 23 as well as SRO-rep 78, overall resulting in higher confidence intervals of the Grand averaged ERP in study 2. Note, that there is a time shift of about 40 ms between the two data sets due to different hardware in both recording setups.

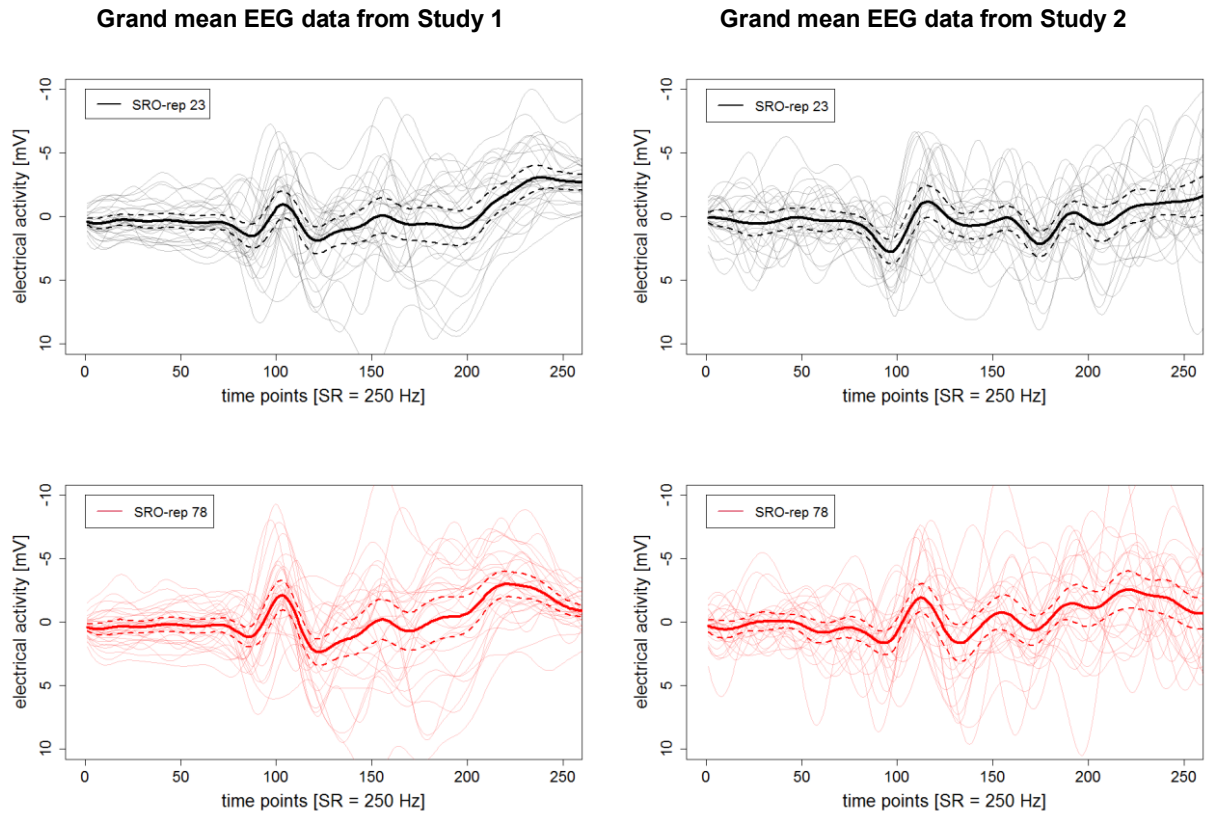

Figure 20: Stimulus-locked EEG activation at electrode OZ in study 1 and its corresponding electrode of study 2. The bold line represents the grand average ERP over all subjects, the dashed line represents the corresponding confidence interval. The transparent curves are the subject-wise ERP curves.

Single trial data level

On the level of segmented single trials even greater differences between the two data sets can be observed. The plots in Figure 21 depict segmented ERP data on a single trial level. The segments are locked to the visual stimulus. On the y-axis all trials across the entire learning phase are plotted on top of each other. This kind of plot can be used to inspect how stable ERP components are on the single trial level or to observe temporal shifts in ERP onsets. Ideally, one would observe slim vertical columns of positivity or negativity as seen in both EEG only single trial plots.

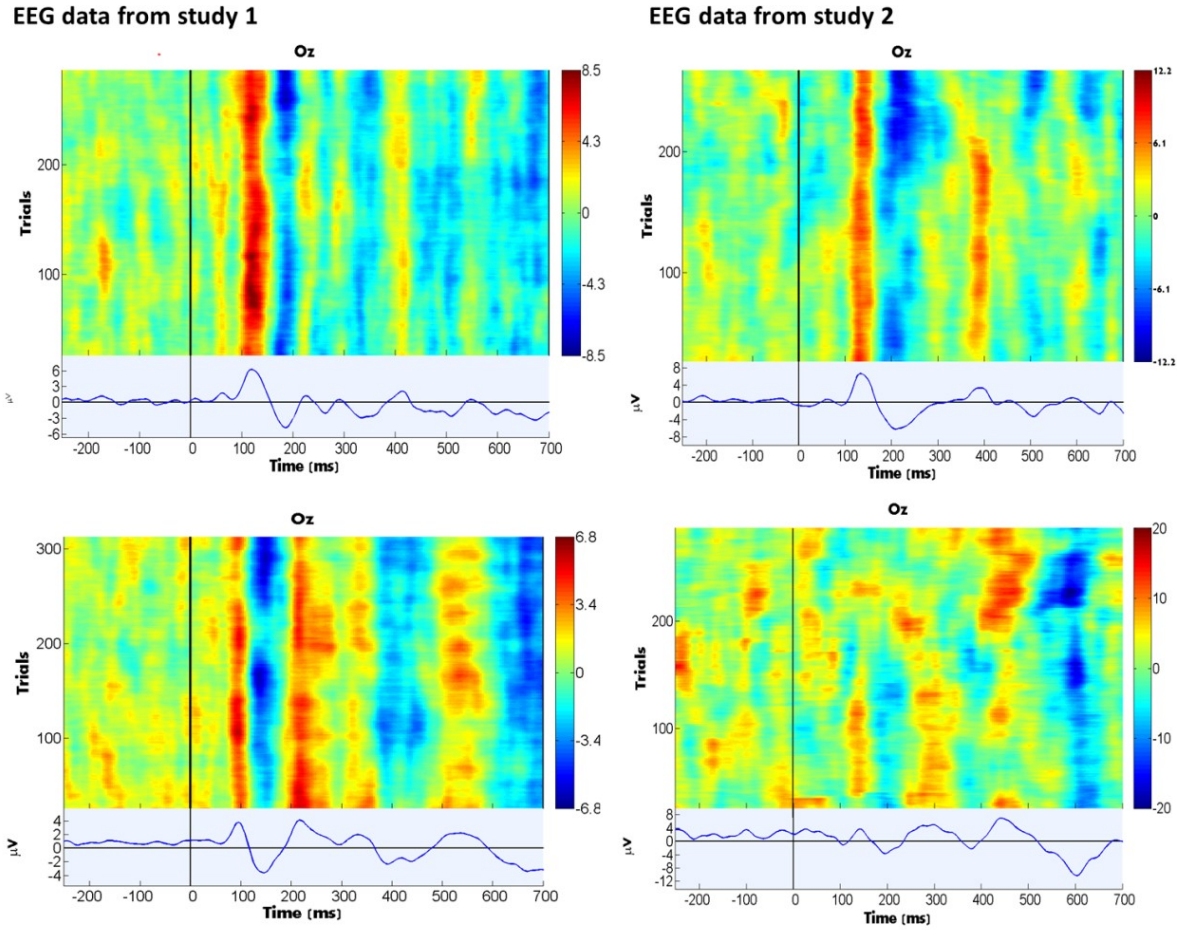

Figure 21: Single trial stimulus-locked EEG data at electrode OZ in study 1 and its corresponding electrode in study 2.

The averaged P1 and N1 are strongly expressed in almost every single trial across the entire session with no temporal deviation. On the right side of the figure two exemplary cases of single trial plots are depicted for EEG data from study 2. The upper one represents a subject in which ERP component resolution is close to the EEG only data. In this case again the P1

and N1 are also expressed well in almost each single trial. However, this fact does not hold for every subject and there is a tremendous amount of variation within the dataset. The lower plot depicts a case in which ERP components are virtually not identifiable on single trial level. This great variation among trials also contributes to the fact that the averaged plot for that subject lacks prominent shaped ERP components. While a loss in data quality of EEG data acquired from co-registered EEG-fMRI can be compensated for by the averaging procedure of the ERP method this does not apply when trying to analyze the data on a single trial level and a higher noise ratio in this case may cause problems concerning effect strength or power.

O-R outcome related response-locked anterior/central negativity

The analysis identified a maximum difference in electrical activity between SRO-rep 23 and SRO-rep 78 at the electrode equivalent to FC3 in a time range 268 to 316 ms [$t(25) = 2.69$, $p = .012$]. This negativity increase was significantly correlated with the response time O-R compatibility effect [$R^2_{adj.} = .21$, $F(3, 25) = 4.32$, $p = .026$]. However, this correlation pointed towards the opposite direction compared to the correlation observed in study 1 with greater differences being associated with greater compatibility effects [$b = .019$, $t(25) = 2.13$, $p = .044$]. Likewise to study 1, I also observed a significant increase in negativity prior to the peak of the post-response anterior negativity as well as another massive negativity increase at a central cluster of electrodes over the learning course ranging from 400 to 626 ms post-response and maximizing at 484 ms at electrode CPz (see Figure 22). These differences, however, were not correlated with the behavioral marker of O-R compatibility or any other behavioral marker.

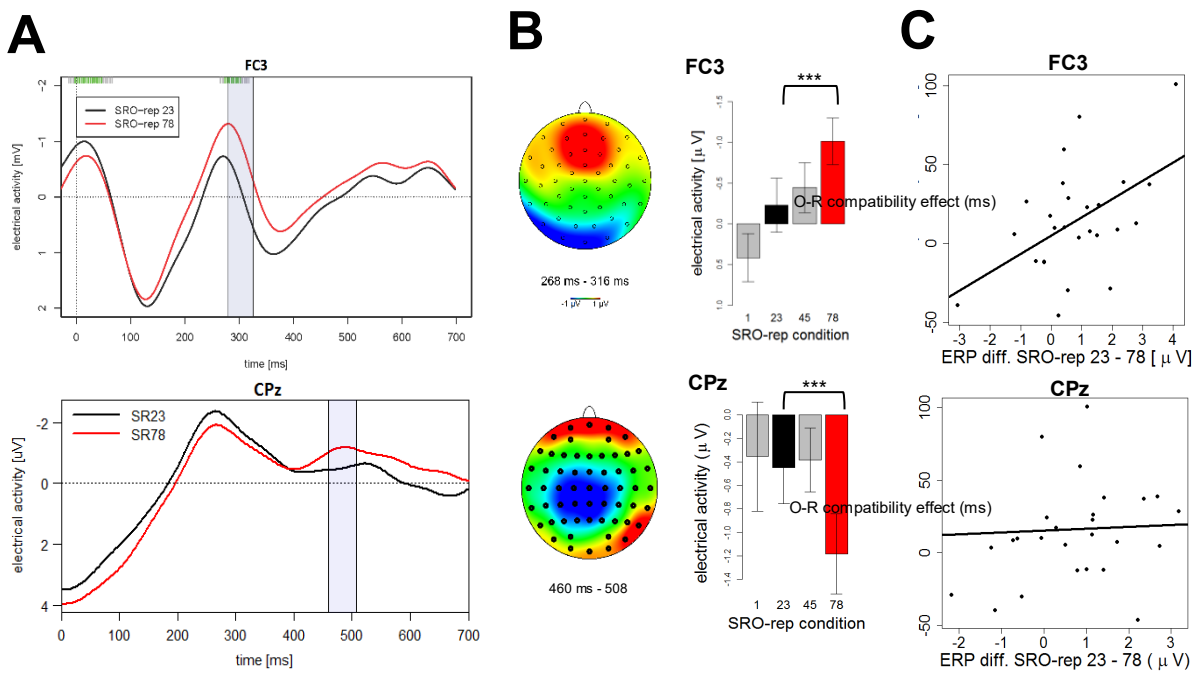

Figure 22: Response-locked grand average waveforms exhibiting significant learning-related effects across SRO-rep 23 and SRO-rep 78. The interval highlighted in light blue represents the time interval which was used for statistical analysis. The upper border of the plot displays time points at which the difference in electrical activity between SRO-rep 23 and 78 showed a significant correlation with the compatibility effect (gray: $p < .1$, green: $p < .05$, red: $p < .01$). Time point zero indicates the time of responding. The onset of the auditory outcome was at 150 ms. (B) Averaged topographical map of the difference in electrical activity between SRO-rep 23 and 78 within the specified time windows. Bar graphs for average electrical activity within the extracted time window are plotted for all factor levels that were used in both main and control analysis with the two levels depicted in ERP plots highlighted in black and red. (C) Scatter plots of electrical activity difference (for the time window in which the ERP difference was maximal) in relation to the O-R compatibility effect.

<u>O-R outcome related stimulus-locked modulation of the visual P1-N1 complex</u>

The analysis replicated previous findings of an increase in negativity in visual P1-N1 range at posterior sites, maximazing at O2 [$t(25) = 3.86$, $p < .001$, see Figure 23]. Just as in study 1, this modulation was correlated inversely with the O-R compatibility effect [$R^2_{adj.} = .2$, $F(3, 25) = 4.12$, $p = .026$]. Hence, smaller differences in EEG activity were associated with stronger compatibility effects [$b = -.032$, $t(25) = -2.67$, $p = .014$]. Likewise to study 1, I also observed this effect at frontal electrode sites as well as another maximum difference between early and late learning conditions peaking at around 600 ms at posterior sites. However, these differences were not correlated with the compatibility effect or any other behavioral marker.

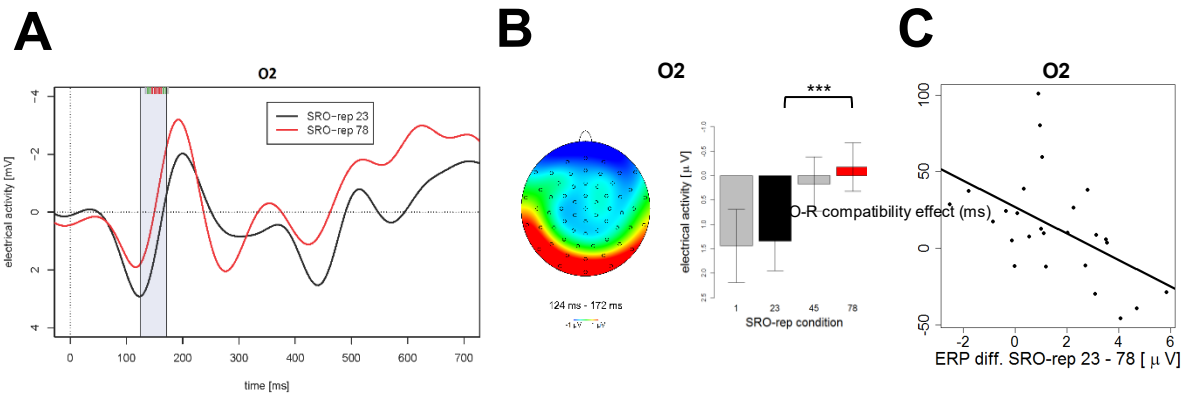

Figure 23: (A) Stimulus-locked grand average waveforms exhibiting significant learning-related effects across SRO-rep 23 and 78 at occipital electrode Oz. The intervals highlighted in light blue represent the time intervals which were used for statistical analysis. The upper border of the plot displays time points at which the difference in electrical activity between SRO-rep 23 and 78 showed a significant correlation with the compatibility effect (gray: p < .1, green: p < .05, red: p < .01). Time point zero indicates the time of visual stimulus onset. (B) Averaged topographical map of the difference in electrical activity between SRO-rep 23 and 78 within the specified time window (124 ms - 172 ms). Bar graphs for average electrical activity within the extracted time window are plotted for all factor levels that were used in both main and control analysis with the two levels depicted in ERP plots highlighted in black and red. (C) Scatter plots of electrical activity difference in relation to the O-R compatibility effect (for the time window in which the ERP difference was maximal).

S-R learning-related stimulus locked frontal positivity

The change in positivity about 488 ms after presentation of the imperative stimulus was also prominent in this study at similar electrode sites [$t(25) = -2.87$, $p = .008$]. In this study, the correlation of this EEG effect with error rates at SRO-rep 4 was not replicated (see Figure 24).

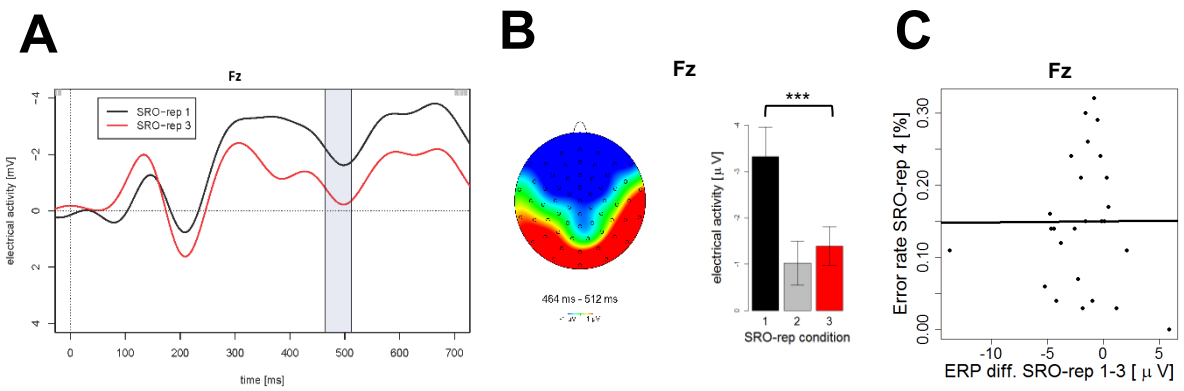

Figure 24: (A) Stimulus-locked grand average waveforms exhibiting significant learning-related effects across SRO-rep 1 and 3. The interval highlighted in blue represents the time interval which was used for statistical analysis. The upper border of the plot displays time points at which the difference in electrical activity between SRO-rep 23 and 78 showed a significant correlation with the compatibility effect (gray: p < .1, green: p < .05, red: p < .01). Time point zero indicates the time of visual stimulus onset. (B) Averaged topographical map of the difference in electrical activity between SRO-rep 1 and 3 within the specified time window (464 ms – 512 ms). Bar graphs of average electrical activity in all three guided SRO repetitions. (C) Scatter plots of electrical activity difference in relation to error rates at SRO-rep 4 (for the time window in which the ERP difference was maximal). Note that the depicted error rate values are rescaled as an impact of regressing out the RT speed-up from SRO-rep 1 to SRO-rep 3 and only correct trials were included in the ERP analysis and contributed to the plotted results.

EEG-informed fMRI analysis

Feasibility analysis

Table 12 shows the results of the analysis. Correlating the EEG motor signal at the time of the response with the fMRI signal resulted in significant bilateral activation of the postcentral gyrus as well as the right insula. The activation clusters of the postcentral gyrus also extended into the parietal operculum which is a functional equivalent to the secondary motor cortex (Beudel, Zijlstra, Mulder, Zijdewind, & de Jong, 2011; Eickhoff, Grefkes, Zilles, & Fink, 2007). The activation in those regions was positively correlated with response time differences between SRO-rep 23 and 78. The stimulus-locked visual N1 peak amplitude or the response-locked auditory N1 peak amplitude were not associated with any significant activation in the brain.

Table 12: Predicted brain activation by response-locked EEG motor response signal (centro-parietal electrode cluster).

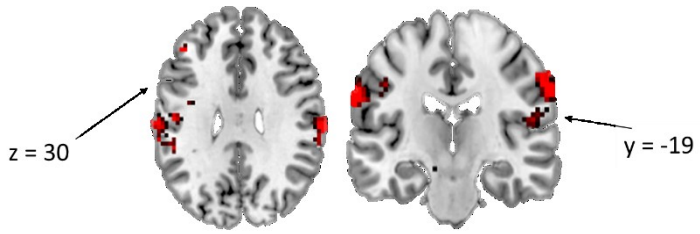

Brain region	MNI coordinates			Activation SRO-rep 1 to 8 associated with RT difference SRO-rep 23-78				
	x	y	z	*t*	*z*	*p* Voxel (FWE-corr.)	Cluster Size	*p* (FWE-corr.)
Right postcentral gyrus	60	-19	40	4.50	3.75	.60	127	.02
Left postcentral gyrus	-51	-10	22	4.49	3.74	.6	219	.002
Right insula	36	17	-8	4.42	3.7	.655	102	.009

FMRI activation associated with post-response EEG activation

In the EEG analysis I identified a post outcome increase in negativity from early to late learning stages at the electrode equivalent to FC3 in a time range from 268 to 316 ms. Contrary to study 1, this increase was even greater for high R-O learners (i.e. subjects that exhibited a particularly strong O-R compatibility effect). This EEG parameter was used to modulate the standard fMRI task regressor (SRO-rep level) in the EEG informed analysis. This procedure resulted in an increased coupling between the EEG negativity and activation in the right pre-motor cortex from early to late stages of learning (PMC, see Table 13). The analysis exhibited no significant correlation with any behavioral marker of R-O learning.

Table 13: Functional coupling with post-response EEG negativity (268 - 316ms) during S-R-O learning.

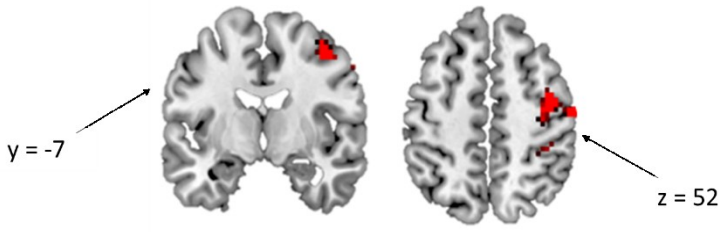

Brain region	MNI coordinates			Activation SRO-rep 23-78				
	x	y	z	*t*	*z*	*p* Voxel (FWE-corr.)	Cluster Size	*p* (FWE-corr.)
Right Premotor cortex	42	-7	52	5.97	4.47	.111	174	.001

Correlation at peak Voxel [42 -7 52]

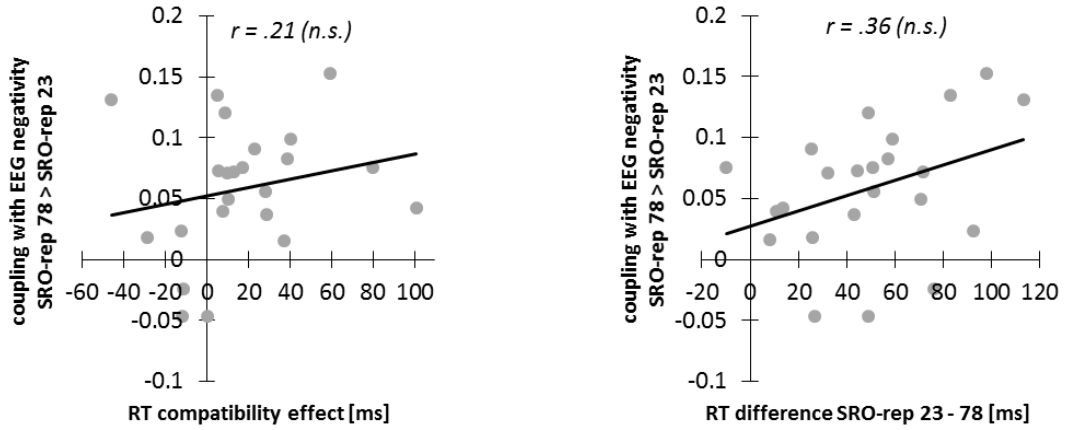

In the exploratory analysis, I used the late increase in negativity ranging from 400 to 626 ms subsequent to the response. The effect had a central local maximum peaking at 484 ms after the response and was not correlated with any behavioral marker of O-R learning. I clustered four central electrodes (equivalents to Cz, C1, C2, CPz) and used the averaged potential to modulate the standard fMRI regressors per SRO-rep level. This analysis resulted in a differential pattern with different coupling effects correlating with different behavioral markers of O-R outcome integration. An increased coupling between the late EEG negativity and activation in the SMA was positively correlated with the O-R compatibility effect (see Table 14).

Table 14: Correlation between functional coupling with post-response EEG negativity (460 - 508 ms) and RT compatibility effect during S-R-O learning.

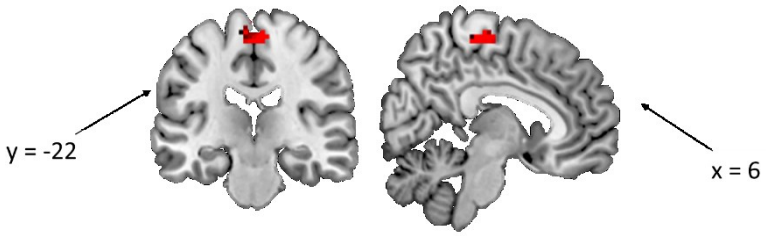

Brain region	MNI coordinates			Activation SRO-rep 23-78 associated with RT compatibility effect				
	x	y	z	*t*	*z*	*p* Voxel (FWE-corr.)	Cluster Size	*p* (FWE-corr.)
Supplementary motor area (SMA)	6	-22	64	5.16	4.07	.315	98	.024

Correlation at peak Voxel [6 -22 64]

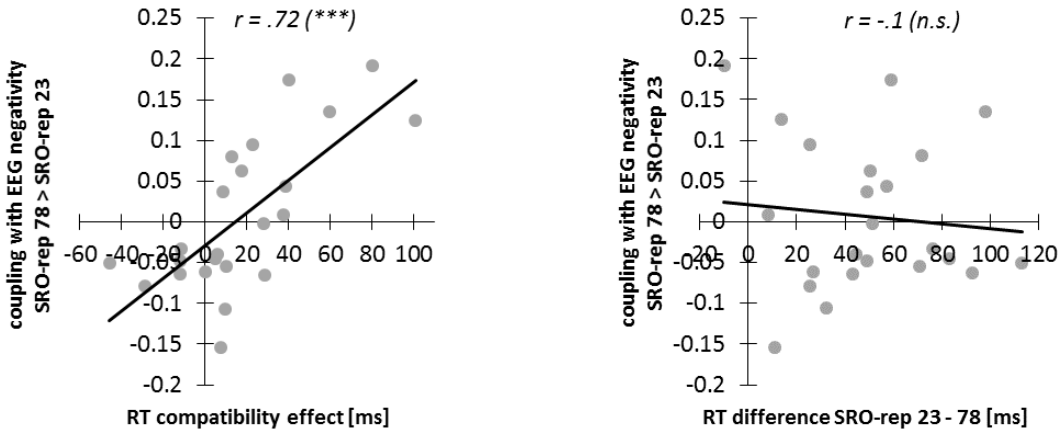

Increased couplings between the late EEG negativity and activation in the somatosensory cortex as well as the dorsal lateral caudate, on the other hand, were positively correlated with reaction time differences between SRO-rep 23 and SRO-rep 78 during S-R-O learning (see Table 15). Note, that the coupling effect in the cluster of the dorsal caudate also extended into the white matter as well as some parts of the medial prefrontal cortex (mPFC).

Table 15: Correlation between functional coupling with post-response EEG negativity (460 - 508 ms) and RT difference SRO-rep 23 - 78 of during S–R–O learning.

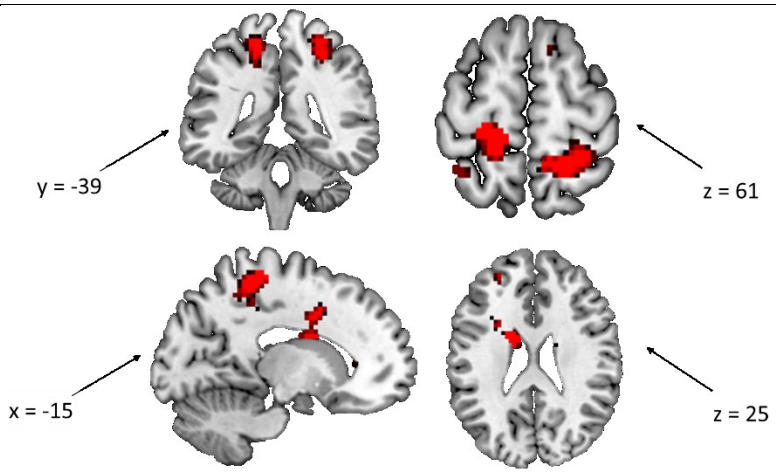

Brain region	MNI coordinates			Activation SRO-rep 23-78 associated with RT difference SRO-rep 23-78				
	x	y	z	*t*	*z*	*p* Voxel (FWE-corr.)	Cluster Size	*p* (FWE-corr.)
Somatosensory cortex (r)	21	-46	67	7.66	5.18	.006	745	.000
Somatosensory cortex (l)	-15	-34	61	7.37	5.07	.011		
Left caudate	-15	2	25	6.91	4.89	.023	229	.000

Correlation at peak Voxel [21 -46 67]

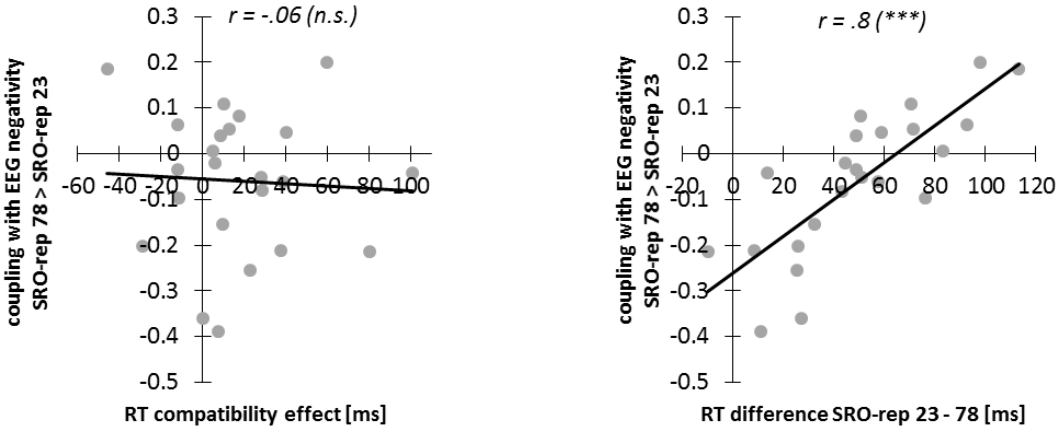

Correlation at peak Voxel [-15 2 25]

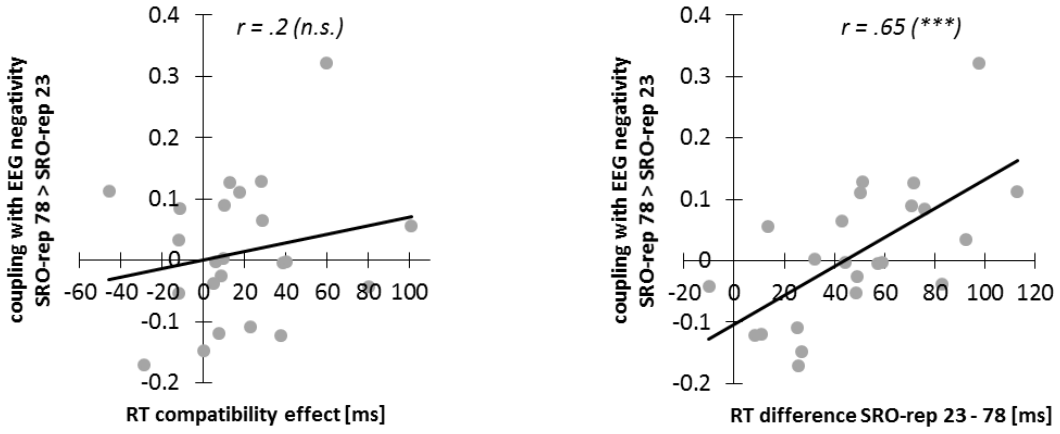

Study 2 - Within trial distinction of O-R learning-related BOLD activity with the means of co-registered EEG information

FMRI activation associated with pre-response EEG activation

In the EEG analysis, I identified an increase in negativity in the visual P1-N1 (124 – 172 ms) range at posterior sites, maximizing at electrode O2. This increasing negativity, however, was attenuated for high R-O learners resulting in an inverse correlation with the behavioral RT compatibility effect. I used the visual P1-N1 component in the fMRI analysis to allow for a gradual change of the standard fMRI task regressors (SRO-rep level). The analysis revealed an increasing coupling between the P1-N1 modulation and activation in the orbital frontal cortex (OFC), more specifically the right orbital inferior frontal gyrus (OIFG, see Table 16). Furthermore, this coupling effect was positively correlated with the RT difference between SRO-rep 23 and 78.

Table 16: Correlation between O-R usage and functional coupling with pre-response EEG negativity (124 - 172 ms) during S-R-O learning

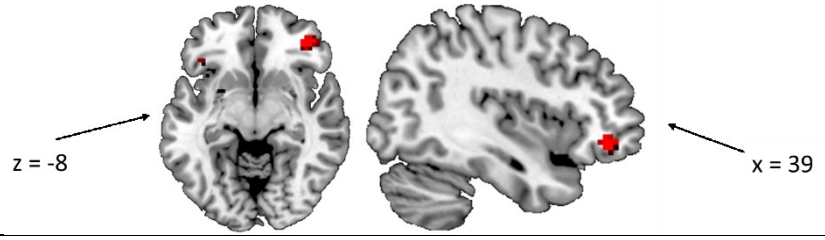

Brain region	MNI coordinates			Activation SRO-rep 23-78 associated with RT difference SRO-rep 23-78				
	x	y	z	*t*	*z*	*p* Voxel (FWE-corr.)	Cluster Size	*p* (FWE-corr.)
Right orbital inferior frontal gyrus	39	44	-8	6.89	4.98	.01	75	.06

Correlation at peak Voxel [39 44 -8]

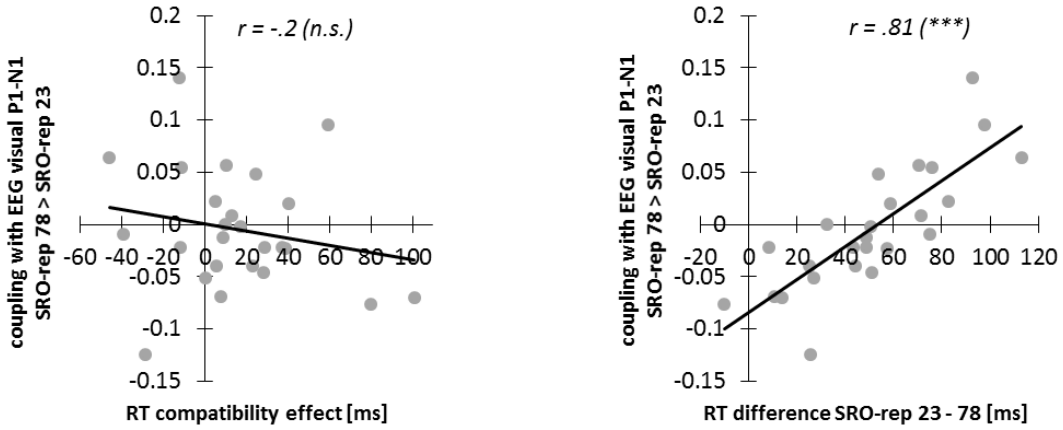

There was no significant BOLD activation associated with the pre-selected S-R learning-related pre-response EEG signal (see Figure 24). Additional explorative analysis with

stimulus-locked local maxima (e.g. using the late posterior peak around 600 ms at O2) also did not yield any significant results.

5.4 Discussion

This study followed up on the results of study 1 using the same paradigm. Its overarching goals were to reproduce the learning-related EEG parameters observed in study 1 and to utilize them in a joint EEG-fMRI analysis. With this type of analysis I strived to make use of specific EEG parameter information in order to disentangle temporarily overlaying information in the fMRI BOLD signal. Specifically, I tried to separate learning-related pre-response brain activation, associated with action selection and initiation, from post-response activation potentially reflecting outcome integration processes.

Additionally, this study served to replicate earlier findings of Ruge and Wolfensteller (2015). They found that O-R encoding strength is associated with LPFC-putamen coupling, prompting that this particular brain region is involved into the formation O-R associations. The active usage of O-R associations on the other hand correlated with LPFC-caudate coupling. They concluded that the caudate therefore seems to act as a control instance for goal-directed actions, especially in an instruction-based learning environment.

FMRI PPI replication

I again observed previously reported general patterns of increasing functional coupling from early to late S-R-O learning trials between LPFC and anterior caudate as well as LPFC and OFC (Ruge & Wolfensteller, 2013, 2015). However, I did not replicate earlier findings of a distinction of functional fronto-striatal couplings related to distinct behavioral markers of either O-R encoding strength or active O-R usage. Additionally, there was an increased coupling between LPFC and SMA as S-R-O learning progressed. Functional connections between SMA and PFC have been reported before (Rowe, Robinson, & Gordon, 2005). Although this coupling was not correlated with markers related to response-outcome learning later results of the EEG-informed analysis might point towards the nature of these effects. The reason why I could not identify or replicate correlations with these behavioral markers remains unknown. One reason might lie in in a lack of power of these markers in this study itself. Although present and significant, the O-R compatibility effect was not as pronounced as expected from previous studies, potentially resulting in a non-significant correlation in the PPI analysis.

EEG analysis

Regarding EEG data quality, there already was a greater amount of noise visible in the extracted EEG signal from the simultaneous EEG-fMRI session when compared to the data from the EEG only set up. Thus, the Grand Average ERP from this study exhibited broader confidence intervals in comparison to EEG data acquired outside the scanner. This could already have had an effect on the power of individual EEG effects and also its potential correlations with behavioral indices.

In the confirmatory analysis, the primary goal was to elaborate on those spatiotemporal ROIs that showed a clear correlation with one of the behavioral markers of either R-O outcome integration or S-R learning. Exploratory analysis included a shift in time windows or clustering of multiple electrodes. Furthermore, I performed an additional exploratory analysis regarding a strongly pronounced late response-locked EEG effect that was present in both studies, although it was not correlated with any behavioral marker. In general, study 2 was only partially able to replicate the EEG activity dynamics related to the formation of bidirectional R-O associations that were observed in study 1.

EEG-informed fMRI analysis

Feasibility analysis

The goal of this procedure was to check if the chosen means of fusing two different data modalities in a joint analysis would produce plausible results. Eventually, only one of the three chosen EEG parameters could be associated with brain activity. The ERP motor signal predicted significant activation in a cluster including the postcentral gyrus as well as the parietal operculum. The latter region has been marked as functionally corresponding to the secondary motor cortex (SII, Beudel et al., 2011; Eickhoff et al., 2007). There was no coupling between the stimulus-locked visual N1 nor the response-locked auditory N1 and activation in respective sensory areas of the brain. The coupling between the EEG motor signal and activation in the postcentral gyrus and SII was also positively correlated with a general decrease in response times between early and late stages of learning. Hence, it was stronger for subjects exhibiting greater reaction response time decreases. This could be due to the fact that those subjects are better learners, thus exhibiting stronger neural activity. Overall, with only one of the three analyses being significant (and only in combination with a behavioral marker), this sheds only a dim light on answering the question if EEG parameters and fMRI BOLD activation can be reliably fused with the means of EEG-informed analyses.

FMRI activation associated with post-response EEG activation

In this study, I observed an increased coupling between electrical activity in the post-response post N1 signal and activation in the premotor cortex (PMC) between early and late stages of learning. The coupling increase was not correlated with any behavioral marker of outcome-response learning. Regarding the EEG negativity effect found in this study, it is most likely not related to the sensory attenuation effects already observed in study 1 as several considerations indicate. First of all, the correlation points in the exact opposite direction compared to study 1, meaning that greater O-R compatibility effects were associated with greater increases in negativity. Secondly, the effect in this study is located subsequent to the peak amplitude while in in study 1 the corresponding effect was observed prior to the peak amplitude. Finally, the effect itself was not as pronounced and as prolonged as it was in study 1. Together with the fact that the time window and the electrode used in the analysis were slightly shifted (see chapter 5.2) it is reasonable to assume that the effect of sensory attenuation observed in study 1 was not replicated in this study. So how can the increased coupling between post response EEG negativity and activation in the PMC be interpreted? The PMC has been suggested to play a role in action-related processes (Picard & Strick, 1996, 2001). It has been found that in outcome-response learning there seems to be an engagement of this region in preparatory processes if the action is associated with a distinct effect which is also pre-activated via action codes (Ruge, Muller, & Braver, 2010). The results of this study prompt the interpretation that this mechanism could also be at play here. Moreover, the coupling increase between post-response negativity in the EEG signal (which in itself was positively associated with O-R encoding) and activation in the PMC further strengthens the point that PMC involvement in motor processes of an action is directly linked to the processing of its ensuing effect.

Additional exploratory analysis

The EEG analysis also identified a recurring post-outcome effect at central electrode sites which expressed a stronger negativity in late compared to early learning stages. This effect showed no correlation with any of the behavioral markers of learning in both studies. However, since this effect was very pronounced and was reliably observed in both studies I also performed an additional explorative EEG-informed fMRI analysis using this parameter. The analysis resulted in a pattern of distinct couplings with different brain regions, each correlated with different behavioral markers of S-R-O learning.

First of all, the analysis identified an increased coupling between the late EEG negativity and activation in the SMA that was positively correlated with the O-R compatibility effect. Thus, high R-O learners exhibited stronger coupling than low R-O learners. This correlation, together with the fact that SMA activation is correlated with a post-response EEG marker of O-R encoding, gives way to the interpretation that the SMA is involved in synchronizing the motor program of the just performed action to the sensory processing of the ensuing effect. Previous works have already suggested that this region plays a crucial part in post-response processes related to outcome integration. A number of studies have reported relevant SMA activation when perceiving outcome stimuli following extensive phases of R-O learning (Elsner et al., 2002; Melcher et al., 2008; Melcher et al., 2013). Bonini et al. (2014) suggested that early evaluation of the outcomes of actions is performed by the SMA. In accordance with Frimmel et al. (2016), the results of this study promote outcome-related SMA activation in extremely early stages of S-R-O learning. Moreover, they could shed light on the controversy if the SMA is involved rather in pre or post-response processes related with outcome response learning (Nachev et al., 2008). The correlation of SMA activation with a post-response post outcome EEG signal is a strong indicator favoring the later assumption. As the PPI analysis of the fMRI only data revealed, activation in the SMA was equally functionally connected to activation in the LPFC (see paragraph *fMRI PPI replication* above). Overall, this might suggest that additionally to monitoring of actions in relation to its outcomes, the motor program of the performed action is linked to the internal representation of R-O contingencies cached in the LPFC “procedural working memory” (Oberauer, 2009). If so, this established link might enable a later pro-active activation of the motor program in anticipation of the desired outcome which would work independent of a stimulus triggering the response. Hence, post-response activation of the SMA and its functional coupling with the LPFC might enable actions to become anticipatory, i.e. goal-directed, in the absence of an imperative stimulus in the first place. This mechanism would be equivalent to the second phase in the two-phase model of goal-directed action according to ideomotor theory (Shin et al., 2010).

Secondly, the analysis revealed an increased coupling between the late EEG negativity and activation in the somatosensory cortex as well as the dorsal caudate that were positively correlated with reaction time differences between SRO-rep 23 and SRO-rep 78 over the S-R-O learning course. Activation in the anterior caudate is generally believed to be involved in the establishment of goal-directed action (J. O'Doherty et al., 2004; Tanaka et al., 2008; Tricomi et al., 2004) and has already been demonstrated in various studies (Ruge & Wolfensteller, 2010; Stocco, Lebiere, O'Reilly, & Anderson, 2012). Ruge and Wolfensteller (2015) reported an increased coupling of activation between LPFC and anterior caudate in a PPI analysis that was associated with the behavioral marker of response slowing. The coupling effect in this

study with the late negativity in the EEG signal, however, showed activation in the dorsal parts of the caudate which has not been brought primarily into connection with the effects described above. The results of this study could prompt the conclusion that caudate involvement into processes of O-R learning, more specifically active monitoring of the learning process, can also be generalized to more dorsal parts of this region. This hypothesis, however, must remain speculative based on the exploratory results of the analysis approach and the fact that it is not supported by other research so far. But there is existing evidence that the dorsal striatum, and the dorsal part of the caudate in particular, are critical in the formation and control of habitual action (Burton, Nakamura, & Roesch, 2015; Haber & Knutson, 2010). Thus, another hypothesis regarding the coupling effect in the dorsal caudate could be that it might be connected to an early automatization of the acquired behavior. Automatization in this case would refer to the ongoing consolidation of the learned S-R-O contingency in a sense that the agent has to rely less and less on an explicit evaluation of the outcome. This, however, has to be distinguished from an automatization in a sense of a habitualization of behavior as a result of long term learning. In summary, no final answer regarding the true nature of the coupling effect in the dorsal caudate can be given up to this point. However, it seems reasonable that the dorsal caudate functions as a region in which the acquired behavior might already be prepared to work in a more automatized manner without relying on the online evaluation of the ensuing effect. On a concluding note, it has to be kept in mind that activation in the basal ganglia is prone to artifacts due to its proximity to the cerebrospinal fluid in the ventricles. The cluster identified in this study also extended from the caudate over the white matter into the medial PFC. However, peak activation of this cluster was located in the dorsal caudate.

The coupling effect in the somatosensory cortex is likely related to R-O learning and a post-response consolidation of the just performed motor program. The superior postcentral gyrus has been described as being part of the cortical network that generates the readiness potential (Arezzo, Vaughan, & Koss, 1977; Ikeda & Shibasaki, 1992; Urbano, Babiloni, Onorati, & Babiloni, 1996). Furthermore, the somatosensory cortex projects to primary motor areas and in this way may essentially contribute to the preparation and execution of movements (Pleger et al., 2006; Porter, 1991, 1997). In this sense, increased activation in this area might also relate to the coupling effect seen in the SMA and could support the establishment of a more stimulus-independent use of the acquired R-O associations as the motor program could be activated by anticipation of the effect alone, as postulated by ideomotor theory.

Both, the coupling effect in the caudate as well as activation in the somatosensory cortex were correlated with response time differences between early and late stages of learning. Correlating reaction time differences between early and late stages of learning with the compatibility effect from the test phase revealed a significant response slowing for those

subjects that exhibited a particularly high compatibility effect in terms of reaction times. The original interpretation of this phenomenon was that it represents some kind of “monitoring cost” in the acquisition process that naturally is higher for better R-O learners. That is why this marker has been branded as a marker of O-R usage in previous studies (Ruge & Wolfensteller, 2015) as well as in the present one. Thus, if the neuronal coupling effect is connected to O-R usage, one would expect a negative correlation between coupling and reaction time differences between early and late learning stages. However, the analysis identified a positive correlation as a greater decrease in response times yielded a greater coupling between the EEG negativity increase and activation in these brain areas. This, however, seems to be contrary to the interpretation of this behavioral marker as a correlate of O-R usage. This issue suggests that the behavioral correlation with the coupling effect is not triggered by the response slowing rather than by the decrease in response times from early to late stages of learning itself. Another consideration could support this hypothesis. The response slowing effect in high R-O learners was initially interpreted as an “active usage of increasingly learned O–R associations through the S-O → O-R chain” (Ruge & Wolfensteller, 2015). Thus, it would make much more sense to see a correlation of this marker with neuronal activity in connection with response preparation or initiation, i.e. functional couplings with ERP parameters prior to the response.

But why does the late post-response post-outcome negativity difference in EEG signal was coupled with such seemingly distinct processes as O-R encoding in the SMA as well as response time decreases in the caudate and in the parietal lobe? The most reasonable answer might be that this late EEG signal is not a correlate of one process but a mixture between two different superimposed ERP components that are distinctly associated with either one of the activation patterns. This also might explain the missing correlation to a behavioral marker of R-O learning on the EEG data level in both studies as correlations of these distinct sub-processes to two different markers might have canceled each other out.

FMRI activation associated with pre-response EEG activation

I observed that learning-related modulations of the P1-N1 complex were increasingly associated with activation in the orbital Frontal cortex (OFC), specifically the orbital inferior frontal gyrus (OIFG) over the course of learning. Furthermore, that coupling was positively correlated with the RT difference between SRO-rep 23 and 78.

First of all, as this EEG attenuation effect could be perfectly replicated in this study it proves itself as a pronounced and reliable effect. Secondly, results from the EEG-informed

analysis do not seem to support my previously formed hypothesis that this effect mirrors early multisensory outcome integration processes (Murray et al., 2015). Multisensory integration describes the interaction between stimulus processing in different sensory modalities. In this case it refers to the visual imperative stimulus and the auditory outcome. Moreover, in this study multisensory effects would be based solely on the prior presentation of the bimodal information, i.e. the visuo-auditory stimulus outcome mapping. I speculated that visual outcome anticipation is triggered by the presentation of the visual stimulus, thus resulting in an attenuation of the P1-N1 ERP complex. Furthermore, I hypothesized that this attenuation effect could supposedly be coupled to increased activation in either primary visual or auditory cortex, or both. However, there was no activation in either of the primary sensory cortices that was associated with the attenuation effect in the P1-N1. Although the ventro-lateral prefrontal cortex has also been associated as a brain region involved in multisensory integration (Sugihara, Diltz, Averbeck, & Romanski, 2006) the question must be raised if the observed P1-N1 attenuation effect really reflects a pure correlate of multisensory integration (at least to a major part, see 6.2.1 for a discussion of this matter).

Then, how does the coupling increase between the P1-N1 complex in the EEG signal and activation in the OIFG fit into the picture? I speculate that the OIFG is a brain region that is highly associated with the representation of S-O information. The OIFG has been reported as part of the so called ventral visual stream which mainly has been associated with handling purely perceptual or working memory processes (Goldman-Rakic, 1987). However, Toni, Ramnani, Josephs, Ashburner, and Passingham (2001) found increasing activation in the OIFG in a supervised learning task of arbitrary sensorimotor associations. Subjects had to acquire knowledge about which key to press based on the visual presentation of an abstract symbol. The authors attributed increasing activation in the OIFG to the increased identification of the visual stimuli and their growing associative meaning to the correct response as learning progressed. Their results suggested that non-spatial visual information affects motor responses through a cortico-cortical route from the inferior temporal cortex to the ventral prefrontal convexity and the orbital surface. A review of the connectivity of these regions seemed to support their argument (Passingham, Toni, & Rushworth, 2000). Moreover, in this work they reviewed evidence that the prefrontal cortex, and even more specifically the inferior frontal gyrus is able to represent cues, responses, and outcomes. They concluded that the inferior temporal and the ventral prefrontal cortex are critical in integrating perceptual information with executive processes and their outcomes. Together with the results presented in this study, this suggests that the OIFG might serve as an interface of early outcome integration utilizing forward associations between the imperative stimulus and the anticipated outcome. These S-O couplings, are further used to form contingencies between the actual

required response and its consecutive (desired) outcome. The earlier an outcome is anticipated (based on stimulus outcome associations), the better it will be associated with its response, hence leading to stronger O-R compatibility effects later on seen on the EEG level. This account is consistent with the general notion that more salient events (here outcomes that are pre-activated sooner) will be associated with other events (here the action) more easily and more rapidly (Mackintosh, 1975; Le Pelley and McLaren, 2003). This could also explain the positive correlation with response time differences between early and late stages of learning seen on the fMRI level. As already discussed above, this fact also rules out an interpretation of the association as an instance of O-R usage as it would require a negative association between neural activity and RT differences.

Absence of FMRI activation associated with pre-response EEG activation connected to S-R learning

In both studies, I observed an increased learning-related frontal positivity in the mid-latency range between 464 and 512 ms post-stimulus. However, opposed to study 1, this change in activation was not correlated with any behavioral marker. Since in this case trial aggregation was done containing only one SRO repetition level (SRO-rep 1 or 3, as opposed to SRO-rep 2 and 3 or 7 and 8 in the slower time interval) it might be the case that this contrast lacked the statistical power to compensate the additional noise in the EEG data introduced by the MR environment. This might also the reason I did not observe any effects in the EEG-informed analysis using this EEG parameter.

6 Concluding general discussion

6.1 Brief assessment of study objectives

This dissertation set out to investigate neurocognitive mechanisms of instructed outcome-response learning. This was done employing two different imaging methods, namely EEG and fMRI. The first study aimed to identify potential EEG markers of rapid instructed learning. EEG and fMRI were then used in a consecutive combined study. The central goal was to use the additional EEG information to allow for a better within trial resolution of the otherwise temporarily coarse fMRI BOLD signal. This work could partially prove that learning-related EEG parameters can be reliably identified in repeated studies. Furthermore, pre- and post-response EEG markers could be associated with distinct brain activation and related to distinct sub-process of goal-directed action. In this concluding discussion results of both studies and its implications will be debated in an overarching context. Hereafter, the focus will lie on addressing several points regarding limitations of this work in terms of interpretations and conclusions that can be drawn from it. This will particularly include still existing data quality issues and resulting limitations on potentially more elaborate analysis methods of combined EEG-fMRI data. Eventually, strategies on how to possibly build upon the presented work will be debated.

6.2 Novel insights into rapid instruction based S-R-O learning?

The experimental paradigm used in both studies was specifically designed to investigate neurophysiological dynamics associated with the initial learning of bi-directional R-O associations under forced choice conditions by assessing correlations with the post-learning behavioral O-R compatibility effect as an index of the previously acquired association strength. This goes beyond earlier EEG (Waszak et al., 2012) and fMRI studies (Kuhn et al., 2010; Pfister, Melcher, Kiesel, Dechent, & Gruber, 2014; Ruge & Wolfensteller, 2010; Zwosta, Ruge, & Wolfensteller, 2015) which have revealed neurophysiological markers related to the impact of learnt R-O associations but which have not yet investigated the initial learning of such associations.

Study 1 prepared the combined main analysis by providing a blue print both in terms of EEG data quality as well as expected ERP parameters. Assessing ERPs provides the advantage to disentangle potential pre-response and post-response activation of goal-directed behavior as it was being learned. Study 2 comprised the simultaneous EEG-fMRI study. In the joint EEG-fMRI analysis the EEG signal served as additional information by correlating a specific ERP component that has been associated with distinct learning-related sub processes

in advance with the fMRI signal. In other words, the ERP signal served as a tool to dissect specific event-related BOLD information. Due to the sluggish nature of the BOLD response this was difficult to assess in previous sole fMRI studies which have begun to characterize the evolution of R-O integration processes across learning trials on multiple time scales of learning (Frimmel et al., 2016; Melcher et al., 2013; Mohr et al., 2015; Ruge & Wolfensteller, 2013, 2015).

6.2.1 Early stimulus outcome information retrieval indicates the transition from stimulus based behavior to goal-directed action

Study 1 identified stimulus-triggered pre-response outcome integration processes within the visual N1 latency range. In the later co-registered EEG-fMRI study this effect was replicated. Furthermore, EEG-informed fMRI analysis revealed that learning-related modulations of the P1-N1 are functionally coupled to increased activation in the orbitofrontal cortex (OFC), specifically the orbital inferior frontal gyruy (OIFG).

The OFC has been thoroughly brought in connection with associative learning, especially in connection with the anticipation with expected outcomes (Noonan et al., 2012; Roesch, Taylor, & Schoenbaum, 2006; Schoenbaum, Chiba, & Gallagher, 1998; Schoenbaum & Roesch, 2005; Schoenbaum, Saddoris, & Stalnaker, 2007). It has been proposed to act as an associative look-up table for the flexible representation of stimulus-outcome associations (Rolls, 1996). Analogously, the significance particularly of the OIFG has also been pointed out in a study employing a trial and error S-R learning paradigm (Toni et al., 2001). Activation in this region was attributed to increased identification of the visual imperative stimuli and their growing associative meaning to the demanded response as learning progressed. Furthermore, in a review from the same research group they presented evidence that the prefrontal cortex, and even more specifically the inferior frontal gyrus is able to represent cues, responses, and outcomes (Passingham et al., 2000). Albeit profound differences there is a general understanding that there seems to be an overlap in neural processing in instructed vs. trial and error learning (Frimmel et al., 2016; Melcher et al., 2013; Ruge & Wolfensteller, 2010). However, to my knowledge no study has linked activation in the OFC or OIFG to markers in the EEG signal, particularly at such an early stage within a trial. So how can the effect of the increased coupling between visual P1-N1 and activation in the OFC be interpreted?

The results indicate that the OFC could serve as a (multimodal) hub for integrating stimulus information and information about its associated outcome in an early pre-stage of action selection and initiation. This prompts the conclusion that this region is already engaged

in the learning process of S-O contingencies. This assumed generalization of the OFC to engagement already in the S-O acquisition process is in line with other studies (Ostlund & Balleine, 2007; Schoenbaum, Roesch, & Stalnaker, 2006; Stalnaker, Cooch, & Schoenbaum, 2015). Learnt S-O contingencies would facilitate initiating the motor program of the action of choice. The earlier an outcome is anticipated (based on stimulus-outcome associations), the better it will be associated with its response, hence leading to stronger O-R compatibility effects later on. This account is consistent with the general notion that more salient events (here outcomes that are pre-activated sooner) will be associated with other events (here the action) more easily and more rapidly (Mackintosh, 1975; Le Pelley and McLaren, 2003). Thus, one could speculate that increased activation in the OFC in response to S-R-O mappings possibly embodies a marker for the ongoing transition from mere stimulus-based behavior to a goal-directed behavior in successful learners.

Does the P1-N1 modulation and its association to increased activation in the OFC reflect a correlate of multisensory integration?

Employing different modalities of stimuli (imperative visual stimulus and auditory outcome) in the learning phase of the experimental paradigm, I initially hypothesized that pre-response stimulus-based outcome integration processes could be related to neural markers typically associated with multi-sensory (here, visuo-auditory) integration processes (Murray et al., 2015). Multi-sensory integration, that is interaction between different sensory modalities, have been identified even in very early stages of stimulus processing (Talsma, Doty, & Woldorff, 2007). Giard and colleagues found that the processing of a stimulus containing redundant bimodal information (e.g. seeing and hearing a barking dog) is more rapid than that of either unimodal stimulus alone (Giard & Peronnet, 1999). This finding was complemented by EEG studies which reported modulations of the visual N1 in response to the bimodal stimulus in comparison to visual modality only (Fort, Delpuech, Pernier, & Giard, 2002; Molholm, Ritter, Javitt, & Foxe, 2004). The question arises if the P1-N1 negativity increase observed in the two studies of this work can really be attributed to multisensory integration to a full extent?

In both studies, I identified an attenuated ERP modulation within the P1-N1 complex in response to the visual stimulus. There is still ongoing controversy about the nature of multisensory integration EEG effects in response to visual stimuli. ERP modulations were repeatedly observed in terms of a positivity as well as a negativity increase of electrical potential (Altieri, Stevenson, Wallace, & Wenger, 2015; Cappe, Thut, Romei, & Murray, 2010; Fort, Delpuech, Pernier, & Giard, 2002; Giard & Peronnet, 1999; Molholm et al., 2002;

Senkowski et al., 2011; Stekelenburg & Vroomen, 2012; Vidal et al., 2008). A similar issue arises when looking at the results of the EEG-informed analysis in which the P1-N1 modulation predicted increasing activation in the OFC over the learning course. The inferior frontal gyrus (IFG) has been brought in connection to multisensory integration processes (Renier et al., 2009), especially in the audio-visual domain (Callan, Jones, & Callan, 2014; Sugihara et al., 2006), though. The majority of the studies, however, demonstrated activation in the primary visual or the primary auditory cortex, or both (Matusz et al., 2015; Meylan & Murray, 2007; Murray et al., 2005; Murray et al., 2004; Thelen et al., 2012; Thelen et al., 2014; Zangenehpour & Zatorre, 2010).

In conclusion, the effects that are present in this study might be influenced by the nature of the bimodality of the stimulus and its corresponding outcome. However, it is safe to assume that they do not represent multisensory integration effects in a classical sense (Murray et al., 2016). Although there have been exceptions to the rule, most of the multisensory integration paradigms work with a) omnipresence of bimodal information and b) are mainly task- and response irrelevant (Gondan & Roder, 2006; Teder-Salejarvi et al., 2002). Presumably, the bimodality of S and O is more or less insignificant in the context of S-R-O learning. What seems to be more important and salient is the S-O contingency itself that can be learned from the mappings. This association is in fact independent from the modality of the presented material. This contingency alone gives an advantage in selecting the corresponding response and it just happens to be bimodal in the experimental design used. However, a final answer to the question raised above cannot be given up to this point.

6.2.2 Post-response encoding and consolidation of O-R contingencies enables goal-directedness of behavior

An increase in late post-response, post-outcome EEG negativity over the course of learning revealed a seemingly two way processing stream of O-R contingencies. First of all, the ERP negativity was functionally coupled to increased activation in the Supplementary Motor Area (SMA) in late learning stages. This activation increase was correlated with the O-R compatibility effect. Thus, high R-O learners exhibited a stronger activation than low learners. Furthermore, the fMRI only PPI-analysis revealed that activation in the SMA was equally functionally connected to activation in the lateral prefrontal cortex (LPFC).

Secondly, the increasing late post-outcome negativity in the EEG signal was also functionally coupled to increasing activation in the dorsal caudate as well as the somatosensory cortex over the learning course. This increased activation in these areas was

positively correlated to a general response time decrease over the S-R-O learning course. Increased coupling between the LPFC and the anterior caudate over the course of learning, although not correlated with any behavioral marker, was as well observed in the fMRI only PPI analysis. With such a differential activation pattern at this late stage within a trial the question arises: What happens in the aftermath of a response and its ensuing effect? Furthermore, which processes are represented by the late EEG negativity increase that is correlated with two separate brain regions (each connected to a different behavioral marker of O-R learning)?

Consolidation of response-outcome contingencies through post-response motor-sensory feedback loops?

The results promote the general idea that the SMA is involved in the acquisition of goal-directed behavior (Elsner et al., 2002; Melcher et al., 2008; Melcher et al., 2013). Together with prior research (Frimmel et al., 2016) this notion can be generalized not only to extensive learning phases but also to learning tasks in which goal-directed behavior is acquired in only few practice trials. However, there is an ongoing debate on whether SMA activation can be clearly linked to sub-processes prior or subsequent to an agent's action (Nachev et al., 2008). With the means of co-registered EEG-fMRI acquisition it is possible to gain a deeper insight in answering this question since it is possible to attain distinct BOLD activation information within a trial with the help of additional EEG information. All in all, study 2 provides additional evidence favoring an involvement of the SMA only following a performed action in response to an imperative stimulus and even more, subsequent to the perception of its ensuing effect. This may give rise to the interpretation that the SMA is associated with linking the motor program of the performed action to the sensory program of the perceived effect, hence establishing and further strengthening O-R contingencies. This link is basically the core of what defines outcome response learning, i.e. acquiring goal-directed behavior according to both instrumental learning as well as ideomotor approaches.

The question arises on where these contingencies are stored. There is a distinction to be made between long term memory areas in the brain (O'Reilly & Rudy, 2001; Rolls, 2010; Rolls & Kesner, 2006; Tulving & Markowitsch, 1998) and areas that provide more of a buffer or cache structure in ongoing tasks or processes (Oberauer, 2009). Concerning long term memory and retrieval processes the hippocampus has been suggested to play a key role in the goal-directed control of action (Fouquet et al., 2013; Johnson, van der Meer, & Redish, 2007; Kennedy & Shapiro, 2009; Zilli & Hasselmo, 2008). In an ongoing task, however, the LPFC has been repeatedly reported to function as a cache memory storage of O-R

contingencies (Dolan & Dayan, 2013; Doll et al., 2009b; Doll, Simon, & Daw, 2012; Glascher, Daw, Dayan, & O'Doherty, 2010; Ramamoorthy & Verguts, 2012).

Unique to the ideomotor approach is the assumption that learnt O-R associations are bidirectional in a sense that they work both ways in terms of directedness. According to phase 2 of the two stage model proposed by Elsner and Hommel (2001), decoupling learnt R-O contingencies from external triggers is an essential step necessary to increase one agent´s degrees of freedom beyond the realm of instrumental behavior, i.e. acting solely based on the presence of an physical stimulus. Study 2 gave indications that the neural representation of the motor program stored in the SMA is linked to the internal representation of response and outcome stored in the LPFC. This link could enable actions to become anticipatory, i.e. goal-directed. Activation of the internal representation of the desired outcome and its required action would activate the neural representation of the corresponding motor program via previously established LPFC-SMA couplings. Hence, coupling between the LPFC and the SMA in the acquisition phase of R-O contingencies might be a key to a postulated fundamental mechanism according to ideomotor theory (Shin et al., 2010) as it would allow for a pro-active activation of the motor program based on an agent´s current goal (O-R).

Consolidation through early automatization of goal-directed behavior in the dorsal caudate?

Activation in anterior parts of the caudate is generally believed to be involved in the establishment of goal-directed actions (J. O'Doherty et al., 2004; Ruge & Wolfensteller, 2010; Tanaka et al., 2008; Tricomi et al., 2004). This has already been demonstrated in various studies (Ruge & Wolfensteller, 2010; Stocco et al., 2012). Based on the results of a PPI analysis Ruge and Wolfensteller (2015) assumed that this region was not engaged in encoding processes of O-R contingencies per se but rather is activated in the active utilization process of O-R contingencies (i.e. in an ongoing S-R-O learning task). The results of the PPI replication analyses (with the one caveat that the correlation with the behavioral marker did not exceed significance level) seem to support this hypothesis. The results of the EEG-informed analysis, however, do not quite fit into the picture. The analysis identified an increased coupling of a late negativity in the EEG signal and activation in dorsal parts of the caudate. The dorsal caudate has not particularly been brought into connection with O-R learning so far. The results of this study could prompt the hypothesis that caudate involvement into processes of O-R learning can also be generalized to more dorsal parts of this region. However, this consideration is highly speculative given the fact that is not backed so far by other research.

Based on the results of this work, what seems to be more likely is that the coupling effect in this part of the caudate reflects an ongoing process of an early automatization of the acquired behavior. It is commonly believed that the dorsal striatum, and the dorsal caudate in particular, are critical in the formation and control of habitual action in long time learning (Burton et al., 2015; Haber & Knutson, 2010). However, the automatization process potentially at work here has to be distinguished from habitual behavior as a result of such long time learning processes. But it has already be shown in a similar paradigm that behavior can show signs of automatization within only few repetitions of novel instructed S-R mappings (Mohr et al., 2016). This automatization process would save potential cognitive resources as it would decouple often performed behavior from anticipation/processing of the outcome. Thus, it might possible that the dorsal caudate functions as a region in which the acquired behavior might already be prepared to work in a more automatized manner without relying on the online evaluation of the ensuing effect.

In conclusion I want to refer to the two opening questions raised at the beginning of this section: What happens in the aftermath of a performed action and its ensuing effect and what does the late post-response EEG negativity really represent? It might be a neurophysiological marker of an overall updating and synchronization process happening at the end of each trial. Thus, it is correlated with several areas in the brain, each involved with distinct feedback mechanisms. On one hand, the SMA seems to be engaged in bidirectional encoding processes of R-O associations, mediated by increased coupling with the LPFC. This association could already set up to be activated independent of the presence of a physical stimulus. On the other hand, there might be an early automatization of the performed behavior, potentially disentangling itself more and more from evaluation of the ensuing effect, reflected by increasing activation in dorsal parts of the caudate as learning progresses.

Is the attenuation of the perceived outcome in response to a performed action part of the learnt O-R contingency?

Regarding post-response effects of O-R learning, in study 1 I observed a learning-related attenuation effect in the auditory N1 range following in response to the presentation of the auditory outcome. This suggested that the phenomenon of neurophysiological sensory attenuation as a direct result of outcome integration processes can be generalized to a context of rapid instruction-based S-R-O learning and can be established within few initial learning trials. This effect however has not been replicated in the confirmatory analysis of study 2. EEG data in this case pointed towards the reverse effect of an increase in negativity in subjects exhibiting stronger O-R compatibility effects. The reason why this effect could not be observed

in study 2 remains elusive. However, with the effect being very prominent in study 1 it might be worthwhile investigating this phenomenon in a further isolated study. Sensory attenuation of self-generated stimuli is commonly accounted for by forward models of motor control (Miall & Wolpert, 1996). According to such models, information about the motor command, the so called *corollary discharge* (Sperry, 1950), or *efference copy* (Von Holst & Mittelstaedt, 1950), is used to make predictions about the sensory outcomes of the initiated action. The actual outcome of the action is then compared to this predicted outcome. If both match, the response is attenuated (Curio, Neuloh, Numminen, Jousmaki, & Hari, 2000; Ford, Mathalon, Heinks, et al., 2001; Ford, Mathalon, Kalba, et al., 2001; Heinks-Maldonado, Mathalon, Gray, & Ford, 2005; Houde, Nagarajan, Sekihara, & Merzenich, 2002; Martikainen et al., 2005; McCarthy & Donchin, 1976; Schafer & Marcus, 1973). Consistent with the forward model, less attenuation is found when the actual effect does not match the expected effect (Bays, Wolpert, & Flanagan, 2005; Blakemore, Frith, & Wolpert, 1999; Heinks-Maldonado et al., 2005; Heinks-Maldonado, Nagarajan, & Houde, 2006; Houde et al., 2002). This could in fact be used in a proceeding EEG experiment, which could test specifically on the presence of sensory attenuation effects. One would only have to introduce an additional manipulation in the learning phase of the paradigm in which half of the S-R mappings are followed by arbitrary outcomes so that no R-O contingencies could be acquired. Hence, one would expect an attenuated EEG response to the outcome in the contingency condition and less to no attenuation in the random outcome manipulation.

6.3 Critical reflection of the methodology and outlook

6.3.1 Strengths and limitations of this work

This work set out to disentangle neurophysiological correlates of instructed outcome response learning using the means of co-registered EEG-fMRI. There are an abundance of either EEG or fMRI studies in the field approaching neural mechanisms on the acquisition of goal-directed behavior in humans. However, to be able to split the fMRI BOLD signal with additional information that relied on information of both modalities posed a novelty. The studies presented here were particularly designed to contribute distinct activation in the brain to either response preparation/initiation or to post-response outcome integration processes.

A great strength of this work lies in the fact that the same exact paradigm has been used in all of its parts. Together with previously reported work (Ruge & Wolfensteller, 2015) a total of three separate studies, each with a distinct research focus, can be integrated. Even more, each consecutive study was able to serve as a replication study to probe previously

found effects. The value in this test of reliability of results cannot be stressed enough in the course of the strongly debated “replication crisis” in the science community (Maxwell, Lau, & Howard, 2015; Open Science, 2015; Stroebe & Strack, 2014). In this sense, the PPI analysis performed in the very first attempt to this experimental design (Ruge & Wolfensteller, 2015) could be probed with this work. Moreover, EEG ROIs that were explored in study 1 of this dissertation could be either rejected or confirmed in study 2 and further be utilized in the EEG-informed analyses. In this regard, it has to be highlighted that due to the partially explorative nature of the EEG-informed analysis, the interpretations drawn are still to be viewed speculative. Every slight change concerning the EEG regressor in the joint fMRI analysis, may it be a shift of the time window, using a different electrode, or clustering more than one electrodes, requires setting up a new GLM 1 in the EEG-informed analysis. This could ultimately result in an inflation of estimated GLMs, potentially cumulating the Type I statistical error. This issue is currently not accounted for in the present work. Therefore, it would be strongly suggested to verify the results of the EEG-informed analysis in an additional confirmative study.

6.3.2 Data quality assessment

I observed a considerable amount of noise already in the Grand Average ERP signal in the co-registered EEG data of study 2 when compared to the data from the EEG only set up of study 1. Additionally, there was an even greater amount of noise on the single trial level in the EEG-fMRI data set. This loss in data quality could already have had an effect on the power of individual EEG effects and also its potential correlations with behavioral indices. In fact, it might have been one of the reasons why key effects observed in study 1 could not be replicated in study 2. While a loss in data quality can be compensated for by the averaging procedure of the ERP method, this does not apply to the single trial level. Eventually, this lack in data quality made more sophisticated methods based on single trials hard, if not impossible, to realize. For this reason the employment of an exemplary symmetric data fusion method was dropped. As already laid out in the general objectives section (see chapter 3) the initial plan was to also apply a joint ICA approach to the data. Ideally, this could have led to a comparison of both methods concerning feasibility, assumptions, practicability, and interpretations that could be drawn from either method. Ultimately, guidelines on if, when and how to apply either method could have been formulated. However, single trial ICAs of the EEG data absolutely lacked any usefulness. ICs where highly polluted with noise that could not be compensated for in any way. Hence, the joint ICA idea was abandoned to fully concentrate on the EEG-informed analysis approach. It cannot be stressed enough that on the single trial level there remains massive

room for data quality improvement. For future projects, there are several options that could help to improve EEG data quality even on the level of individual trials.

First of all, in the present study the Helium pump artifact was avoided by switching the Helium pump off during simultaneous EEG-fMRI scanning sessions. However, there are many scanning setups in which switching off the Helium pump is not allowed or feasible resulting in the inevitable HE artifact to be present in the EEG data. If this is the case, one can utilize a recent trend in EEG-fMRI. This novel method relies on reference signals in the artifact correction preprocessing pipeline to be used in the correction of the HE and BCG artifact (Chowdhury, Mullinger, Glover, & Bowtell, 2014; Luo, Huang, & Glover, 2014). One way of obtaining these kind of signals is by using “carbon-wire loops” (Abbott et al., 2015; Masterton, Abbott, Fleming, & Jackson, 2007; Negishi, Abildgaard, Laufer, Nixon, & Constable, 2008; J. N. van der Meer et al., 2016). Carbon wire loops (CWLs) are added to the existing EEG cap and measure movement-induced signals based on Faraday´s magnetic induction law. This motion information then assists in the removal of movement-induced artifacts in the EEG in a linear regression, based on a sliding window approach. It has been shown that the CWL correction method not only corrects for the helium pump artifact but also seems to be superior to conventional BCG correction methods, such as AAS or OBS (J. N. van der Meer et al., 2016).

Secondly, on the software side, the method of wavelet denoising (Quiroga, 2000) has been proven to be a powerful tool in smoothing single trial EEG data, thus cleansing it from confounding noise. The wavelet transformation provides a time-frequency representation of the ERP signal with an optimal resolution, both in the time and in the frequency domain. Additionally, this method does not rely on the requirement of stationarity of the signal (Quiroga & Garcia, 2003). In the denoising process the averaged ERP is decomposed into different frequency bands and times using the wavelet multi-resolution decomposition. Wavelet coefficients, correlated with the ERPs are identified, while the remaining are set to zero. The coefficients of interest thereby are supposed to cover a time range in which the single-trial ERPs are expected to occur. Afterwards, the inverse transformation is applied, thus providing the denoised averaged ERP. Ultimately, this scheme is also applied on the single trial data level. The strength of this method lies in its ability to provide almost as equally clean individual trial data as averaged ERPs. However, this method has so far been tested by the authors mentioned above only in cases in which almost pure and prominent ERPs, namely the P1-N1 complex and the P300 component, were present. Data on how the wavelet denoising method would perform in cases in which multiple event related potentials simultaneously present, resulting in a temporal overlap, or when dealing with components that are not characterized by high amplitudes, have not been published so far. The main reason I restrained from using

this method concerns the ambiguous issue if such a profound data transformation technique can still be considered data cleaning rather than data manipulation. Especially in the case of single trial data it may be the case that the wavelet denoising method eradicates trial-to-trial individuality and variance information in the smoothing process that is so desired to be accounted for in the first place.

In conclusion, there are methods to even further improve EEG data quality in co-registration settings. In my point of view it is preferable to prioritized optimization of the acquisition environment over any other means. Getting as clean as possible data will save a lot of preprocessing and correction steps in the later course. Perfect synchronization between EEG amplifier and the fMRI sequence seem to play a key part in controlling the Gradient artifact. To further optimize correction of the Cardioballistic artifact and Helium pump artifact, J. N. van der Meer et al. (2016) promote a fundamental benefit of including additional carbon wires in the set up.

6.3.3 A common neural foundation for EEG and fMRI?

One of the main motivations on going to the lengths of co-registered EEG-fMRI data acquisition is based on the fundamental assumption that both imaging methods produce markers that basically share a common neural basis. In alignment with this common understanding I also performed additional simple EEG-fMRI-coupled analyses independent of the primary research questions. The focus lied on prominent and well-established ERP components that usually exhibit huge amplitudes in the EEG spectrum and supposedly can unambiguously be assigned to specific areas in the brain. Namely, I used the visual N1 in response to the visual imperative stimulus, the EEG correlate of the motor response, as well as the auditory N1 in response to the auditory outcome subsequent to the response. I assumed that these components would be tightly coupled to activation in the primary visual cortex (visual N1), premotor or motor areas (ERP motor signal) and the primary auditory cortex (auditory N1). However, performing an EEG-informed fMRI analysis concatenated over the entire learning course (SRO-rep 1 to SRO-rep 8), yielded mixed results. Only the ERP motor signal predicted significant activation in parts of the postcentral gyrus as well as the parietal operculum. This coupling was only visible if response time differences between early and late stages of learning were entered as an additional covariate into the model. Including either the visual N1 or the auditory N1 did not lead to any significant activation in the brain. On first sight, these results do not seem to shed a good light on the question, if EEG and fMRI data fusion using the means of EEG-informed analysis is able to produce stable and sound results. Thus,

the question on empirical evidence from other studies supporting the axiom of converging imaging methods based on a universal neurological measure arises.

The electrophysiological basis of neurophysiological markers has been investigated thoroughly in the past years (Logothetis & Pfeuffer, 2004). One common presumption is that the BOLD signal itself is tightly coupled to local field potentials (LFPs) in the brain reflecting dendritic activity (Logothetis et al., 2001). Thus, increasing and decreasing brain activity should be able to be picked up by the fMRI BOLD signal (Shmuel, Augath, Oeltermann, & Logothetis, 2006) as well as by electroencephalography as LFP power signal. Based on this understanding many studies trying to gain an understanding on the common nature of fMRI and EEG correlates focused around comparing the BOLD estimate to EEG-LFP power measures (Buzsaki & Draguhn, 2004; Engel & Singer, 2001; Fries, 2005; Goense & Logothetis, 2008; Knight, 2007; Linkenkaer-Hansen, Nikulin, Palva, Ilmoniemi, & Palva, 2004; Ohara et al., 2001). However, much fewer is known on the link of EEG scalp potentials to the BOLD signal. Some research was done revolving around cortical surface negativities (Brunia & van Boxtel, 2001; Rosler, Heil, & Roder, 1997) such as the readiness potential (RP, Kornhuber & Deecke, 1990)), a slow negative shift mainly picked up by electrodes at motor cortex sites, or the contingent negative variation (CNV, (Birbaumer, Elbert, Canavan, & Rockstroh, 1990). It has been shown that cortical surface negativity is reflected by depolarization of the apical dendrites of large pyramidal cells (Mitzdorf, 1989). Regarding visual and auditory perception Lakatos, Karmos, Mehta, Ulbert, and Schroeder (2008) were able to demonstrate that increased attention to an auditory or visual stimulus is associated to depolarization within upper layers of either the primary visual or auditory cortex. Thus, at least for slow cortical potentials (SCPs), this suggests a link to neuroimaging in terms of a measurable “activation level” imaged by BOLD fMRI. There seems to be a rule of an inverse proportionality regarding the temporal frequency and the spatial scale of synchronous activity (Bullock et al., 1995; Leopold, Murayama, & Logothetis, 2003; Varela, Lachaux, Rodriguez, & Martinerie, 2001). This means that phase coherence in higher frequencies is often observed on a scale of mm while SCPs (usually in the range of 1 Hz and less) are synchronized over many centimeters. Potential changes in behavior, i.e. in response to stimuli, increase the spatial range of phase coherent activity. This effect is most prominent at lower frequencies (Gross et al., 2004; Kahana, 2006; Saalmann, Pigarev, & Vidyasagar, 2007). This has generally led to the conclusion that event-related changes in neuronal synchronization are at least to a certain degree responsible for changes in the fMRI BOLD signal during task performance.

Is there a definitive explanation on why couplings of ERP components and BOLD signal on such a fundamental level could only be observed in partial in the present EEG-fMRI study? A final answer to this question cannot be given. To my knowledge there has not been

systematic research on the convergence of ERPs other than the RP and the CNV. It might be that a common neural foundation between short lived ERPs (compared to the temporarily elongated RP/CNV) is much harder to grasp with the method of EEG-informed analysis. Additionally, it has been proposed that EEG and fMRI are symmetrically complementary with regards to function localization. Research shows that certain neuronal processes may be detected by EEG recording but not by fMRI and vice versa (Herrmann & Debener, 2008; Nunez & Silberstein, 2000). This has led to the conclusion that respective weaknesses of each method seem to be symmetrical arrayed. However, this view also has been challenged by various authors (Logothetis, 2002; Ojemann et al., 1997; Shmuel et al., 2006). It could be shown that there seem to be "blind spots" which can pose a problem for both EEG and fMRI, such as the medial temporal lobe (Brazdil et al., 2005; Cohen et al., 1999; Halgren et al., 1995) or the hippocampal system (Fell et al., 2001; Fernandez, Fell, & Fries, 2002). However, these examples only seem to represent more exceptional cases rather than a general rule. Another reason for the missing correlation between sensory ERP potentials and activation in the respective sensory cortices may be found in the design of the paradigm itself. It might be that although the stimulus-locked visual N1 as well as the response-locked auditory N1 were well pronounced, they were not isolated in terms of other temporarily overlapping components. As seen above, both components were already involved in learning-related processes, i.e. response selection/initiation or outcome processing. Hence, there might already be a superimposition of EEG components representing multiple distinct neural processes.

6.3.4 How can co-registered EEG-fMRI contribute to a better understanding of the human brain?

The answer to this question highly depends on the way both data modalities are fused. Data fusion and analysis again should be led primary by the overarching research question that is aimed to be answered. The broad variety of reasons for combining electrophysiology and functional neuroimaging has been reviewed by Ullsperger and Debener (2010). They also introduced a taxonomy for categorizing various types of EEG-fMRI data fusion methods.

One strand of methods revolves around source localization methods of electrophysiological parameters (i.e. EEG or MEG). These methods differ in terms of a priori defined information that are additionally fed into the model. The simplest methods involve no generator or conductivity modeling of the EEG source leaving proximity as only measure for correlating electrophysiological results with brain structure (Nunez & Pilgreen, 1991). The so called *inverse current source localization* constitutes a more sophisticated approach which requires computation of a head conductivity model (Darvas, Ermer, Mosher, & Leahy, 2006;

Rush & Driscoll, 1968). According to this method, the location of generators of electrical current within the brain are deduced by identifying a best fitting model either by brain electrical source analysis (BESA, Scherg & Picton, 1991) or by means of low resolution brain electromagnetic tomography (LOERETA, Pascual-Marqui et al., 1999). Inverse source localization can be unconstrained or constrained with respect to potential regions of interest. In its most elaborated form location and orientation of all current dipoles can be determined by a mixture of anatomical and functional neuroimaging (Dale, Fischl, & Sereno, 1999; Dale & Sereno, 1993; Nunez & Silberstein, 2000). Together with the generator strengths, this head conductivity model fully specifies the electrical state of the system. Thus, generator time courses can by directly drawn from the recorded data by application of the pre-computed forward model.

Other research is more concerned with assigning correspondences between distinct electrophysiological components and functional neuroanatomy. These components can be defined either as event-related potentials (Strobel et al., 2008) or independent components (ICA, Makeig et al., 2004). In general, ICA is more data driven whereas ERP-based analysis strategies tend to be more top-down methods (Ullsperger & Debener, 2010). However, it has to be stressed that even in the ICA method feature components further used in a unified EEG-fMRI model usually represent distinct ERP components. Thus, I will further only relate to ERPs, even if the component in question was produced by the ICA method. The extracted components of interest are correlated with the fMRI BOLD signal, usually on a trial-to-trial basis. Hence, combined ERP-fMRI designs are supposed to capture correlations between EEG electrophysiological and hemodynamic responses in relation to behavioral events (Debener et al., 2006). Several separate studies were able to link specific ERP components to activation in distinct regions in the brain (Calhoun et al., 2006; Eichele et al., 2005; Raichle et al., 2001; Vincent, Kahn, Snyder, Raichle, & Buckner, 2008). For most of the studies simultaneous EEG-fMRI acquisition is mandatory in order to avoid potential training effects by sequential recording. Another advantage in using ERPs in a combined analysis lies in their long research tradition. For prominent ERPs there is already a lot of knowledge about functionality and even possible generator location. Thus, these information could also be used in the combined analysis to help exploring functionality of activated brain areas. Further, in trial-by-trial analyses two distinct variance sources are separable: (1) a deterministic variance component related to the event itself, and (2) a stochastic variance component reflecting trial-by-trial variability within a single subject. With the BOLD signal alone, one is only able to extract the deterministic variance component (by conventional event-related fMRI analysis). Its stochastic component is only accessible by the means of EEG-fMRI acquisition (Ullsperger & Debener, 2010).

6.4 General Conclusion

Combining electroencephalography with functional magnetic resonance tomography in a manner that optimally exploits the respective strengths of each method can provide huge benefits in neuroscientific research. In this dissertation the method was used to investigate neurocognitive mechanisms on the acquisition of goal-directed behavior in an instructed learning paradigm. Temporal highly resolved EEG information was used to break down the fMRI BOLD signal within a trial. EEG-informed analyses brought to light distinct brain activation associated with response selection and initiation as well as brain activation associated with post-response outcome integration, respectively. This would have not been possible applying each of the methods alone.

Prior to the behavioral response, the results point towards the orbital frontal cortex as a region of integrating S-O information enabling an agent to increasingly shift from mere stimulus based behavior towards acting upon achieving a desired goal state. Post-response activations revealed a seemingly two-fold feedback stream of integration of O-R contingencies, each mediated by a late post-outcome negativity in EEG activity. On one hand the SMA was engaged in bidirectional encoding processes of O-R associations, additionally correlated with increased coupling with the LPFC. Hence, the SMA seems to be a key region not only when it comes to establishing goal-directed actions. It might play a central part of making an agents behavior independent from external triggering stimuli, hence enabling anticipatory and pro-active behavior. On the other hand the results probed the hypothesis that the dorsal caudate functions as a region in which the acquired behavior might already be prepared to work in a more automatized manner without relying on the online evaluation of the ensuing effect.

Overall, co-registered EEG-fMRI recording has been proven beneficial in the context of researching underlying mechanisms of goal-directed behavior. The results can provide an additional piece in grasping the complex mechanisms involved into outcome response learning. Due to the highly explorative approach of the studies more confirmatory research is strongly recommended to eventually attain a comprehensive understanding on the neurocognitive mechanisms of outcome response learning. A final assessment regarding the reliable conjunction of these two different data modalities cannot be given based on this work alone.

7 References

Abbott, D. E., Masterton, R. A. J., Archer, J. S., Fleming, S. W., Warren, A. E. L., & Jackson, G. D. (2015). Constructing carbon fiber motion-detection loops for simultaneous EEG-fMRI. *Frontiers in Neurology, 5*. doi:10.3389/fneur.2014.00260

Adams, C. D., & Dickinson, A. (1981). Instrumental responding following reinforcer devaluation. *Quarterly Journal of Experimental Psychology Section B-Comparative and Physiological Psychology, 33*(May), 109-121.

Alain, C., Snyder, J. S., He, Y., & Reinke, K. S. (2007). Changes in auditory cortex parallel rapid perceptual learning. *Cerebral Cortex, 17*(5), 1074-1084. doi:10.1093/cercor/bhl018

Aliu, S. O., Houde, J. F., & Nagarajan, S. S. (2009). Motor-induced suppression of the auditory cortex. *Journal of Cognitive Neuroscience, 21*(4), 791-802. doi:10.1162/jocn.2009.21055

Allen, P. J., Josephs, O., & Turner, R. (2000). A method for removing imaging artifact from continuous EEG recorded during functional MRI. *Neuroimage, 12*(2), 230-239. doi:10.1006/nimg.2000.0599

Allen, P. J., Polizzi, G., Krakow, K., Fish, D. R., & Lemieux, L. (1998). Identification of EEG events in the MR scanner: The problem of pulse artifact and a method for its subtraction. *Neuroimage, 8*(3), 229-239. doi:10.1006/nimg.1998.0361

Altieri, N., Stevenson, R. A., Wallace, M. T., & Wenger, M. J. (2015). Learning to associate auditory and visual stimuli: Behavioral and neural mechanisms. *Brain Topography, 28*(3), 479-493. doi:10.1007/s10548-013-0333-7

Anami, K., Mori, T., Tanaka, F., Kawagoe, Y., Okamoto, J., Yarita, M., . . . Saitoh, O. (2003). Stepping stone sampling for retrieving artifact-free electroencephalogram during functional magnetic resonance imaging. *Neuroimage, 19*(2 Pt 1), 281-295.

Anami, K., Saitoh, O., & Yamoto, M. (2002). *Reduction of ballistocardiogram with a vacuum head-fixating system during simultaneous fMRI and multi-channel nonopolar EEG recording.* Paper presented at the Recent Advances in Human Brain Mapping.

Arezzo, J., Vaughan, H. G., Jr., & Koss, B. (1977). Relationship of neuronal activity to gross movement-related potentials in monkey pre- and postcentral cortex. *Brain Research, 132*(2), 362-369. doi:10.1016/0006-8993(77)90429-2

Ashby, F. G., Turner, B. O., & Horvitz, J. C. (2010). Cortical and basal ganglia contributions to habit learning and automaticity. *Trends in Cognitive Sciences, 14*(5), 208-215. doi:10.1016/j.tics.2010.02.001

Atienza, M., Cantero, J. L., & Dominguez-Marin, E. (2002). The time course of neural changes underlying auditory perceptual learning. *Learning & Memory, 9*(3), 138-150. doi:10.1101/lm.46502

Babiloni, F., Babiloni, C., Carducci, F., Del Gratta, C., Romani, G. L., Rossini, P. M., & Cincotti, F. (2002). Cortical source estimate of combined high resolution EEG and fMRI data related to voluntary movements. *Methods of Information in Medicine, 41*(5), 443-450.

References

Babiloni, F., Carducci, F., Cincotti, F., Del Gratta, C., Roberti, G. M., Romani, G. L., . . . Babiloni, C. (2000). Integration of high resolution EEG and functional magnetic resonance in the study of human movement-related potentials. *Methods of Information in Medicine, 39*(2), 179-182.

Baess, P., Jacobsen, T., & Schroger, E. (2008). Suppression of the auditory N1 event-related potential component with unpredictable self-initiated tones: Evidence for internal forward models with dynamic stimulation. *International Journal of Psychophysiology, 70*(2), 137-143. doi:10.1016/j.ijpsycho.2008.06.005

Baess, P., Widmann, A., Roye, A., Schroger, E., & Jacobsen, T. (2009). Attenuated human auditory middle latency response and evoked 40-Hz response to self-initiated sounds. *Eur J Neurosci, 29*(7), 1514-1521. doi:10.1111/j.1460-9568.2009.06683.x

Balleine, B. W., & Dickinson, A. (1998). Goal-directed instrumental action: Contingency and incentive learning and their cortical substrates. *Neuropharmacology, 37*(4-5), 407-419. doi:10.1016/S0028-3908(98)00033-1

Balleine, B. W., & O'Doherty, J. P. (2010). Human and rodent homologies in action control: Corticostriatal determinants of goal-directed and habitual action. *Neuropsychopharmacology, 35*(1), 48-69. doi:10.1038/npp.2009.131

Balleine, B. W., & Ostlund, S. B. (2007). Still at the choice-point - Action selection and initiation in instrumental conditioning. *Reward and Decision Making in Corticobasal Ganglia Networks, 1104*, 147-171. doi:10.1196/annals.1390.006

Bandettini, P. A., & Ungerleider, L. G. (2001). From neuron to BOLD: New connections. *Nature Neuroscience, 4*(9), 864-866. doi:10.1038/nn0901-864

Bates, D. M. M., M.; Bolker, B. (2012). lme4: Linear mixed-effects models using S4 classes.

Bays, P. M., & Wolpert, D. M. (2007a). Computational principles of sensorimotor control that minimize uncertainty and variability. *J Physiol, 578*(Pt 2), 387-396. doi:10.1113/jphysiol.2006.120121

Bays, P. M., & Wolpert, D. M. (2007b). Predictive attenuation in the perception of touch. In Y. R. P.Haggard, M.Kawato (Eds.) (Ed.), *Sensorimotor foundations of higher cognition, attention and performance* (pp. 339–358). Oxford,England: Oxford UniversityPress.

Bays, P. M., Wolpert, D. M., & Flanagan, J. R. (2005). Perception of the consequences of self-action is temporally tuned and event driven. *Current Biology, 15*(12), 1125-1128. doi:10.1016/j.cub.2005.05.023

Beckers, T., De Houwer, J., & Eelen, P. (2002). Automatic integration of non-perceptual action effect features: The case of the associative affective Simon effect. *Psychological Research-Psychologische Forschung, 66*(3), 166-173. doi:10.1007/s00426-002-0090-9

Benar, C., Aghakhani, Y., Wang, Y., Izenberg, A., Al-Asmi, A., Dubeau, F., & Gotman, J. (2003). Quality of EEG in simultaneous EEG-fMRI for epilepsy. *Clinical Neurophysiology, 114*(3), 569-580.

Benar, C. G., Schon, D., Grimault, S., Nazarian, B., Burle, B., Roth, M., . . . Anton, J. L. (2007). Single-trial analysis of oddball event-related potentials in simultaneous EEG-fMRI. *Human Brain Mapping, 28*(7), 602-613. doi:10.1002/hbm.20289

References

Beudel, M., Zijlstra, S., Mulder, T., Zijdewind, I., & de Jong, B. M. (2011). Secondary sensory area sii is crucially involved in the preparation of familiar movements compared to movements never made before. *Human Brain Mapping, 32*(4), 564-579. doi:10.1002/hbm.21044

Birbaumer, N., Elbert, T., Canavan, A. G., & Rockstroh, B. (1990). Slow potentials of the cerebral cortex and behavior. *Physiological Reviews, 70*(1), 1-41. doi:10.1152/physrev.1990.70.1.1

Blakemore, S. J., Frith, C. D., & Wolpert, D. M. (1999). Spatio-temporal prediction modulates the perception of self-produced stimuli. *Journal of Cognitive Neuroscience, 11*(5), 551-559.

Blakemore, S. J., Wolpert, D., & Frith, C. (2000). Why can't you tickle yourself? *Neuroreport, 11*(11), R11-16.

Blakemore, S. J., Wolpert, D. M., & Frith, C. D. (1998). Central cancellation of self-produced tickle sensation. *Nature Neuroscience, 1*(7), 635-640. doi:10.1038/2870

Bonini, F., Burle, B., Liegeois-Chauvel, C., Regis, J., Chauvel, P., & Vidal, F. (2014). Action monitoring and medial frontal cortex: Leading role of supplementary motor area. *Science, 343*(6173), 888-891. doi:10.1126/science.1247412

Bonmassar, G., Purdon, P. L., Jaaskelainen, I. P., Chiappa, K., Solo, V., Brown, E. N., & Belliveau, J. W. (2002). Motion and ballistocardiogram artifact removal for interleaved recording of EEG and EPs during MRI. *Neuroimage, 16*(4), 1127-1141.

Boynton, G. M., Engel, S. A., Glover, G. H., & Heeger, D. J. (1996). Linear systems analysis of functional magnetic resonance imaging in human V1. *Journal of Neuroscience, 16*(13), 4207-4221.

Brazdil, M., Dobsik, M., Mikl, M., Hlustik, P., Daniel, P., Pazourkova, M., . . . Rektor, I. (2005). Combined event-related fMRI and intracerebral ERP study of an auditory oddball task. *Neuroimage, 26*(1), 285-293. doi:10.1016/j.neuroimage.2005.01.051

Brem, S., Lang-Dullenkopf, A., Maurer, U., Halder, P., Bucher, K., & Brandeis, D. (2005). Neurophysiological signs of rapidly emerging visual expertise for symbol strings. *Neuroreport, 16*(1), 45-48. doi:10.1097/00001756-200501190-00011

Bretz, F., Hothorn, T., & Westfall, P. H. (2011). *Multiple comparisons using R*. Boca Raton, FL: CRC Press.

Brunia, C. H., & van Boxtel, G. J. (2001). Wait and see. *International Journal of Psychophysiology, 43*(1), 59-75. doi:10.1016/s0167-8760(01)00179-9

Budd, T. W., Barry, R. J., Gordon, E., Rennie, C., & Michie, P. T. (1998). Decrement of the N1 auditory event-related potential with stimulus repetition: Habituation vs. refractoriness. *International Journal of Psychophysiology, 31*(1), 51-68.

Bullock, T. H., Mcclune, M. C., Achimowicz, J. Z., Iraguimadoz, V. J., Duckrow, R. B., & Spencer, S. S. (1995). EEG coherence has structure in the millimeter domain - subdural and hippocampal recordings from epileptic patients. *Electroencephalography and Clinical Neurophysiology, 95*(3), 161-177. doi:10.1016/0013-4694(95)93347-A

Burton, A. C., Nakamura, K., & Roesch, M. R. (2015). From ventral-medial to dorsal-lateral striatum: Neural correlates of reward-guided decision-making. *Neurobiology of Learning and Memory, 117*, 51-59. doi:10.1016/j.nlm.2014.05.003

References

Buzsaki, G., & Draguhn, A. (2004). Neuronal oscillations in cortical networks. *Science, 304*(5679), 1926-1929. doi:10.1126/science.1099745

Calhoun, V. D., Adali, T., Pearlson, G. D., & Kiehl, K. A. (2006). Neuronal chronometry of target detection: Fusion of hemodynamic and event-related potential data. *Neuroimage, 30*(2), 544-553. doi:10.1016/j.neuroimage.2005.08.060

Calhoun, V. D., Liu, J., & Adali, T. (2009). A review of group ICA for fMRI data and ICA for joint inference of imaging, genetic, and ERP data. *Neuroimage, 45*(1 Suppl), S163-172. doi:10.1016/j.neuroimage.2008.10.057

Callan, D. E., Jones, J. A., & Callan, A. (2014). Multisensory and modality specific processing of visual speech in different regions of the premotor cortex. *Frontiers in Psychology, 5*, 389. doi:10.3389/fpsyg.2014.00389

Cappe, C., Thut, G., Romei, V., & Murray, M. M. (2010). Auditory-visual multisensory interactions in humans: Timing, topography, directionality, and sources. *Journal of Neuroscience, 30*(38), 12572-12580. doi:10.1523/JNEUROSCI.1099-10.2010

Chowdhury, M. E. H., Mullinger, K. J., Glover, P., & Bowtell, R. (2014). Reference layer artefact subtraction (RLAS): A novel method of minimizing EEG artefacts during simultaneous fMRI. *Neuroimage, 84*, 307-319. doi:10.1016/j.neuroimage.2013.08.039

Clark, K., Appelbaum, L. G., van den Berg, B., Mitroff, S. R., & Woldorff, M. G. (2015). Improvement in visual search with practice: Mapping learning-related changes in neurocognitive stages of processing. *Journal of Neuroscience, 35*(13), 5351-5359. doi:10.1523/Jneurosci.1152-14.2015

Cohen, N. J., Ryan, E., Hunt, C., Romine, L., Wszalek, T., & Nash, C. (1999). Hippocampal system and declarative (relational) memory: Summarizing the data from functional neuroimaging studies. *Hippocampus, 9*(1), 83-98. doi:10.1002/(Sici)1098-1063(1999)9:1<83::Aid-Hipo9>3.0.Co;2-7

Colwill, R. M., & Rescorla, R. A. (1985). Postconditioning devaluation of a reinforcer affects instrumental responding. *Journal of Experimental Psychology-Animal Behavior Processes, 11*(1), 120-132. doi:10.1037//0097-7403.11.1.120

Colwill, R. M., & Rescorla, R. A. (1988). Associations between the discriminative stimulus and the reinforcer in instrumental learning. *Journal of Experimental Psychology-Animal Behavior Processes, 14*(2), 155-164. doi:10.1037/0097-7403.14.2.155

Colwill, R. M., & Rescorla, R. A. (1990). Effect of reinforcer devaluation on discriminative control of instrumental behavior. *Journal of Experimental Psychology: Animal Behavior Processes, 16*(1), 40-47.

Corbit, L. H., & Balleine, B. W. (2005). Double dissociation of basolateral and central amygdala lesions on the general and outcome-specific forms of pavlovian-instrumental transfer. *Journal of Neuroscience, 25*(4), 962-970. doi:10.1523/JNEUROSCI.4507-04.2005

Curio, G., Neuloh, G., Numminen, J., Jousmaki, V., & Hari, R. (2000). Speaking modifies voice-evoked activity in the human auditory cortex. *Human Brain Mapping, 9*(4), 183-191.

Dale, A. M., Fischl, B., & Sereno, M. I. (1999). Cortical surface-based analysis - I. Segmentation and surface reconstruction. *Neuroimage, 9*(2), 179-194. doi:10.1006/nimg.1998.0395

Dale, A. M., Liu, A. K., Fischl, B. R., Buckner, R. L., Belliveau, J. W., Lewine, J. D., & Halgren, E. (2000). Dynamic statistical parametric mapping: Combining fMRI and MEG for high-resolution imaging of cortical activity. *Neuron, 26*(1), 55-67. doi:10.1016/s0896-6273(00)81138-1

Dale, A. M., & Sereno, M. I. (1993). Improved localization of cortical activity by combining eeg and meg with mri cortical surface reconstruction - a linear-approach. *Journal of Cognitive Neuroscience, 5*(2), 162-176. doi:10.1162/jocn.1993.5.2.162

Darvas, F., Ermer, J. J., Mosher, J. C., & Leahy, R. M. (2006). Generic head models for atlas-based EEG source analysis. *Human Brain Mapping, 27*(2), 129-143. doi:10.1002/hbm.20171

de Wit, S., Corlett, P. R., Aitken, M. R., Dickinson, A., & Fletcher, P. C. (2009). Differential engagement of the ventromedial prefrontal cortex by goal-directed and habitual behavior toward food pictures in humans. *Journal of Neuroscience, 29*(36), 11330-11338. doi:10.1523/Jneurosci.1639-09.2009

de Wit, S., & Dickinson, A. (2009). Associative theories of goal-directed behaviour: A case for animal-human translational models. *Psychological Research-Psychologische Forschung, 73*(4), 463-476. doi:10.1007/s00426-009-0230-6

de Wit, S., Kosaki, Y., Balleine, B. W., & Dickinson, A. (2006). Dorsomedial prefrontal cortex resolves response conflict in rats. *Journal of Neuroscience, 26*(19), 5224-5229. doi:10.1523/JNEUROSCI.5175-05.2006

Debener, S., Mullinger, K. J., Mazy, R. K., & Bowtell, R. W. (2008). Properties of the ballistocardiogram artefact as revealed by EEG recordings at 1.5, 3 and 7 T static magnetic field strength. *International Journal of Psychophysiology, 67*(3), 189-199. doi:10.1016/j.ijpsycho.2007.05.015

Debener, S., Strobel, A., Sorger, B., Peters, J., Kranczioch, C., Engel, A. K., & Goebel, R. (2007). Improved quality of auditory event-related potentials recorded simultaneously with 3-T fMRI: Removal of the ballistocardiogram artefact. *Neuroimage, 34*(2), 587-597. doi:10.1016/j.neuroimage.2006.09.031

Debener, S., Ullsperger, M., Fiehler, K., von Cramon, D. Y., & Engel, A. K. (2005). Monitoring error processing by means of simultaneous EEG/fMRI recordings II: Single-trial independent component analysis of the error-related negativity (ERN). *Journal of Psychophysiology, 19*(2), 111-111.

Debener, S., Ullsperger, M., Siegel, M., & Engel, A. K. (2006). Single-trial EEG-fMRI reveals the dynamics of cognitive function. *Trends in Cognitive Sciences, 10*(12), 558-563. doi:10.1016/j.tics.2006.09.010

Debener, S., Ullsperger, M., Siegel, M., Fiehler, K., von Cramon, D. Y., & Engel, A. K. (2005). Trial-by-trial coupling of concurrent electroencephalogram and functional magnetic resonance imaging identifies the dynamics of performance monitoring. *Journal of Neuroscience, 25*(50), 11730-11737. doi:10.1523/Jneurosci.3286-05.2005

Delgado, M. R., Miller, M. M., Inati, S., & Phelps, E. A. (2005). An fMRI study of reward-related probability learning. *Neuroimage, 24*(3), 862-873. doi:10.1016/j.neuroimage.2004.10.002

Dempsey, M. F., & Condon, B. (2001). Thermal injuries associated with MRI. *Clinical Radiology, 56*(6), 457-465. doi:10.1053/crad.2000.0688

Dempsey, M. F., Condon, B., & Hadley, D. M. (2001). Investigation of the factors responsible for burns during MRI. *Journal of Magnetic Resonance Imaging, 13*(4), 627-631.

Dickinson, A., & Balleine, B. (1994). Motivational control of goal-directed action. *Animal Learning & Behavior, 22*(1), 1-18.

Dickinson, A., & de Wit, S. (2003). The interaction between discriminative stimuli and outcomes during instrumental learning. *Quarterly Journal of Experimental Psychology Section B-Comparative and Physiological Psychology, 56*(1), 127-139. doi:10.1080/02724990244000223

Dickinson, A., Squire, S., Varga, Z., & Smith, J. W. (1998). Omission learning after instrumental pretraining. *Quarterly Journal of Experimental Psychology Section B-Comparative and Physiological Psychology, 51*(3), 271-286.

Dolan, R. J., & Dayan, P. (2013). Goals and habits in the brain. *Neuron, 80*(2), 312-325. doi:10.1016/j.neuron.2013.09.007

Doll, B. B., Jacobs, W. J., Sanfey, A. G., & Frank, M. J. (2009). Instructional control of reinforcement learning: a behavioral and neurocomputational investigation. *Brain Research, 1299*, 74-94. doi:10.1016/j.brainres.2009.07.007

Doll, B. B., Simon, D. A., & Daw, N. D. (2012). The ubiquity of model-based reinforcement learning. *Current Opinion in Neurobiology, 22*(6), 1075-1081. doi:10.1016/j.conb.2012.08.003

Drost, U. C., Rieger, M., Brass, M., Gunter, T. C., & Prinz, W. (2005). Action-effect coupling in pianists. *Psychological Research, 69*(4), 233-241. doi:10.1007/s00426-004-0175-8

Dumontheil, I., Thompson, R., & Duncan, J. (2011). Assembly and use of new task rules in fronto-parietal cortex. *Journal of Cognitive Neuroscience, 23*(1), 168-182. doi:10.1162/jocn.2010.21439

Eckert, M. A., Kamdar, N. V., Chang, C. E., Beckmann, C. F., Greicius, M. D., & Menon, V. (2008). A cross-modal system linking primary auditory and visual cortices: evidence from intrinsic fMRI connectivity analysis. *Human Brain Mapping, 29*(7), 848-857. doi:10.1002/hbm.20560

Eichele, T., Calhoun, V. D., Moosmann, M., Specht, K., Jongsma, M. L. A., Quiroga, R. Q., . . . Hugdahl, K. (2008). Unmixing concurrent EEG-fMRI with parallel independent component analysis. *International Journal of Psychophysiology, 67*(3), 222-234. doi:10.1016/j.ijpsycho.2007.04.010

Eichele, T., Moosmann, M., Wu, L., Gutberlet, I., & Debener, S. (2010). Removal of MRI artifacts from EEG recordings. In M. Ullsperger & S. Debener (Eds.), *Simultaneous EEG and fMRI*: Oxford University Press.

Eichele, T., Rachakonda, S., Brakedal, B., Eikeland, R., & Calhoun, V. D. (2011). EEGIFT: Group independent component analysis for event-related EEG data. *Computational Intelligence and Neuroscience*. doi:Artn 12936510.1155/2011/129365

Eichele, T., Rachakonda, S., & Calhoun, V. D. (2008). EEGIFT: A toolbox for group independent component analysis of event-related EEG. *Psychophysiology, 45*, S118-S118.

Eichele, T., Specht, K., Moosmann, M., Jongsma, M. L., Quiroga, R. Q., Nordby, H., & Hugdahl, K. (2005). Assessing the spatiotemporal evolution of neuronal activation with single-trial event-related potentials and functional MRI. *Proceedings of the National Academy of Sciences of the United States of America, 102*(49), 17798-17803. doi:10.1073/pnas.0505508102

Eickhoff, S. B., Grefkes, C., Zilles, K., & Fink, G. R. (2007). The somatotopic organization of cytoarchitectonic areas on the human parietal operculum. *Cerebral Cortex, 17*(8), 1800-1811. doi:10.1093/cercor/bhl090

Elsner, B., & Hommel, B. (2001). Effect anticipation and action control. *Journal of Experimental Psychology-Human Perception and Performance, 27*(1), 229-240. doi:Doi 10.1037//0096-1523.27.1.229

Elsner, B., & Hommel, B. (2004). Contiguity and contingency in action-effect learning. *Psychological Research-Psychologische Forschung, 68*(2-3), 138-154. doi:10.1007/s00426-003-0151-8

Elsner, B., Hommel, B., Mentschel, C., Drzezga, A., Prinz, W., Conrad, B., & Siebner, H. (2002). Linking actions and their perceivable consequences in the human brain. *Neuroimage, 17*(1), 364-372. doi:10.1006/nimg.2002.1162

Engel, A. K., & Singer, W. (2001). Temporal binding and the neural correlates of sensory awareness. *Trends in Cognitive Sciences, 5*(1), 16-25. doi:10.1016/s1364-6613(00)01568-0

Felblinger, J., Slotboom, J., Kreis, R., Jung, B., & Boesch, C. (1999). Restoration of electrophysiological signals distorted by inductive effects of magnetic field gradients during MR sequences. *Magnetic Resonance in Medicine, 41*(4), 715-721. doi:10.1002/(Sici)1522-2594(199904)41:4<715::Aid-Mrm9>3.0.Co;2-7

Fell, J., Klaver, P., Lehnertz, K., Grunwald, T., Schaller, C., Elger, C. E., & Fernandez, G. (2001). Human memory formation is accompanied by rhinal-hippocampal coupling and decoupling. *Nature Neuroscience, 4*(12), 1259-1264. doi:10.1038/nn759

Fernandez, G., Fell, J., & Fries, P. (2002). Response: The birth of a memory. *Trends in Neurosciences, 25*(6), 281-282. doi:10.1016/S0166-2236(02)02177-X

Ford, J. M., Mathalon, D. H., Heinks, T., Kalba, S., Faustman, W. O., & Roth, W. T. (2001). Neurophysiological evidence of corollary discharge dysfunction in schizophrenia. *American Journal of Psychiatry, 158*(12), 2069-2071. doi:10.1176/appi.ajp.158.12.2069

Ford, J. M., Mathalon, D. H., Kalba, S., Whitfield, S., Faustman, W. O., & Roth, W. T. (2001). Cortical responsiveness during inner speech in schizophrenia: an event-related potential study. *American Journal of Psychiatry, 158*(11), 1914-1916. doi:10.1176/appi.ajp.158.11.1914

Fort, A., Delpuech, C., Pemier, J., & Giard, M. H. (2002). Early auditory-visual interactions in human cortex during nonredundant target identification. *Cognitive Brain Research, 14*(1), 20-30. doi:10.1016/S0926-6410(02)00058-7

Fort, A., Delpuech, C., Pernier, J., & Giard, M. H. (2002). Dynamics of cortico-subcortical cross-modal operations involved in audio-visual object detection in humans. *Cerebral Cortex, 12*(10), 1031-1039. doi:10.1093/cercor/12.10.1031

Fouquet, C., Babayan, B. M., Watilliaux, A., Bontempi, B., Tobin, C., & Rondi-Reig, L. (2013). Complementary roles of the hippocampus and the dorsomedial striatum during spatial and sequence-based navigation behavior. *PLoS One, 8*(6), e67232. doi:10.1371/journal.pone.0067232

Fries, P. (2005). A mechanism for cognitive dynamics: Neuronal communication through neuronal coherence. *Trends in Cognitive Sciences, 9*(10), 474-480. doi:10.1016/j.tics.2005.08.011

Frimmel, S., Wolfensteller, U., Mohr, H., & Ruge, H. (2016). The neural basis of integrating pre- and post-response information for goal-directed actions. *Neuropsychologia, 80*, 56-70. doi:10.1016/j.neuropsychologia.2015.10.035

Friston, K. J., Buechel, C., Fink, G. R., Morris, J., Rolls, E., & Dolan, R. J. (1997). Psychophysiological and modulatory interactions in neuroimaging. *Neuroimage, 6*(3), 218-229. doi:10.1006/nimg.1997.0291

Garreffa, G., Carni, M., Gualniera, G., Ricci, G. B., Bozzao, L., De Carli, D., . . . Maraviglia, B. (2003). Real-time MR artifacts filtering during continuous EEG/fMRI acquisition. *Magnetic Resonance Imaging, 21*(10), 1175-1189.

Giard, M. H., & Peronnet, F. (1999). Auditory-visual integration during multimodal object recognition in humans: A behavioral and electrophysiological study. *Journal of Cognitive Neuroscience, 11*(5), 473-490. doi:10.1162/089892999563544

Gitelman, D. R., Penny, W. D., Ashburner, J., & Friston, K. J. (2003). Modeling regional and psychophysiologic interactions in fMRI: The importance of hemodynamic deconvolution. *Neuroimage, 19*(1), 200-207. doi:10.1016/S1053-8119(03)00058-2

Glascher, J., Daw, N., Dayan, P., & O'Doherty, J. P. (2010). States versus rewards: Dissociable neural prediction error signals underlying model-based and model-free reinforcement learning. *Neuron, 66*(4), 585-595. doi:10.1016/j.neuron.2010.04.016

Goense, J. B., & Logothetis, N. K. (2008). Neurophysiology of the BOLD fMRI signal in awake monkeys. *Current Biology, 18*(9), 631-640. doi:10.1016/j.cub.2008.03.054

Goldman-Rakic, P. S. (1987). Motor control function of the prefrontal cortex. *Ciba Foundation Symposium, 132*, 187-200.

Goldman, R. I., Stern, J. M., Engel, J., & Cohen, M. S. (2000). Acquiring simultaneous EEG and functional MRI. *Clinical Neurophysiology, 111*(11), 1974-1980. doi:10.1016/S1388-2457(00)00456-9

Gondan, M., & Roder, B. (2006). A new method for detecting interactions between the senses in event-related potentials. *Brain Research, 1073-1074*, 389-397. doi:10.1016/j.brainres.2005.12.050

Goschke, T. (2002). Volition und kognitive Kontrolle. In J. Müsseler & W. Prinz (Eds.), *Allgemeine Psychologie* (1st ed., pp. 270-335). Heidelberg: Spektrum Akademischer Verlag.

Goschke, T. (2004). Vom freien Willen zur Selbstdetermination: Kognitive und volitionale Mechanismen der intentionalen Handlungssteuerung. *Psychologische Rundschau, 55*(4), 186-197.

Gratton, G., Coles, M. G. H., & Donchin, E. (1983). A new method for off-line removal of ocular artifact. *Electroencephalography and Clinical Neurophysiology, 55*(4), 468-484. doi:10.1016/0013-4694(83)90135-9

Gray, P. (2011). *Psychology* (6th ed.). New York: Worth.

Grech, R., Cassar, T., Muscat, J., Camilleri, K. P., Fabri, S. G., Zervakis, M., . . . Vanrumste, B. (2008). Review on solving the inverse problem in EEG source analysis. *Journal of NeuroEngineering and Rehabilitation, 5*, 25. doi:10.1186/1743-0003-5-25

Greenwald, A. G. (1970). Sensory feedback mechanisms in performance control - with special reference to ideo-motor mechanism. *Psychological Review, 77*(2), 73-99. doi:10.1037/H0028689

Gross, J., Schmitz, F., Schnitzler, I., Kessler, K., Shapiro, K., Hommel, B., & Schnitzler, A. (2004). Modulation of long-range neural synchrony reflects temporal limitations of visual attention in humans. *Proceedings of the National Academy of Sciences of the United States of America, 101*(35), 13050-13055. doi:10.1073/pnas.0404944101

Haber, S. N., & Knutson, B. (2010). The reward circuit: Linking primate anatomy and human imaging. *Neuropsychopharmacology, 35*(1), 4-26. doi:10.1038/npp.2009.129

Haggard, P., & Clark, S. (2003). Intentional action: Conscious experience and neural prediction. *Consciousness and Cognition, 12*(4), 695-707.

Halgren, E., Baudena, P., Clarke, J. M., Heit, G., Liegeois, C., Chauvel, P., & Musolino, A. (1995). Intracerebral potentials to rare target and distractor auditory and visual stimuli. I. Superior temporal plane and parietal lobe. *Electroencephalography and Clinical Neurophysiology, 94*(3), 191-220. doi:10.1016/0013-4694(94)00259-n

Hamalainen, M. S., & Ilmoniemi, R. J. (1994). Interpreting magnetic fields of the brain: minimum norm estimates. *Medical & Biological Engineering & Computing, 32*(1), 35-42. doi:10.1007/BF02512476

Hamandi, K., Laufs, H., Noth, U., Carmichael, D. W., Duncan, J. S., & Lemieuxa, L. (2008). BOLD and perfusion changes during epileptic generalised spike wave activity. *Neuroimage, 39*(2), 608-618. doi:10.1016/j.neuroimage.2007.07.009

Hartstra, E., Kuhn, S., Verguts, T., & Brass, M. (2011). The implementation of verbal instructions: an fMRI study. *Human Brain Mapping, 32*(11), 1811-1824. doi:10.1002/hbm.21152

Haxby, J. V., Horwitz, B., Ungerleider, L. G., Maisog, J. M., Pietrini, P., & Grady, C. L. (1994). The functional organization of human extrastriate cortex: A PET-rCBF study of selective attention to faces and locations. *Journal of Neuroscience, 14*(11 Pt 1), 6336-6353.

Heinks-Maldonado, T. H., Mathalon, D. H., Gray, M., & Ford, J. M. (2005). Fine-tuning of auditory cortex during speech production. *Psychophysiology, 42*, 180–190.

Heinks-Maldonado, T. H., Nagarajan, S. S., & Houde, J. F. (2006). Magnetoencephalographic evidence for a precise 4b forwardmodel in speech production. *Neuroreport, 17*, 1375–1379.

Heinze, H. J., Mangun, G. R., Burchert, W., Hinrichs, H., Scholz, M., Munte, T. F., . . . et al. (1994). Combined spatial and temporal imaging of brain activity during visual selective attention in humans. *Nature, 372*(6506), 543-546. doi:10.1038/372543a0

Henson, R. N., Rylands, A., Ross, E., Vuilleumeir, P., & Rugg, M. D. (2004). The effect of repetition lag on electrophysiological and haemodynamic correlates of visual object priming. *Neuroimage, 21*(4), 1674-1689. doi:10.1016/j.neuroimage.2003.12.020

Herrmann, C. S., & Debener, S. (2008). Simultaneous recording of EEG and BOLD responses: A historical perspective. *International Journal of Psychophysiology, 67*(3), 161-168. doi:10.1016/j.ijpsycho.2007.06.006

Herwig, A., Prinz, W., & Waszak, F. (2007). Two modes of sensorimotor integration in intention-based and stimulus-based actions. *Quarterly Journal of Experimental Psychology, 60*(11), 1540-1554. doi:10.1080/17470210601119134

Hill, R. A., Chiappa, K. H., Huang-Hellinger, F., & Jenkins, B. G. (1995). EEG during MR imaging: Differentiation of movement artifact from paroxysmal cortical activity. *Neurology, 45*(10), 1942-1943.

Hoffman, J., Butz, M. V., Herbort, O., Kiesel, A., & Lenhard, A. (2007). Spekulationen zur Struktur ideo-motorischer Beziehungen. *Zeitschrift für Sportpsychologie, 14*, 95-104.

Hoffmann, A., Jager, L., Werhahn, K. J., Jaschke, M., Noachtar, S., & Reiser, M. (2000). Electroencephalography during functional echo-planar imaging: Detection of epileptic spikes using post-processing methods. *Magnetic Resonance in Medicine, 44*(5), 791-798. doi:10.1002/1522-2594(200011)44:5<791::Aid-Mrm17>3.0.Co;2-2

Hoffmann, J., Butz, M. V., Herbort, O., Kiesel, A., & Lenhard, A. (2007). Speculations about the structure of ideomotor relations. *Zeitschrift für Sportpsychologie, 14*(3), 95-103. doi:10.1026/1612-5010.14.3.95

Hoffmann, J., & Engelkamp, J. (2013). *Lern- und Gedächtnispsychologie.* . Heidelberg: Springer-Verlag.

Holland, P. C. (2004). Relations between Pavlovian-instrumental transfer and reinforcer devaluation. *Journal of Experimental Psychology-Animal Behavior Processes, 30*(2), 104-117. doi:10.1037/0097-7403.30.2.104

Holroyd, C. B., & Coles, M. G. (2002). The neural basis of human error processing: reinforcement learning, dopamine, and the error-related negativity. *Psychological Review, 109*(4), 679-709.

Hommel, B. (1996). The cognitive representation of action: Automatic integration of perceived action effects. *Psychological Research-Psychologische Forschung, 59*(3), 176-186. doi:10.1007/Bf00425832

Hommel, B. (2009). Action control according to TEC (theory of event coding). *Psychological Research, 73*(4), 512-526. doi:10.1007/s00426-009-0234-2

Hommel, B. (2013). Ideomotor action control: On the perceptual grounding of voluntary actions and agents. In W. Prinz, M. Beisert, & A. Herwig (Eds.), *Action science: Foundations of an emerging discipline*. Cambridge, MA: MIT Press.

Hommel, B., Musseler, J., Aschersleben, G., & Prinz, W. (2001). The Theory of Event Coding (TEC): A framework for perception and action planning. *Behavioral and Brain Sciences, 24*(5), 849-878; discussion 878-937.

Hothorn, T., Bretz, F., & Westfall, P. (2008). Simultaneous inference in general parametric models. *Biometrical Journal, 50*(3), 346-363. doi:10.1002/bimj.200810425

Houde, J. F., Nagarajan, S. S., Sekihara, K., & Merzenich, M. M. (2002). Modulation of the auditory cortex during speech: an MEG study. *J Cogn Neurosci, 14*(8), 1125-1138. doi:10.1162/089892902760807140

Huang, T. R., Hazy, T. E., Herd, S. A., & O'Reilly, R. C. (2013). Assembling old tricks for new tasks: a neural model of instructional learning and control. *J Cogn Neurosci, 25*(6), 843-851. doi:10.1162/jocn_a_00365

Huettel, S. A., Song, A. W., & McCarthy, G. (2009). *Functional Magnetic Resonance Imaging*. Sunderland, MA: Sunderland Associates.

Hughes, G., Desantis, A., & Waszak, F. (2013a). Attenuation of auditory N1 results from identity-specific action-effect prediction. *European Journal of Neuroscience, 37*(7), 1152-1158. doi:10.1111/ejn.12120

Hughes, G., Desantis, A., & Waszak, F. (2013b). Mechanisms of intentional binding and sensory attenuation: The role of temporal prediction, temporal control, identity prediction, and motor prediction. *Psychological Bulletin, 139*(1), 133-151. doi:10.1037/a0028566

Hughes, G., & Waszak, F. (2011). ERP correlates of action effect prediction and visual sensory attenuation in voluntary action. *Neuroimage, 56*(3), 1632-1640. doi:10.1016/j.neuroimage.2011.02.057

Hull, C. L. (1930). Knowledge and purpose as habit mechanisms. *Psychological Review, 37*, 511-525. doi:10.1037/h0072212

Huster, R. J., Debener, S., Eichele, T., & Herrmann, C. S. (2012). Methods for simultaneous EEG-fMRI: An introductory review. *Journal of Neuroscience, 32*(18), 6053-6060. doi:10.1523/Jneurosci.0447-12.2012

Huster, R. J., Eichele, T., Enriquez-Geppert, S., Wollbrink, A., Kugel, H., Konrad, C., & Pantev, C. (2011). Multimodal imaging of functional networks and event-related potentials in performance monitoring. *Neuroimage, 56*(3), 1588-1597. doi:10.1016/j.neuroimage.2011.03.039

Ikeda, A., & Shibasaki, H. (1992). Invasive recording of movement-related cortical potentials in humans. *Journal of Clinical Neurophysiology, 9*(4), 509-520. doi:10.1097/00004691-199210000-00005

James, C. J., & Hesse, C. W. (2005). Independent component analysis for biomedical signals. *Physiological Measurement, 26*(1), R15-39. doi:10.1088/0967-3334/26/1/r02

James, W. (1890). *The principles of psychology, Vol. 2*. New York: Dover Publications.

Jäncke, L. (2005). *Methoden der Bildgebung in der Psychologie n den kognitiven Neurowissenschaften*. Stuttgart: Kohlhammer.

Janczyk, M., Skirde, S., Weigelt, M., & Kunde, W. (2009). Visual and tactile action effects determine bimanual coordination performance. *Human Movement Science, 28*(4), 437-449. doi:10.1016/j.humov.2009.02.006

Jann, K., Dierks, T., Boesch, C., Kottlow, M., Strik, W., & Koenig, T. (2009). BOLD correlates of EEG alpha phase-locking and the fMRI default mode network. *Neuroimage, 45*(3), 903-916. doi:10.1016/j.neuroimage.2009.01.001

Jasper, H. H. (1958). The ten±twenty electrode system of the International Federation. *Electroencephalography and Clinical Neurophysiology, 10*, 371-375.

Johnson, A., van der Meer, M. A., & Redish, A. D. (2007). Integrating hippocampus and striatum in decision-making. *Current Opinion in Neurobiology, 17*(6), 692-697. doi:10.1016/j.conb.2008.01.003

Kahana, M. J. (2006). The cognitive correlates of human brain oscillations. *Journal of Neuroscience, 26*(6), 1669-1672. doi:10.1523/JNEUROSCI.3737-05c.2006

Kawashima, R., O'Sullivan, B. T., & Roland, P. E. (1995). Positron-emission tomography studies of cross-modality inhibition in selective attentional tasks: Closing the "mind's eye". *Proceedings of the National Academy of Sciences of the United States of America, 92*(13), 5969-5972. doi:10.1073/pnas.92.13.5969

Keller, P. E., & Koch, I. (2006). The planning and execution of short auditory sequences. *Psychonomic Bulletin & Review, 13*(4), 711-716. doi:Doi 10.3758/Bf03193985

Keller, P. E., Wascher, E., Prinz, W., Waszak, F., Koch, I., & Rosenbaum, D. A. (2006). Differences between intention-based and stimulus-based actions. *Journal of Psychophysiology, 20*(1), 9-20. doi:10.1027/0269-8803.20.1.9

Kennedy, P. J., & Shapiro, M. L. (2009). Motivational states activate distinct hippocampal representations to guide goal-directed behaviors. *Proceedings of the National Academy of Sciences of the United States of America, 106*(26), 10805-10810. doi:10.1073/pnas.0903259106

Kiesel, A., & Koch, I. (2012). *Lernen. Grundlagen der Lernpsychologie.* Wiesbaden: VS Verlag.

Klem, G. H., Luders, H. O., Jasper, H. H., & Elger, C. (1999). The ten-twenty electrode system of the International Federation. The International Federation of Clinical Neurophysiology. *Electroencephalography and Clinical Neurophysiology, 52*, 3-6.

Knight, R. T. (2007). Neuroscience - Neural networks debunk phrenology. *Science, 316*(5831), 1578-1579. doi:10.1126/science.1144677

Konings, M. K., Bartels, L. W., Smits, H. F., & Bakker, C. J. (2000). Heating around intravascular guidewires by resonating RF waves. *Journal of Magnetic Resonance Imaging, 12*(1), 79-85.

Kornhuber, H. H., & Deecke, L. (1990). readiness for movement - the bereitschaftspotential story - a citation classic commentary on changes in brain potentials with willful and passive movement in humans - the readiness potential and reafferent potentials, by Kornhuber,H.H., and Deecke,L. *Current Contents/Clinical Medicine*(4), 14-14.

Krakow, K., Allen, P. J., Symms, M. R., Lemieux, L., Josephs, O., & Fish, D. R. (2000). EEG recording during fMRI experiments: image quality. *Human Brain Mapping, 10*(1), 10-15.

Kriegeskorte, N., Simmons, W. K., Bellgowan, P. S. F., & Baker, C. I. (2009). Circular analysis in systems neuroscience: The dangers of double dipping. *Nature Neuroscience, 12*(5), 535-540. doi:10.1038/nn.2303

Kuhn, S., Seurinck, R., Fias, W., & Waszak, F. (2010). The internal anticipation of sensory action effects: When action induces ffa and ppa activity. *Frontiers in Human Neuroscience, 4*, 54. doi:10.3389/fnhum.2010.00054

Kunde, W. (2001a). Exploring the hyphen in ideo-motor action. *Behavioral and Brain Sciences, 24*(5), 891-+.

Kunde, W. (2001b). Response-effect compatibility in manual choice reaction tasks. *Journal of Experimental Psychology-Human Perception and Performance, 27*(2), 387-394. doi:10.1037//0096-1523.27.2.387

Kunde, W. (2003). Temporal response-effect compatibility. *Psychological Research, 67*(3), 153-159. doi:10.1007/s00426-002-0114-5

Kunde, W. (2004). Response priming by supraliminal and subliminal action effects. *Psychological Research, 68*(2-3), 91-96. doi:10.1007/s00426-003-0147-4

Kunde, W. (2006). Antezedente Effektrepräsentationen in der Verhaltenssteuerung. *Psychologische Rundschau, 57*(1), 34-42.

Kunde, W., Koch, I., & Hoffmann, J. (2004). Anticipated action effects affect the selection, initiation, and execution of actions. *The Quarterly Journal of Experimental Psychology, 57*(1), 87-106. doi:10.1080/02724980343000143

Lakatos, P., Karmos, G., Mehta, A. D., Ulbert, I., & Schroeder, C. E. (2008). Entrainment of neuronal oscillations as a mechanism of attentional selection. *Science, 320*(5872), 110-113. doi:10.1126/science.1154735

Lange, K. (2011). The reduced N1 to self-generated tones: An effect of temporal predictability? *Psychophysiology, 48*(8), 1088-1095. doi:10.1111/j.1469-8986.2010.01174.x

Laurienti, P. J., Burdette, J. H., Wallace, M. T., Yen, Y. F., Field, A. S., & Stein, B. E. (2002). Deactivation of sensory-specific cortex by cross-modal stimuli. *Journal of Cognitive Neuroscience, 14*(3), 420-429. doi:10.1162/089892902317361930

Le Pelley, M. E., & McLaren, I. P. L. (2003). Learned associability and associative change in human causal learning. *Quarterly Journal of Experimental Psychology Section B-Comparative and Physiological Psychology, 56*(1), 68-79. doi:10.1080/02724990244000179

Lemieux, L., Allen, P. J., Franconi, F., Symms, M. R., & Fish, D. R. (1997). Recording of EEG during fMRI experiments: Patient safety. *Magnetic Resonance Imaging, 38*(6), 943-952.

Leopold, D. A., Murayama, Y., & Logothetis, N. K. (2003). Very slow activity fluctuations in monkey visual cortex: Implications for functional brain imaging. *Cerebral Cortex, 13*(4), 422-433. doi: 10.1093/cercor/13.4.422

Li, J., Delgado, M. R., & Phelps, E. A. (2011). How instructed knowledge modulates the neural systems of reward learning. *Proceedings of the National Academy of Sciences of the United States of America, 108*(1), 55-60. doi:10.1073/pnas.1014938108

Linkenkaer-Hansen, K., Nikulin, V. V., Palva, S., Ilmoniemi, R. J., & Palva, J. M. (2004). Prestimulus oscillations enhance psychophysical performance in humans. *Journal of Neuroscience, 24*(45), 10186-10190. doi:10.1523/Jneurosci.2584-04.2004

Logothetis, N. K. (2002). The neural basis of the blood-oxygen-level-dependent functional magnetic resonance imaging signal. *Philosophical Transactions of the Royal Society of London, 357*(1424), 1003-1037. doi:10.1098/rstb.2002.1114

Logothetis, N. K. (2008). What we can do and what we cannot do with fMRI. *Nature, 453*(7197), 869-878. doi:10.1038/nature06976

Logothetis, N. K., Pauls, J., Augath, M., Trinath, T., & Oeltermann, A. (2001). Neurophysiological investigation of the basis of the fMRI signal. *Nature, 412*(6843), 150-157. doi:10.1038/35084005

Logothetis, N. K., & Pfeuffer, J. (2004). On the nature of the BOLD fMRI contrast mechanism. *Magnetic Resonance Imaging, 22*(10), 1517-1531. doi:10.1016/j.mri.2004.10.018

Lotze, R. H. (1896). Medicinische Psychologie, Oder, Physiologie der Seele.

Luck, S. J. (2005). *An introduction to the event-related potential technique.* Cambridge, Massachusetts: The MIT Press.

Luo, Q. F., Huang, X. S., & Glover, G. H. (2014). Ballistocardiogram artifact removal with a reference layer and standard EEG cap. *Journal of Neuroscience Methods, 233*, 137-149. doi:10.1016/j.jneumeth.2014.06.021

Luque, D., Moris, J., Rushby, J. A., & Le Pelley, M. E. (2015). Goal-directed EEG activity evoked by discriminative stimuli in reinforcement learning. *Psychophysiology, 52*(2), 238-248. doi:10.1111/psyp.12302

Mackintosh, N. J. (1975). A theory of attention: Variations in the associability of stimuli with reinforcement. 4.

Makeig, S., Delorme, A., Westerfield, M., Jung, T. P., Townsend, J., Courchesne, E., & Sejnowski, T. J. (2004). Electroencephalographic brain dynamics following manually responded visual targets. *Plos Biology, 2*(6), 747-762. doi:ARTN e17610.1371/journal.pbio.0020176

Mansfield, P., & Maudsley, A. A. (1976). Line scan proton spin imaging in biological structures by NMR. *Physics in Medicine and Biology, 21*(5), 847-852.

Martikainen, M. H., Kaneko, K., & Hari, R. (2005). Suppressed responses to self-triggered sounds in the human auditory cortex. *Cereb Cortex, 15*(3), 299-302. doi:10.1093/cercor/bhh131

Masterton, R. A. J., Abbott, D. F., Fleming, S. W., & Jackson, G. D. (2007). Measurement and reduction of motion and ballistocardiogram artefacts from simultaneous EEG and fMRI recordings. *Neuroimage, 37*(1), 202-211. doi:10.1016/j.neuroimage.2007.02.060

Matusz, P. J., Thelen, A., Amrein, S., Geiser, E., Anken, J., & Murray, M. M. (2015). The role of auditory cortices in the retrieval of single-trial auditory-visual object memories. *European Journal of Neuroscience, 41*(5), 699-708. doi:10.1111/ejn.12804

Maxwell, S. E., Lau, M. Y., & Howard, G. S. (2015). Is psychology suffering from a replication crisis? What does "failure to replicate" really mean? *American Psychology, 70*(6), 487-498. doi:10.1037/a0039400

McCarthy, G., & Donchin, E. (1976). The effects of temporal and event uncertainty in determining the waveforms of the auditory event related potential (ERP). *Psychophysiology, 13*(6), 581-590.

McLaren, D. G., Ries, M. L., Xu, G. F., & Johnson, S. C. (2012). A generalized form of context-dependent psychophysiological interactions (gPPI): A comparison to standard approaches. *Neuroimage, 61*(4), 1277-1286. doi:10.1016/j.neuroimage.2012.03.068

Melcher, T., Weidema, M., Eenshuistra, R. M., Hommel, B., & Gruber, O. (2008). The neural substrate of the ideomotor principle: An event-related fMRI analysis. *Neuroimage, 39*(3), 1274-1288. doi:10.1016/j.neuroimage.2007.09.049

Melcher, T., Winter, D., Hommel, B., Pfister, R., Dechent, P., & Gruber, O. (2013). The neural substrate of the ideomotor principle revisited: Evidence for asymmetries in action-effect learning. *Neuroscience, 231*, 13-27. doi:10.1016/j.neuroscience.2012.11.035

Menon, R. S., Ogawa, S., Kim, S. G., Ellermann, J. M., Merkle, H., Tank, D. W., & Ugurbil, K. (1992). Functional brain mapping using magnetic resonance imaging. Signal changes accompanying visual stimulation. *Investigative Radiology, 27 Suppl 2*, S47-53.

Meylan, R. V., & Murray, M. M. (2007). Auditory-visual multisensory interactions attenuate subsequent visual responses in humans. *Neuroimage, 35*(1), 244-254. doi:10.1016/j.neuroimage.2006.11.033

Miall, R. C., & Wolpert, D. M. (1996). Forward models for physiological motor control. *Neural Networks, 9*(8), 1265-1279. doi:Doi 10.1016/S0893-6080(96)00035-4

Michel, C. M., Murray, M. M., Lantz, G., Gonzalez, S., Spinelli, L., & Grave de Peralta, R. (2004). EEG source imaging. *Clinical Neurophysiology, 115*(10), 2195-2222. doi:10.1016/j.clinph.2004.06.001

Mifsud, N. G., Oestreich, L. K., Jack, B. N., Ford, J. M., Roach, B. J., Mathalon, D. H., & Whitford, T. J. (2016). Self-initiated actions result in suppressed auditory but amplified visual evoked components in healthy participants. *Psychophysiology*. doi:10.1111/psyp.12605

Minati, L., Rosazza, C., Zucca, I., D'Incerti, L., Scaioli, V., & Bruzzone, M. G. (2008). Spatial correspondence between functional MRI (fMRI) activations and cortical current density maps of event-related potentials (ERP): A study with four tasks. *Brain Topography, 21*(2), 112-127. doi:10.1007/s10548-008-0064-3

Mishra, J., Rolle, C., & Gazzaley, A. (2015). Neural plasticity underlying visual perceptual learning in aging. *Brain Research, 1612*, 140-151. doi:10.1016/j.brainres.2014.09.009

Mitzdorf, U. (1989). Current-Source-Density Analysis of Evoked-Potentials. *Perception, 18*(4), 549-549.

Mizuhara, H., Wang, L. Q., Kobayashi, K., & Yamaguchi, Y. (2005). Long-range EEG phase synchronization during an arithmetic task indexes a coherent cortical network simultaneously measured by fMRI. *Neuroimage, 27*(3), 553-563. doi:10.1016/j.neuroimage.2005.04.030

Mohr, H., Wolfensteller, U., Betzel, R. F., Misic, B., Sporns, O., Richiardi, J., & Ruge, H. (2016). Integration and segregation of large-scale brain networks during short-term task automatization. *Nature Communications, 7*, 13217. doi:10.1038/ncomms13217

Mohr, H., Wolfensteller, U., Frimmel, S., & Ruge, H. (2015). Sparse regularization techniques provide novel insights into outcome integration processes. *Neuroimage, 104*, 163-176. doi:10.1016/j.neuroimage.2014.10.025

Molholm, S., Ritter, W., Javitt, D. C., & Foxe, J. J. (2004). Multisensory visual-auditory object recognition in humans: A high-density electrical mapping study. *Cerebral Cortex, 14*(4), 452-465. doi:10.1093/cercor/bhh007

Molholm, S., Ritter, W., Murray, M. M., Javitt, D. C., Schroeder, C. E., & Foxe, J. J. (2002). Multisensory auditory-visual interactions during early sensory processing in humans: A high-density electrical mapping study. *Cognitive Brain Research, 14*(1), 115-128. doi:10.1016/S0926-6410(02)00066-6

Moosmann, M., Eichele, T., Nordby, H., Hugdahl, K., & Calhoun, V. D. (2008). Joint independent component analysis for simultaneous EEG-MRI: Principle and simulation (vol 67, pg 212, 2008). *International Journal of Psychophysiology, 68*(1), 81-81. doi:10.1016/j.ijpsycho.2007.08.003

Moosmann, M., Schonfelder, V. H., Specht, K., Scheeringa, R., Nordby, H., & Hugdahl, K. (2009). Realignment parameter-informed artefact correction for simultaneous EEG-fMRI recordings. *Neuroimage, 45*(4), 1144-1150. doi:10.1016/j.neuroimage.2009.01.024

Mozolic, J. L., Hugenschmidt, C. E., Peiffer, A. M., & Laurienti, P. J. (2008). Modality-specific selective attention attenuates multisensory integration. *Experimental Brain Research, 184*(1), 39-52. doi:10.1007/s00221-007-1080-3

Murray, M. M., Foxe, J. J., & Wylie, G. R. (2005). The brain uses single-trial multisensory memories to discriminate without awareness. *Neuroimage, 27*(2), 473-478. doi:10.1016/j.neuroimage.2005.04.016

Murray, M. M., Michel, C. M., Grave de Peralta, R., Ortigue, S., Brunet, D., Gonzalez Andino, S., & Schnider, A. (2004). Rapid discrimination of visual and multisensory memories revealed by electrical neuroimaging. *Neuroimage, 21*(1), 125-135. doi:10.1016/j.neuroimage.2003.09.035

Murray, M. M., Thelen, A., Thut, G., Romei, V., Martuzzi, R., & Matusz, P. J. (2015). The multisensory function of the human primary visual cortex. *Neuropsychologia, 11*(15), 30127-30125.

Naatanen, R., & Picton, T. (1987). The N1 wave of the human electric and magnetic response to sound: A review and an analysis of the component structure. *Psychophysiology, 24*(4), 375-425.

Nachev, P., Kennard, C., & Husain, M. (2008). Functional role of the supplementary and pre-supplementary motor areas. *Nature Reviews Neuroscience, 9*(11), 856-869. doi:10.1038/nrn2478

Nakamura, W., Anami, K., Mori, T., Saitoh, O., Cichocki, A., & Amari, S. (2006). Removal of ballistocardiogram artifacts from simultaneously recorded EEG and fMRI data using independent component analysis. *Ieee Transactions on Biomedical Engineering, 53*(7), 1294-1308. doi:10.1109/Tmbe.2006.875718

Negishi, M., Abildgaard, M., Laufer, I., Nixon, T., & Constable, R. T. (2008). An EEG (electroencephalogram) recording system with carbon wire electrodes for simultaneous EEG-fMRI (functional magnetic resonance imaging) recording. *Journal of Neuroscience Methods, 173*(1), 99-107. doi:10.1016/j.jneumeth.2008.05.024

Negishi, M., Abildgaard, M., Nixon, T., & Constable, R. T. (2004). Removal of time-varying gradient artifacts from EEG data acquired during continuous fMRI. *Clinical Neurophysiology, 115*(9), 2181-2192. doi:10.1016/j.clinph.2004.04.005

Niazy, R. K., Beckmann, C. F., Iannetti, G. D., Brady, J. M., & Smith, S. M. (2005). Removal of FMRI environment artifacts from EEG data using optimal basis sets. *Neuroimage, 28*(3), 720-737. doi:10.1016/j.neuroimage.2005.06.067

Nierhaus, T., Gundlach, C., Goltz, D., Thiel, S. D., Pleger, B., & Villringer, A. (2013). Internal ventilation system of MR scanners induces specific EEG artifact during simultaneous EEG-fMRI. *Neuroimage, 74*, 70-76. doi:10.1016/j.neuroimage.2013.02.016

Nitz, W. R., Oppelt, A., Renz, W., Manke, C., Lenhart, M., & Link, J. (2001). On the heating of linear conductive structures as guide wires and catheters in interventional MRI. *Journal of Magnetic Resonance Imaging, 13*(1), 105-114.

Noonan, M. P., Kolling, N., Walton, M. E., & Rushworth, M. F. (2012). Re-evaluating the role of the orbitofrontal cortex in reward and reinforcement. *European Journal of Neuroscience, 35*(7), 997-1010. doi:10.1111/j.1460-9568.2012.08023.x

Noonan, M. P., Mars, R. B., & Rushworth, M. F. S. (2011). Distinct roles of three frontal cortical areas in reward-guided behavior. *Journal of Neuroscience, 31*(40), 14399-14412. doi:10.1523/Jneurosci.6456-10.2011

Nunez, P. L., & Pilgreen, K. L. (1991). The Spline-Laplacian in Clinical Neurophysiology - a Method to Improve EEG spatial-resolution. *Journal of Clinical Neurophysiology, 8*(4), 397-413. doi:Doi 10.1097/00004691-199110000-00005

Nunez, P. L., & Silberstein, R. B. (2000). On the relationship of synaptic activity to macroscopic measurements: Does co-registration of EEG with fMRI make sense? *Brain Topography, 13*(2), 79-96. doi:Doi 10.1023/A:1026683200895

O'Doherty, J., Dayan, P., Schultz, J., Deichmann, R., Friston, K., & Dolan, R. J. (2004). Dissociable roles of ventral and dorsal striatum in instrumental conditioning. *Science, 304*(5669), 452-454. doi:10.1126/science.1094285

O'Doherty, J. P. (2011). Contributions of the ventromedial prefrontal cortex to goal-directed action selection. *Annals of the New York Academy of Sciences, 1239*, 118-129. doi:10.1111/j.1749-6632.2011.06290.x

O'Reilly, R. C., & Rudy, J. W. (2001). Conjunctive representations in learning and memory: principles of cortical and hippocampal function. *Psychological Review, 108*(2), 311-345. doi:10.1037/0033-295x.108.2.311

Oberauer, K. (2009). Design for a working memory. *The psychology of learning and motivation: Advances in research and theory* (pp. 45 - 100). San Diego, CA: Elsevier.

Ogawa, S., Lee, T. M., Kay, A. R., & Tank, D. W. (1990). Brain magnetic resonance imaging with contrast dependent on blood oxygenation. *Proceedings of the National Academy of Sciences of the United States of America, 87*(24), 9868-9872.

Ogawa, S., Lee, T. M., Nayak, A. S., & Glynn, P. (1990). Oxygenation-sensitive contrast in magnetic resonance image of rodent brain at high magnetic fields. *Magnetic Resonance in Medicine, 14*(1), 68-78.

Ogawa, S., Menon, R. S., Tank, D. W., Kim, S. G., Merkle, H., Ellermann, J. M., & Ugurbil, K. (1993). Functional brain mapping by blood oxygenation level-dependent contrast magnetic resonance imaging. A comparison of signal characteristics with a biophysical model. *Biophysiological Journal, 64*(3), 803-812. doi:10.1016/S0006-3495(93)81441-3

Ogawa, S., Tank, D. W., Menon, R., Ellermann, J. M., Kim, S. G., Merkle, H., & Ugurbil, K. (1992). Intrinsic signal changes accompanying sensory stimulation: functional brain mapping with magnetic resonance imaging. *Proceedings of the National Academy of Sciences of the United States of America, 89*(13), 5951-5955.

Ohara, S., Mima, T., Baba, K., Ikeda, A., Kunieda, T., Matsumoto, R., . . . Shibasaki, H. (2001). Increased synchronization of cortical oscillatory activities between human supplementary motor and primary sensorimotor areas during voluntary movements. *Journal of Neuroscience, 21*(23), 9377-9386. doi:10.1523/Jneurosci.21-23-09377.2001

Ojemann, J. G., Akbudak, E., Snyder, A. Z., McKinstry, R. C., Raichle, M. E., & Conturo, T. E. (1997). Anatomic localization and quantitative analysis of gradient refocused echo-planar fMRI susceptibility artifacts. *Neuroimage, 6*(3), 156-167. doi:10.1006/nimg.1997.0289

Onton, J., Westerfield, M., Townsend, J., & Makeig, S. (2006). Imaging human EEG dynamics using independent component analysis. *Neurosci Biobehav Rev, 30*(6), 808-822. doi:10.1016/j.neubiorev.2006.06.007

Open Science, C. (2015). Psychology. Estimating the reproducibility of psychological science. *Science, 349*(6251), aac4716. doi:10.1126/science.aac4716

Ostlund, S. B., & Balleine, B. W. (2007). Orbitofrontal cortex mediates outcome encoding in Pavlovian but not instrumental conditioning. *Journal of Neuroscience, 27*(18), 4819-4825. doi:10.1523/JNEUROSCI.5443-06.2007

Ou, W. M., Nummenmaa, A., Ahveninen, J., Belliveau, J. W., Hamalainen, M. S., & Golland, P. (2010). Multimodal functional imaging using fMRI-informed regional EEG/MEG source estimation. *Neuroimage, 52*(1), 97-108. doi:10.1016/j.neuroimage.2010.03.001

Pascual-Marqui, R. D., Lehmann, D., Koenig, T., Kochi, K., Merlo, M. C. G., Hell, D., & Koukkou, M. (1999). Low resolution brain electromagnetic tomography (LORETA) functional imaging in acute, neuroleptic-naive, first-episode, productive schizophrenia. *Psychiatry Research-Neuroimaging, 90*(3), 169-179. doi:10.1016/S0925-4927(99)00013-X

Passingham, R. E., Toni, I., & Rushworth, M. F. (2000). Specialisation within the prefrontal cortex: the ventral prefrontal cortex and associative learning. *Experimental Brain Research, 133*(1), 103-113. doi:10.1007/s002210000405

Pavlov, I. V. (1927). *Conditioned reflexes*. Oxford: Oxford University Press.

Pfister, R., Kiesel, A., & Melcher, T. (2010). Adaptive control of ideomotor effect anticipations. *Acta Psychologica, 135*(3), 316-322. doi:10.1016/j.actpsy.2010.08.006

Pfister, R., & Kunde, W. (2013). Dissecting the response in response-effect compatibility. *Experimental Brain Research, 224*(4), 647-655. doi:10.1007/s00221-012-3343-x

Pfister, R., Melcher, T., Kiesel, A., Dechent, P., & Gruber, O. (2014). Neural correlates of ideomotor effect anticipations. *Neuroscience, 259*, 164-171. doi:10.1016/j.neuroscience.2013.11.061

Picard, N., & Strick, P. L. (1996). Motor areas of the medial wall: a review of their location and functional activation. *Cerebral Cortex, 6*(3), 342-353. doi:10.1093/cercor/6.3.342

Picard, N., & Strick, P. L. (2001). Imaging the premotor areas. *Current Opinion in Neurobiology, 11*(6), 663-672. doi:10.1016/s0959-4388(01)00266-5

Pictet, J., Meuli, R., Wicky, S., & van der Klink, J. J. (2002). Radiofrequency heating effects around resonant lengths of wire in MRI. *Physics in Medicine and Biology, 47*(16), 2973-2985.

Pleger, B., Blankenburg, F., Bestmann, S., Ruff, C. C., Wiech, K., Stephan, K. E., . . . Dolan, R. J. (2006). Repetitive transcranial magnetic stimulation-induced changes in sensorimotor coupling parallel improvements of somatosensation in humans. *Journal of Neuroscience, 26*(7), 1945-1952. doi:10.1523/JNEUROSCI.4097-05.2006

Porter, L. L. (1991). Patterns of connectivity in the cat sensory-motor cortex: A light and electron microscope analysis of the projection arising from area 3a. *J Comp Neurol, 312*(3), 404-414. doi:10.1002/cne.903120308

Porter, L. L. (1997). Morphological Characterization of a Cortico-cortical relay in the cat sensorimotor cortex. *Cerebral Cortex, 7*(2), 100-109. doi:10.1093/cercor/7.2.100

Prinz, W. (1990). A common coding approach to perception and action. In O. Neumann & W. Prinz (Eds.), *Relationships between perception and action* (pp. 167-201). Berlin: Springer.

Prinz, W. (1997). Perception and action planning. *European Journal of Cognitive Psychology, 9*(2), 129-154. doi:10.1080/713752551

Quiroga, R. Q. (2000). Obtaining single stimulus evoked potentials with wavelet denoising. *Physica D-Nonlinear Phenomena, 145*(3-4), 278-292. doi:10.1016/S0167-2789(00)00116-0

Quiroga, R. Q., & Garcia, H. (2003). Single-trial event-related potentials with wavelet denoising. *Clinical Neurophysiology, 114*(2), 376-390. doi:10.1016/S1388-2457(02)00365-6

R Core Team. (2012). R: A language and envireonment for statistical computing.

Raichle, M. E., MacLeod, A. M., Snyder, A. Z., Powers, W. J., Gusnard, D. A., & Shulman, G. L. (2001). A default mode of brain function. *Proceedings of the National Academy of Sciences of the United States of America, 98*(2), 676-682. doi:10.1073/pnas.98.2.676

Raij, T., Ahveninen, J., Lin, F. H., Witzel, T., Jaaskelainen, I. P., Letham, B., . . . Belliveau, J. W. (2010). Onset timing of cross-sensory activations and multisensory interactions in auditory and visual sensory cortices. *European Journal of Neuroscience, 31*(10), 1772-1782. doi:10.1111/j.1460-9568.2010.07213.x

Ramamoorthy, A., & Verguts, T. (2012). Word and deed: A computational model of instruction following. *Brain Research, 1439*, 54-65. doi:10.1016/j.brainres.2011.12.025

Renier, L. A., Anurova, I., De Volder, A. G., Carlson, S., VanMeter, J., & Rauschecker, J. P. (2009). Multisensory integration of sounds and vibrotactile stimuli in processing streams for "what" and "where". *Journal of Neuroscience, 29*(35), 10950-10960. doi:10.1523/JNEUROSCI.0910-09.2009

Rescorla, R. A. (1966). Predictability and number pairings in Pavlovian fear conditioning. *Psychonomic Science, 4*, 383-384.

Rescorla, R. A. (1968). Probability of shock in the presence and absence of CS in fear conditioning. *Journal of Comparative and Physiological Psychology, 66*(1), 1-5.

Rescorla, R. A. (1994). Transfer of instrumental control mediated by a devalued outcome. *Animal Learning & Behavior, 22*(1), 27-33. doi:10.3758/Bf03199953

Rescorla, R. A., & Solomon, R. L. (1967). Two-process learning theory: Relationships between Pavlovian conditioning and instrumental learning. *Psychological Review, 74*(3), 151-182.

Rieger, M. (2007). Letters as visual action-effects in skilled typing. *Acta Psychologica, 126*(2), 138-153. doi:10.1016/j.actpsy.2006.11.006

Riera, J. J., & Sumiyoshi, A. (2010). Brain oscillations: ideal scenery to understand the neurovascular coupling. *Curr Opin Neurol, 23*(4), 374-381. doi:10.1097/WCO.0b013e32833b769f

Roesch, M. R., Taylor, A. R., & Schoenbaum, G. (2006). Encoding of time-discounted rewards in orbitofrontal cortex is independent of value representation. *Neuron, 51*(4), 509-520. doi:10.1016/j.neuron.2006.06.027

Rolls, E. T. (1996). The orbitofrontal cortex. *Philosophical Transactions of the Royal Society of London, 351*(1346), 1433-1443. doi:10.1098/rstb.1996.0128

Rolls, E. T. (2010). A computational theory of episodic memory formation in the hippocampus. *Behavioural Brain Research, 215*(2), 180-196. doi:10.1016/j.bbr.2010.03.027

Rolls, E. T., & Kesner, R. P. (2006). A computational theory of hippocampal function, and empirical tests of the theory. *Progress in Neurobiology, 79*(1), 1-48. doi:10.1016/j.pneurobio.2006.04.005

Rorden, C., Karnath, H. O., & Bonilha, L. (2007). Improving lesion-symptom mapping. *Journal of Cognitive Neuroscience, 19*(7), 1081-1088. doi:10.1162/jocn.2007.19.7.1081

Rosa, M. J., Daunizeau, J., & Friston, K. J. (2010). EEG-fMRI integration: a critical review of biophysical modeling and data analysis approaches. *J Integr Neurosci, 9*(4), 453-476.

Rosler, F., Heil, M., & Roder, B. (1997). Slow negative brain potentials as reflections of specific modular resources of cognition. *Biological Psychology, 45*(1-3), 109-141. doi:10.1016/s0301-0511(96)05225-8

Roussel, C., Hughes, G., & Waszak, F. (2013). A preactivation account of sensory attenuation. *Neuropsychologia, 51*(5), 922-929. doi:10.1016/j.neuropsychologia.2013.02.005

Roussel, C., Hughes, G., & Waszak, F. (2014). Action prediction modulates both neurophysiological and psychophysical indices of sensory attenuation. *Frontiers in Human Neuroscience, 8*. doi:10.3389/fnhum.2014.00115

Rowe, D. L., Robinson, P. A., & Gordon, E. (2005). Stimulant drug action in attention deficit hyperactivity disorder (ADHD): inference of neurophysiological mechanisms via quantitative modelling. *Clinical Neurophysiology, 116*(2), 324-335. doi:10.1016/j.clinph.2004.08.001

Ruge, H., Krebs, R. M., & Wolfensteller, U. (2012). Early markers of ongoing action-effect learning. *Frontiers in Psychology, 3*, 522. doi:10.3389/fpsyg.2012.00522

Ruge, H., Muller, S. C., & Braver, T. S. (2010). Anticipating the consequences of action: an fMRI study of intention-based task preparation. *Psychophysiology, 47*(6), 1019-1027. doi:10.1111/j.1469-8986.2010.01027.x

Ruge, H., & Wolfensteller, U. (2010). Rapid formation of pragmatic rule representations in the human brain during instruction-based learning. *Cerebral Cortex, 20*(7), 1656-1667. doi:10.1093/cercor/bhp228

Ruge, H., & Wolfensteller, U. (2013). Functional integration processes underlying the instruction-based learning of novel goal-directed behaviors. *Neuroimage, 68*, 162-172. doi:10.1016/j.neuroimage.2012.12.003

Ruge, H., & Wolfensteller, U. (2015). Distinct fronto-striatal couplings reveal the double-faced nature of response-outcome relations in instruction-based learning. *Cognitive Affective Behavioral Neuroscience, 15*(2), 349-364. doi:10.3758/s13415-014-0325-4

Ruge, H., & Wolfensteller, U. (2016). Towards an understanding of the neural dynamics of intentional learning: Considering the timescale. *Neuroimage*. doi:10.1016/j.neuroimage.2016.06.006

Rugg, M. D., & Coles, M. G. (1995). *Electrophysiology of Mind: Event-Related Brain Potentials and Cognition*. Oxford: Oxford University Press.

Rush, S., & Driscoll, D. A. (1968). Current distribution in the brain from surface electrodes. *Anesthesia & Analgesia, 47*(6), 717-723.

Rüsseler, J., & Münte, T. F. (2005). Kognitive Potenziale (ereigniskorrelierte Potenziale, EKP). In J. Noth (Ed.), *Evozierte Potenziale, Neurovegetative Diagnostik, Okulographie. Methodik und klinische Anwendung*. Stuttgart: Thieme-Verlag.

Saalmann, Y. B., Pigarev, I. N., & Vidyasagar, T. R. (2007). Neural mechanisms of visual attention: How top-down feedback highlights relevant locations. *Science, 316*(5831), 1612-1615. doi:10.1126/science.1139140

Sammer, G., Blecker, C., Gebhardt, H., Kirsch, P., Stark, R., & Vaitl, D. (2005). Acquisition of typical EEG waveforms during fMRI: SSVEP, LRP, and frontal theta. *Neuroimage, 24*(4), 1012-1024. doi:10.1016/j.neuroimage.2004.10.026

Sanmiguel, I., Todd, J., & Schroger, E. (2013). Sensory suppression effects to self-initiated sounds reflect the attenuation of the unspecific N1 component of the auditory ERP. *Psychophysiology, 50*(4), 334-343. doi:10.1111/psyp.12024

Schafer, E. W., & Marcus, M. M. (1973). Self-stimulation alters human sensory brain responses. *Science, 181*(4095), 175-177.

Scheeringa, R., Petersson, K. M., Oostenveld, R., Norris, D. G., Hagoort, P., & Bastiaansen, M. C. (2009). Trial-by-trial coupling between EEG and BOLD identifies networks related to alpha and theta EEG power increases during working memory maintenance. *Neuroimage, 44*(3), 1224-1238. doi:10.1016/j.neuroimage.2008.08.041

Scherg, M., & Picton, T. W. (1991). Separation and identification of event-related potential components by brain electric source analysis. *Electroencephalography and Clinical Neurophysiology*, 24-37.

Schoenbaum, G., Chiba, A. A., & Gallagher, M. (1998). Orbitofrontal cortex and basolateral amygdala encode expected outcomes during learning. *Nature Neuroscience, 1*(2), 155-159. doi:10.1038/407

Schoenbaum, G., & Roesch, M. (2005). Orbitofrontal cortex, associative learning, and expectancies. *Neuron, 47*(5), 633-636. doi:10.1016/j.neuron.2005.07.018

Schoenbaum, G., Roesch, M. R., & Stalnaker, T. A. (2006). Orbitofrontal cortex, decision-making and drug addiction. *Trends in Neurosciences, 29*(2), 116-124. doi:10.1016/j.tins.2005.12.006

Schoenbaum, G., Saddoris, M. P., & Stalnaker, T. A. (2007). Reconciling the roles of orbitofrontal cortex in reversal learning and the encoding of outcome expectancies. *Annals of the New York Academy of Sciences, 1121*, 320-335. doi:10.1196/annals.1401.001

Senkowski, D., Saint-Amour, D., Hofle, M., & Foxe, J. J. (2011). Multisensory interactions in early evoked brain activity follow the principle of inverse effectiveness. *Neuroimage, 56*(4), 2200-2208. doi:10.1016/j.neuroimage.2011.03.075

Shin, Y. K., Proctor, R. W., & Capaldi, E. J. (2010). A review of contemporary ideomotor theory. *Psychological Bulletin, 136*(6), 943-974. doi:10.1037/a0020541

Shmuel, A., Augath, M., Oeltermann, A., & Logothetis, N. K. (2006). Negative functional MRI response correlates with decreases in neuronal activity in monkey visual area V1. *Nature Neuroscience, 9*(4), 569-577. doi:10.1038/nn1675

Sijbers, J., Michiels, I., Verhoye, M., Van Audekerke, J., Van der Linden, A., & Van Dyck, D. (1999). Restoration of MR-induced artifacts in simultaneously recorded MR/EEG data. *Magnetic Resonance Imaging, 17*(9), 1383-1391. doi:10.1016/S0730-725x(99)00096-X

Sijbers, J., Van Audekerke, J., Verhoye, M., Van der Linden, A., & Van Dyck, D. (2000). Reduction of ECG and gradient related artifacts in simultaneously recorded human EEG/MRI data. *Magnetic Resonance Imaging, 18*(7), 881-886. doi:10.1016/S0730-725x(00)00178-8

Silvetti, S., & Verguts, T. (2012). Reinforcement learning, high-level cognition, and the human brain. In P. Bright (Ed.), *Neuroimaging.*: Intech.

Skinner, B. F. (1938). *The behavior of organisms: An experimental analysis.* New York: Appleton-Century-Crofts.

Song, Y., Ding, Y. L., Fan, S. L., Qu, Z., Xu, L., Lu, C. M., & Peng, D. (2005). Neural substrates of visual perceptual learning of simple and complex stimuli. *Clinical Neurophysiology, 116*(3), 632-639. doi:10.1016/j.clinph.2004.019

Spence, K. W. (1950). Cognitive Versus Stimulus Response Theories of Learning. *Psychological Review, 57*(3), 159-172. doi:10.1037/h0058250

Sperry, R. W. (1950). Neural basis of the spontaneous optokinetic response produced by visual inversion. *Journal of Comparative and Physiological Psychology, 43*(6), 482-489. doi:10.1037/h0055479

Srivastava, G., Crottaz-Herbette, S., Lau, K. M., Glover, G. H., & Menon, V. (2005). ICA-based procedures for removing ballistocardiogram artifacts from EEG data acquired in the MRI scanner. *Neuroimage, 24*(1), 50-60. doi:10.1016/j.neuroimage.2004.09.041

Stalnaker, T. A., Cooch, N. K., & Schoenbaum, G. (2015). What the orbitofrontal cortex does not do. *Nature Neuroscience, 18*(5), 620-627. doi:10.1038/nn.3982

Stekelenburg, J. J., & Vroomen, J. (2012). Electrophysiological correlates of predictive coding of auditory location in the perception of natural audiovisual events. *Frontiers in Integrative Neuroscience, 6*, 26. doi:10.3389/fnint.2012.00026

Stocco, A., Lebiere, C., O'Reilly, R. C., & Anderson, J. R. (2012). Distinct contributions of the caudate nucleus, rostral prefrontal cortex, and parietal cortex to the execution of instructed tasks. *Cognitive Affective Behavioral Neuroscience, 12*(4), 611-628. doi:10.3758/s13415-012-0117-7

Stock, A., & Stock, C. (2004). A short history of ideo-motor action. *Psychological Research, 68*(2-3), 176-188. doi:10.1007/s00426-003-0154-5

Strobel, A., Debener, S., Sorger, B., Peters, J. C., Kranczioch, C., Hoechstetter, K., . . . Goebel, R. (2008). Novelty and target processing during an auditory novelty oddball: A simultaneous event-related potential and functional magnetic resonance imaging study. *Neuroimage, 40*(2), 869-883. doi:10.1016/j.neuroimage.2007.10.065

Stroebe, W., & Strack, F. (2014). The alleged crisis and the illusion of exact replication. *Perspectives on Psychological Science, 9*(1), 59-71. doi:10.1177/1745691613514450

Sugihara, T., Diltz, M. D., Averbeck, B. B., & Romanski, L. M. (2006). Integration of auditory and visual communication information in the primate ventrolateral prefrontal cortex. *Journal of Neuroscience, 26*(43), 11138-11147. doi:10.1523/JNEUROSCI.3550-06.2006

Sun, L. M., & Hinrichs, H. (2009). Simultaneously recorded EEG-fMRI: Removal of gradient artifacts by subtraction of head movement related average artifact waveforms. *Human Brain Mapping, 30*(10), 3361-3377. doi:10.1002/hbm.20758

Talsma, D., Doty, T. J., & Woldorff, M. G. (2007). Selective attention and audiovisual integration: Is attending to both modalities a prerequisite for early integration? *Cerebral Cortex, 17*(3), 679-690. doi:10.1093/cercor/bhk016

Tanaka, S. C., Balleine, B. W., & O'Doherty, J. P. (2008). Calculating consequences: Brain systems that encode the causal effects of actions. *Journal of Neuroscience, 28*(26), 6750-6755. doi:10.1523/Jneurosci.1808-08.2008

Teder-Salejarvi, W. A., McDonald, J. J., Di Russo, F., & Hillyard, S. A. (2002). An analysis of audio-visual crossmodal integration by means of event-related potential (ERP) recordings. *Brain Research. Cognitive Brain Research, 14*(1), 106-114. doi:10.1016/s0926-6410(02)00065-4

Tenforde, T. S., Gaffey, C. T., Moyer, B. R., & Budinger, T. F. (1983). Cardiovascular Alterations in Macaca Monkeys Exposed to Stationary Magnetic-Fields - Experimental-Observations and Theoretical-Analysis. *Bioelectromagnetics, 4*(1), 1-9. doi:10.1002/bem.2250040102

Thelen, A., Cappe, C., & Murray, M. M. (2012). Electrical neuroimaging of memory discrimination based on single-trial multisensory learning. *Neuroimage, 62*(3), 1478-1488. doi:10.1016/j.neuroimage.2012.05.027

Thelen, A., Matusz, P. J., & Murray, M. M. (2014). Multisensory context portends object memory. *Current Biology, 24*(16), R734-735. doi:10.1016/j.cub.2014.06.040

Thorndike, E. L. (1905). *The elements of psychology*. New York: A. G. Seiler.

Thorndike, E. L. (1911). *Animal intelligence experimental studies*. New York: Macmillan.

Thorndike, E. L. (1927). A Fundamental Theorem in Modifiability. *Proc Natl Acad Sci U S A, 13*(1 Pt 1), 15-18. doi:10.1073/pnas.13.1.15

Thorndike, E. L. (1933). A Proof of the Law of Effect. *Science, 77*(1989), 173-175. doi:10.1126/science.77.1989.173-a

Toni, I., Ramnani, N., Josephs, O., Ashburner, J., & Passingham, R. E. (2001). Learning arbitrary visuomotor associations: Temporal dynamic of brain activity. *Neuroimage, 14*(5), 1048-1057. doi:10.1006/nimg.2001.0894

Trapold, M. A. (1970). Are expectancies based upon different positive reinforcing events discriminably different. *Learning and Motivation, 1*(2), 129-140. doi:10.1016/0023-9690(70)90079-2

Tricomi, E. M., Delgado, M. R., & Fiez, J. A. (2004). Modulation of caudate activity by action contingency. *Neuron, 41*(2), 281-292. doi:10.1016/S0896-6273(03)00848-1

Tulving, E., & Markowitsch, H. J. (1998). Episodic and declarative memory: Role of the hippocampus. *Hippocampus, 8*(3), 198-204. doi:10.1002/(SICI)1098-1063(1998)8:3<198::AID-HIPO2>3.0.CO;2-G

Tzourio-Mazoyer, N., Landeau, B., Papathanassiou, D., Crivello, F., Etard, O., Delcroix, N., . . . Joliot, M. (2002). Automated anatomical labeling of activations in SPM using a macroscopic anatomical parcellation of the MNI MRI single-subject brain. *Neuroimage, 15*(1), 273-289. doi:10.1006/nimg.2001.0978

Ullsperger, M., & Debener, S. (2010). *Simultaneous EEG and fMRI*. Oxford: Oxford University Press.

Urbano, A., Babiloni, C., Onorati, P., & Babiloni, F. (1996). Human cortical activity related to unilateral movements. A high resolution EEG study. *Neuroreport, 8*(1), 203-206. doi:10.1097/00001756-199612200-00041

Urcuioli, P. J. (2005). Behavioral and associative effects of differential outcomes in discrimination learning. *Learn Behav, 33*(1), 1-21.

Valdes-Sosa, P. A., Sanchez-Bornot, J. M., Sotero, R. C., Iturria-Medina, Y., Aleman-Gomez, Y., Bosch-Bayard, J., . . . Ozaki, T. (2009). Model driven EEG/fMRI fusion of brain oscillations. *Human Brain Mapping, 30*(9), 2701-2721. doi:10.1002/hbm.20704

Valentin, V. V., Dickinson, A., & O'Doherty, J. P. (2007). Determining the neural substrates of goal-directed learning in the human brain. *Journal of Neuroscience, 27*(15), 4019-4026. doi:10.1523/JNEUROSCI.0564-07.2007

van der Meer, J. N., Pampel, A., Van Someren, E. J., Ramautar, J. R., van der Werf, Y. D., Gomez-Herrero, G., . . . Walter, M. (2016). Carbon-wire loop based artifact correction outperforms post-processing EEG/fMRI corrections-A validation of a real-time simultaneous EEG/fMRI correction method. *Neuroimage, 125*, 880-894. doi:10.1016/j.neuroimage.2015.10.064

Van Der Meer, M., & Redish, A. D. (2010). Expectancies in decision making, reinforcement learning, and ventral striatum. *Frontiers in Neuroscience, 3*(6). doi:10.3389/neuro.01.006.2010

Varela, F., Lachaux, J. P., Rodriguez, E., & Martinerie, J. (2001). The brainweb: Phase synchronization and large-scale integration. *Nature Reviews Neuroscience, 2*(4), 229-239. doi:10.1038/35067550

Vidal, J., Giard, M. H., Roux, S., Barthelemy, C., & Bruneau, N. (2008). Cross-modal processing of auditory-visual stimuli in a no-task paradigm: a topographic event-related potential study. *Clinical Neurophysiology, 119*(4), 763-771. doi:10.1016/j.clinph.2007.11.178

Vincent, J. L., Kahn, I., Snyder, A. Z., Raichle, M. E., & Buckner, R. L. (2008). Evidence for a frontoparietal control system revealed by intrinsic functional connectivity. *Journal of Neurophysiology, 100*(6), 3328-3342. doi:10.1152/jn.90355.2008

Vincent, J. L., Larson-Prior, L. J., Zempel, J. M., & Snyder, A. Z. (2007). Moving GLM ballistocardiogram artifact reduction for EEG acquired simultaneously with fMRI. *Clinical Neurophysiology, 118*(5), 981-998. doi:10.1016/j.clinph.2006.12.017

Von Holst, E., & Mittelstaedt, H. (1950). Das Reafferenzprinzip - (Wechselwirkungen Zwischen Zentralnervensystem Und Peripherie). *Naturwissenschaften, 37*(20), 464-476.

Waszak, F., Cardoso-Leite, P., & Hughes, G. (2012). Action effect anticipation: Neurophysiological basis and functional consequences. *Neuroscience and Biobehavioral Reviews, 36*(2), 943-959. doi:10.1016/j.neubiorev.2011.11.004

Waszak, F., Wascher, E., Keller, P., Koch, I., Aschersleben, G., Rosenbaum, D. A., & Prinz, W. (2005). Intention-based and stimulus-based mechanisms in action selection. *Experimental Brain Research, 162*(3), 346-356. doi:10.1007/s00221-004-2183-8

Watson, J. B. (1913). Psychology as the Behaviorist views it. *Psychological Review*(20), 158-177.

Wolfensteller, U., & Ruge, H. (2011). On the timescale of stimulus-based action-effect learning. *The Quarterly Journal of Experimental Psychology, 64*(7), 1273-1289. doi:10.1080/17470218.2010.546417

Wolfensteller, U., & Ruge, H. (2012). Frontostriatal mechanisms in instruction-based learning as a hallmark of flexible goal-directed behavior. *Frontiers in Psychology, 3*, 192. doi:10.3389/fpsyg.2012.00192

Wolfensteller, U., & Ruge, H. (2014). Response selection difficulty modulates the behavioral impact of rapidly learnt action effects. *Frontiers in Psychology, 5*, 1382. doi:10.3389/fpsyg.2014.01382

Yin, H. H., & Knowlton, B. J. (2006). The role of the basal ganglia in habit formation. *Nature Reviews Neuroscience, 7*(6), 464-476. doi:10.1038/nrn1919

Zangenehpour, S., & Zatorre, R. J. (2010). Crossmodal recruitment of primary visual cortex following brief exposure to bimodal audiovisual stimuli. *Neuropsychologia, 48*(2), 591-600. doi:10.1016/j.neuropsychologia.2009.10.022

Ziessler, M., Nattkemper, D., & Frensch, P. A. (2004a). The role of anticipation and intention in the learning of effects of self-performed actions. *Psychol Res, 68*(2-3), 163-175. doi:10.1007/s00426-003-0153-6

Ziessler, M., Nattkemper, D., & Frensch, P. A. (2004b). The role of anticipation and intention in the learning of effects of self-performed actions. *Psychological Research, 68*(2-3), 163-175. doi:10.1007/s00426-003-0153-6

Zilli, E. A., & Hasselmo, M. E. (2008). Modeling the role of working memory and episodic memory in behavioral tasks. *Hippocampus, 18*(2), 193-209. doi:10.1002/hipo.20382

Zschocke, S. (2002). *Klinische Elektroenzephalographie*. Berlin: Springer.

Zwosta, K., Ruge, H., & Wolfensteller, U. (2013). No anticipation without intention: Response-effect compatibility in effect-based and stimulus-based actions. *Acta Psychologica, 144*(3), 628-634. doi:10.1016/j.actpsy.2013.09.014

Zwosta, K., Ruge, H., & Wolfensteller, U. (2015). Neural mechanisms of goal-directed behavior: Outcome-based response selection is associated with increased functional coupling of the angular gyrus. *Frontiers in Human Neuroscience, 9*. doi:10.3389/fnhum.2015.00180

Danksagung

Ich möchte hiermit die Gelegenheit nutzen, mich bei allen Personen zu bedanken, mit deren Hilfe es möglich wurde, dass diese Arbeit angefertigt werden konnte.

An erster Stelle möchte ich Prof. Dr. Hannes Ruge und Dr. Uta Wolfensteller danken für die Möglichkeit, in ihrer Arbeitsgruppe mitzuarbeiten. Sie halfen mir stets in allen fachlichen Belangen und standen bei Problemen immer mit Rat und Tat zur Seite. Ein ganz besonderer Dank geht außerdem an Hannes für die stete Navigation durch die Untiefen der EEG- und fMRT- Auswertung.

Ich danke außerdem Prof. Dr. Thomas Goschke, der mir die Gelegenheit gab, meine Dissertationsarbeit als Mitglied des Sonderforschungsbereichs 940 durchzuführen. Ein weiterer Dank geht an die DFG, durch deren Finanzierung der Sonderforschungsbereich erst Realität wurde.

Danken möchte ich auch allen guten Seelen des SFB und des Graduiertenkollegs des SFB. Ich denke dabei ganz besonders an Frau Petra Makowski, die sich stets rückhaltlos für mich eingesetzt und Lösungen bei Problemen jeglicher Art gefunden hat. Auch danke ich Prof. Dr. Alexander Strobel, Dr. Diana Armbruster und ganz besonders Frau Bianka Fricke dafür, dass sie immer ein offenes Ohr für die Belange der Doktorandinnen und Doktoranden des SFB hatten.

Ein weiterer Dank gebührt meiner langjährigen Büromitbewohnerin Ulrike Schulz für die vielen aufmunternden Gespräche und die stets launige Arbeitsatmosphäre. Weiterhin danke ich allen engagierten „Freunden des Kickertisches“, die regelmäßig für die nötige Zerstreuung und ein angenehmes Arbeitsklima gesorgt haben.

Weiterhin möchte ich meiner Familie, allen voran meinen Eltern, Jutta und Klaus-Dieter Baum für ihre Unterstützung danken und dafür, dass sie immer an mich geglaubt haben! Besonders bedanken möchte ich mich auch bei meiner Frau Susan Schurig. Sie gab mir den nötigen Rückhalt und ermutigte mich an Tagen, an denen die Motivation meinerseits nicht sehr groß war, mich dennoch nochmal an die Arbeit zu setzen. Weiterhin danke ich ihr für das finale Korrekturlesen der Arbeit und die vielen wertvollen Hinweise zur Formatierung.

Zu guter Letzt möchte ich Prof. Dr. Hannes Ruge sowie Prof. Dr. Alexander Strobel dafür danken, dass sie sich zur Begutachtung der Dissertationsarbeit bereit erklärt haben.

Erklärung

Hiermit versichere ich, dass ich die vorliegende Arbeit ohne unzulässige Hilfe Dritter und ohne Benutzung anderer als der angegebenen Hilfsmittel angefertigt habe; die aus fremden Quellen direkt oder indirekt übernommenen Gedanken sind als solche kenntlich gemacht. Die Arbeit wurde am Institut für Allgemeine Psychologie, Biopsychologie und Methoden der Psychologie, Professur Allgemeine Psychologie, der Technischen Universität Dresden unter wissenschaftlicher Betreuung von Prof. Dr. Hannes Ruge sowie Dr. Uta Wolfensteller angefertigt. Die Arbeit wurde bisher weder im Inland noch im Ausland in gleicher oder ähnlicher Form einer anderen Prüfungsbehörde vorgelegt. Ich erkenne die Promotionsordnung der Technischen Universität Dresden, Fakultät Mathematik und Naturwissenschaften, vom 23.02.2011 an.

Dresden, 30.07.2020

Fabian Baum